Ultra-long haul optical fibre transmission systems.

Terence Widdowson

Doctor of Philosophy

THE UNIVERSITY OF ASTON IN BIRMINGHAM

February 1995

Thesis Summary.

This thesis examines experimentally options for optical fibre transmission over oceanic distances. Its format follows the chronological evolution of ultra-long haul optical systems, commencing with opto-electronic regenerators as repeaters, progressing to optically amplified NRZ systems and finally solitonic propagation. In each case recirculating loop techniques are deployed to simplify the transmission experiments.

Advances in high speed electronics has allowed regenerators operating at 10 Gbit/s to become a practical reality. By augmenting such devices with optical amplifiers it is possible to greatly enhance the repeater spacing. Work detailed in this thesis has culminated in the propagation of 10 Gbit/s data over 400,000 km with a repeater spacing of 160 km. System reliability and robustness are enhanced by the use of a directly modulated DFB laser transmitter and total insensitivity of the system to the signal state of polarisation.

Optically amplified ultra-long haul NRZ systems have taken on particular importance with the impending deployment of TAT 12/13 and TPC 5. The performance of these systems is demonstrated to be primarily limited by analogue impairments such as the accumulation of amplifier noise, polarisation effects and optical non-linearities. These degradations may be reduced by the use of appropriate dispersion maps and by scrambling the transmitted state of signal polarisation. A novel high speed optically passive polarisation scrambler is detailed for the first time. At bit rates in excess of 10 Gbit/s it is shown that these systems are severely limited and do not offer the advantages that might be expected over regenerated links.

Propagation using solitons as the data bits appears particularly attractive since the dispersive and non-linear effects of the fibre allow distortion free transmission. However, the generation of pure solitons is difficult but must be achieved if the uncontrolled transmission distance is to be maximised. This thesis presents a new technique for the stabilisation of an erbium fibre ring laser that has allowed propagation of 2.5 Gbit/s solitons to the theoretical limit of ~18,000 km. At higher bit rates temporal jitter becomes a significant impairment and to allow an increase in the aggregate line rate multiplexing in both time and polarisation domains has been proposed. These techniques are shown to be of only limited benefit in practical systems and ultimately some form of soliton transmission control is required. The thesis demonstrates synchronous retiming by amplitude modulation that has allowed 20 Gbit/s data to propagate 125,000 km error free with an amplifier spacing approaching the soliton period. Ultimately the speed of operation of such systems is limited by the electronics used and, thus, a new form of soliton control is demonstrated using all optical techniques to achieve synchronous phase modulation.

Acknowledgements

During the period that I have undertaken this project I have been extremely fortunate with the number of people who have offered their help, time and ideas. I owe a great deal to my friend and mentor Derek Malyon who cheerfully accepted the responsibility of 'showing me the ropes' in optical fibre communications and worked with me on much of the early part of this thesis.

I must also mention Andrew Ellis, Dave Spirit, Jel Hueting and Phil Watkinson as providers of good counsel, support and sarcasm. Also, of course Nick Doran who enthusiastically accepted the responsibility of supervising the project.

T.W.

Contents

Figure Captions

Chapter 1

1. Introduction

Ultra-long haul transmission systems interconnecting different countries and continents are the prerequisite for global information technology. Where the capacity demands are high enough it becomes commercially viable to utilise optical fibre based systems as opposed to those based on satellites. To date there are several such links spanning the ~6,400 km of the Atlantic and landing in the UK. In this thesis various techniques and technologies are investigated for application to future high capacity transoceanic optical fibre transmission systems. As such the work embodies the concepts of both linear and non-linear optics, communications theory and high speed electronics. The main thrust is to evaluate the options experimentally, with numerical analysis and modelling used to confirm the results obtained.

1.1 Historical background

Historically, transoceanic communication via cable commenced in 1866 with the installation of an electrical telegraphy circuit capable of transmitting three words per minute. In 1956 the first transatlantic telephony cable was installed between the UK and the United States with a capacity of 36 circuits. The demand for voice and telegraph channels has increased with an almost constant growth rate of about 25% a year for both transatlantic and transpacific routes since that time. With the enhanced capacity the cost of each channel reduced and further stimulated demand. Initially, the capacity requirements were met by increasing the diameter, and hence bandwidth, of the coaxial cables used. Ultimately, there is a limit placed on the practically realisable dimensions of the cable due to both economic and mechanical considerations. Additionally, as the bandwidth of these systems increases there is a corresponding decrease in repeater spacing adversely affecting system cost and reliability.

In the 1970's development of optical fibre systems commenced in laboratories world wide. The technology that ensued resulted in the first deep water repeated optical fibre system to be installed in 1985 in the Canary Islands and the first transoceanic optical systems in

1988. The capacities of these systems were much greater than those possible with coaxial cable resulting in more economic use of the line plant. Figure 1.1 details the evolution with time of the 'real' cost of a three minute call to the USA from the UK.

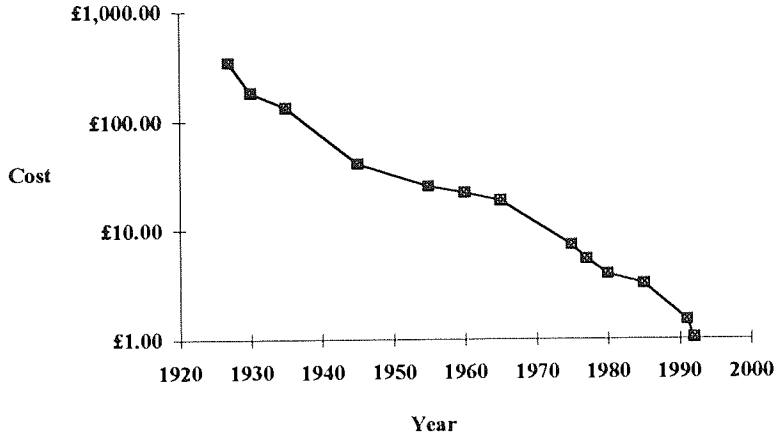

Figure 1.1. Evolution of cost of a 3 minute call to the USA from the UK with time.

These early optical systems utilised opto-electronic regenerators at regular intervals along the fibre in order to reform the distorted and attenuated pulses, e.g. TransAtlantic Telegraphy 8 (TAT 8). This process involved converting the optical signal to an electronic one via a photodiode before reshaping the pulses prior to retransmission at a higher intensity into the following section of the link. The next generation of transoceanic communications systems, TAT-12/13 to be installed in 1995, is to use optical amplifiers to compensate for the fibre attenuation resulting in an entirely optical transmission path.

1.2 Current options for transoceanic optical communications system

One of the advantages of regenerative systems is that they enable the pulses transmitted from each section of the system to be identical, since, noise and distortions do not accumulate. However, increasing the aggregate capacity of these systems by electronic multiplexing requires expensive and cumbersome parallel processing techniques at every repeater. Thus, in general, the bit rate of the system is fixed once installed precluding future upgradability. Ultimately it is the regenerator electronics that limits the utilisation of the massive bandwidth available from the transmission medium.

The alternative approach of optical amplification is in general bit rate independent, allowing amplified systems to be upgraded in principle by replacing the terminal equipment

only. Increases in the aggregate capacity of the system may be achieved by multiplexing in time, wavelength and polarisation in addition to the utilisation of higher speed transmitter and receiver electronics. As such these systems have been considered as the transparent optical pipe. However, due to the 'analogue' nature of the link the reshaping and retiming functions of regenerators are lost and transmission impairments and amplifier noise accumulate with distance even though conventional digital terminal equipment is employed. Consequently, the bit rate achievable by these systems over oceanic distances is limited.

Pulses of a particular shape, optical solitons, provide an opportunity to balance the effects of fibre dispersion and non-linearity and thus allow a pulse to propagate without change in spectral or temporal profile. Additionally, they are inherently digital in nature, unlike optically amplified NRZ systems. In principle they are the 'Holy Grail' of transmission systems since they allow distortionless propagation over arbitrarily long distances in a dispersive medium. However, temporal jitter in solitonic systems can become a severe limitation and at high bit rates action must be taken to control its accumulation.

1.3 Overview and aims of thesis

The aim of this thesis is to ascertain the viability of various options for transoceanic optical fibre communications systems. In each case extensive experimental investigations are complimented with theoretical analysis where deemed necessary. 1550 nm wavelength operation and the use of erbium doped fibre amplifiers (EDFAs) as the optical gain medium is assumed throughout.

Chapter 2 presents the background material required to understand the remainder of the thesis. Firstly, the linear characteristics of optical fibres are discussed from a transmission systems perspective. The relevant non-linear characteristics are also detailed as are applicable to ultra-long haul propagation. The components and performance of such systems are then discussed before a review of the current world status of experimental ultra-long haul transmission is presented.

Chapter 3 takes a fresh look at the 'old and established' technology of opto-electronic regenerators. To date all installed ultra-long haul optical systems utilise regenerators at periods down the transmission line. The most recent transatlantic link, CANTAT-3, operates at a line rate of 2.488 Gbit/s with a spacing between repeaters of ~120 km. However, the advent of the erbium fibre amplifier has directed communications research laboratories around the world to concentrate on optically amplified transmission systems at the expense of opto-electronically regenerated ones. In this thesis, by utilising new developments in high speed

electronics and by augmenting them with optical amplifiers to enhance the power budget, 10 Gbit/s data has been transmitted over global distances with a repeater spacing of 160 km, far in excess of any other published results. In terms of system reliability, robustness and performance such 'hybrid' links appear to offer the preferred topology for operation at line rates up to 10 Gbit/s.

Erbium doped fibre amplified NRZ systems are currently of particular importance due to the impending installation of systems like TAT 12/13. Initially, these systems were envisaged as an ideal implementation of the transparent optical pipe, allowing upgrades in capacity as required by replacing the terminal equipment only. However, in chapter 4 it is shown that the 'analogue' nature of these systems allows imperfections to accumulate. In particular, the deleterious effects of fibre dispersion, non-linearity, amplifier noise and polarisation fluctuations place an upper limit on the achievable bit-rate. To offset some of these limitations it is shown that novel dispersion management schemes and polarisation scrambling at the transmitter can greatly improve system performance to an acceptable level. This work has permitted 5 Gbit/s data to propagate over 17,600 km, in excess of any results reported to date.

Chapter 5 looks at propagation with optical solitons as the data bits. It is shown that very high quality solitons must be generated at the transmitter if the ultimate in performance is to be realised with a simple transmission path architecture. A new technique for the stabilisation of mode locked erbium fibre ring lasers is presented that has allowed 2.5 Gbit/s data to propagate to the theoretical limit of 18,000 km. This result implies, for the first time, that soliton transmission with significant system margin is possible over global distances without recourse to complex control schemes. Further, it is shown that multiplexing in time and polarisation provides only limited improvement in transmission capacity for practically realisable systems, contrary to that suggested elsewhere. At higher bit rates temporal jitter results in the need for some form of transmission control to be utilised. A synchronous retiming technique is used to allow 20 Gbit/s data to propagate over 125,000 km, the furthest transmission distance achieved at this line rate. Additionally, a new form of transmission control is demonstrated that utilises all optical techniques for the first time. This method shows considerable promise, since, the speed of operation is limited by the response of the fibre non-linearity. Consequently, it should enable very high data rates to propagate over oceanic distances.

To conclude chapter 6 attempts to highlight the advantages and disadvantages of each of the techniques discussed. Future options are considered with the aim of providing an

insight into some of the viable alternatives for the next generation of transoceanic communications system.

Chapter 2.

2. Optical fibres and long haul transmission systems

2.1 Optical fibre characteristics

Optical fibres for communications are very thin strands of glass, the core of which has slightly higher refractive index than the cladding. A light signal incident on one end of the fibre is confined to the core and can be transmitted with minimal loss and distortion to the other end due to the principle of total internal reflection. This chapter details the characteristics of optical fibres from a perspective of long haul communications.

2.1.1 Linear optical fibre effects

2.1.1.1 Fibre loss

Power is lost from optical signals on propagation down a transmission fibre. Excessive loss results in the information being irretrievable at the receiver unless intermediate signal boosting is encountered. Taking P_o as the power transmitted into the fibre, the power at any given point, z, along the fibre is given by[1]:

$$P_T = P_o e^{-\alpha z} \tag{2.1}$$

where α is the attenuation constant. Several mechanisms contribute to fibre loss[2], for instance Rayleigh scattering, OH absorption and infra-red lattice absorption. Consequently fibre attenuation varies with wavelength with a minimum of ~0.20 dB/km in the 1550 nm window and 0.4 dB/km at 1300 nm. For systems of transoceanic length it is desirable to utilise the minimum loss wavelength to reduce the number of intermediate repeaters required.

2.1.1.2 Chromatic dispersion

In general the response of a dielectric to the interaction of electromagnetic radiation with the bound electrons of the medium depends upon the frequency of the wave. This phenomena is referred to as chromatic dispersion and manifests itself through the frequency dependence of the refractive index, $n(\omega)$. Mathematically it is accounted for by expanding the mode propagation constant, $\beta=2\pi n/\lambda$, in a Taylor series about the centre frequency[3], ω_o:

$$\beta(\omega) = n(\omega)\frac{\omega}{c} = \beta\Big|_{\omega=\omega_0} + \frac{d\beta}{d\omega}\Big|_{\omega=\omega_0}(\omega-\omega_o) + \frac{1}{2!}\frac{d^2\beta}{d\omega^2}\Big|_{\omega=\omega_0}(\omega-\omega_o)^2 + \ldots \qquad (2.2)$$

Fibre dispersion plays a vital role in the propagation of short optical pulses[4] since different spectral components travel at speeds given by $c/n(\omega)$. The pulse envelope moves with group velocity, $v_g = d\omega/d\beta$, and is broadened due to second order dispersion, $d^2\beta/d\omega^2$. The wavelength at which the second order dispersion is zero is referred to as the zero dispersion wavelength, λ_0, and third order dispersion, $d^3\beta/d\omega^3$, then dominates.

The material dispersion referred to above relates to that of bulk silica. When silica is used to form a fibre, dielectric waveguiding occurs[5]. The effective mode index is slightly lower than the material index $n(\omega)$ and this reduction is wavelength dependent. The main effect of waveguide dispersion is to shift λ_0 slightly from that of bulk silica.

Most of the installed fibre in inland telecommunications networks is step index fibre, SIF, which has a λ_0 in the 1300 nm window. Dispersion shifted fibre, DSF, utilises waveguide dispersion to move the dispersion zero to the lower loss 1550 nm window and is the preferred choice for future long haul systems. Over distances short enough for fibre non-linearities to be insignificant, it is possible to compensate for dispersion by applying an equalising element with dispersion of equal magnitude but opposite sign[6].

2.1.2 Optical fibre non-linearities

In the previous section the linear fibre characteristics that must be accounted for when designing an optical transmission system were highlighted. These limitations may be overcome by the use of periodic signal boosting to offset attenuation and by operating the system on the fibre dispersion zero to minimise pulse distortion due to chromatic dispersion. However, optical fibres also exhibit a slight non-linearity that can cause severe pulse distortion on systems of oceanic length, even when operated on the dispersion zero. In general

non-linear effects introduce system impairments and attempts are made to avoid them. However, under certain circumstances they can be used to achieve pulse narrowing that can enhance system performance[7] and even allow distortion free transmission over arbitrarily long distances by balancing the effects of non-linearity and dispersion through optical solitons[8]. Consequently, non-linearity in optical fibre transmission has received increasing attention in laboratories world wide over the last decade or so.

At low power levels the fundamental phenomenological equation that describes the response of a dielectric medium to an optical field is[9]:

$$P(\omega) = \varepsilon_0 \chi(\omega) E \tag{2.3}$$

relating the induced polarisation, P, to the electric field, E, through the susceptibility, χ, with ε_o the permittivity of a vacuum. At optical frequencies the polarisation is established by the displacement of electrons relative to the atomic nuclei, so that each atom becomes a dipole oscillating at the frequency of the optical wave. For fields small compared to that which binds an electron to an atom the displacement of electrons is also small and the induced oscillations are essentially harmonic resulting in a constant χ. At higher power levels the applied field causes anharmonic motion of the bound electrons and the relationship between the polarisation vector and the applied field is non-linear[10]:

$$P = \varepsilon_0 \left[\chi^{(1)} E + \chi^{(2)} EE + \chi^{(3)} EEE + \ldots \right] \tag{2.4}$$

This is described by higher order terms in the electric susceptibility. The second order term, $\chi^{(2)}$, is a third rank tensor with 27 elements. However, for media which possess an inversion symmetry such as silica, these elements are zero. The third order term, $\chi^{(3)}$, is a fourth rank tensor with 81 elements. In silica glasses this term is responsible for such effects as four wave mixing, self phase modulation and cross phase modulation. The refractive index of the fibre can be described by its non-linear dependence on the optical intensity, I:

$$n(\omega, I) = n_0 + n_2 I \tag{2.5}$$

where $n_0(\omega)$ is the linear index of refraction. The second order non-linearity is related to the Kerr co-efficient, n_2, by[11]:

$$n_2 = \frac{3\chi^{(3)}_{1111}}{4\varepsilon_0 n_0^2 c} \tag{2.6}$$

assuming that the electric field is linearly polarised so that only one component, $\chi^{(3)}_{1111}$, of the tensor contributes to the refractive index. For an isotropic material such as glass, symmetry requires that[12]:

$$\chi^{(3)}_{1111} = \chi^{(3)}_{2222} = \chi^{(3)}_{3333} \tag{2.7}$$

2.1.2.1 Self phase modulation

Since the refractive index of glass is a function of optical intensity, a high intensity wave propagating in the fibre induces a phase change relative to that of a low intensity wave. This is called the non-linear phase change, ϕ_{NL}[13]:

$$\phi_{NL} = \frac{2\pi n_2 I z_{eff}}{\lambda} = \frac{2\pi n_2}{\lambda A_{eff}} P z_{eff} \tag{2.8}$$

where A_{eff} is the effective area of the mode propagating in the fibre[14] and is typically 50-80 μm^2 for SIF/DSF, P the optical power and z_{eff} the effective length of fibre in which the non-linear phase shift occurs. Since fibre attenuates the signal on propagation the effective non-linearity is reduced. Thus an effective length is defined, z_{eff}:

$$z_{eff} = \frac{1}{\alpha}\left[1 - e^{-\alpha L}\right] \tag{2.9}$$

where, L is the physical length of the fibre. For typical communications fibre with α = 0.2 dB/km $z_{eff} \rightarrow$ 22 km. The non-linearity described by equation 2.8 can be expressed equivalently by considering the dependence of the propagation constant on the refractive index:

$$\beta(\omega, I) = \frac{\omega n(\omega, I)}{c} \tag{2.10}$$

When the intensity, I(t), is modulated the propagation constant varies with time. The instantaneous optical frequency is proportional to the time derivative of the propagation constant. New frequency components are generated due to the intensity variation of the pulse. This effect is known as self phase modulation (SPM) and broadens the optical spectrum. In conjunction with group velocity dispersion SPM can cause both pulse narrowing and severe pulse distortion, see chapter 4.

2.1.2.2 Cross phase modulation

Two co-propagating signals in an optical fibre both experience non-linear phase shifts due to SPM. Additionally, each will encounter phase shifts due to the non-linear refractive index changes caused by intensity modulation on the other signal. This phenomena is known as cross phase modulation, XPM.

Consider the interaction, through the non-linear index n_2, between two waves of field amplitudes A_1 and A_2. In the slowly varying envelope approximation[15] the interaction between the waves can be described by the following pair of normalised coupled equations[16]:

$$i\left(\frac{\delta A_1}{\delta z}+\beta_1\frac{\delta A_1}{\delta t}\right)=|A_1|^2A_1+2|A_2|^2A_1 \qquad (2.11.a)$$

$$i\left(\frac{\delta A_2}{\delta z}+\beta_2\frac{\delta A_2}{\delta t}\right)=\frac{\omega_2}{\omega_1}|A_2|^2A_2+2|A_1|^2A_2 \qquad (2.11b)$$

where, β_1 and β_2 represent the specific group delay for the appropriate waves. The first term on the right hand side of equations 2.11a and 2.11b describes SPM, while the second term describes XPM. It can be seen that a given wave is twice as effective at modulating the phase of another wave, XPM, as it is at modulating its own phase, SPM.

XPM has many applications in all optical signal processing[17,18,19] and since it relies on interaction through Kerr non-linearity it is capable of very high speed operation. For example a high power 'pump' signal pulse can be used to induce a phase profile $\Delta\phi(t)$ on to a lower power 'probe' signal pulse by temporally overlapping them in a length of fibre. If the arrival time of the probe signal varies slightly, i.e. it is jittered, the size and magnitude of the imposed phase shift also varies according to the intensity distribution of the pump. By arranging for the probe signal to subsequently propagate through fibre of the appropriate dispersion it is possible to use the induced phase shifts to correct to some extent for the

original timing jitter. This has important repercussions in the control of ultra-long haul soliton transmission systems, see section 5.3.4.

To ascertain the phase shift induced on to the probe signal by the pump it is necessary to integrate equ.s 2.11. If it is assumed that the high power pump signal is A_1 and the low power probe signal A_2 it can be shown that the phase shift induced on A_2 by A_1 is[20]:

$$\phi = \frac{2\omega_2}{\omega_1} \int_0^L P_{A_1}(t - \Delta\beta z)dz \tag{2.12}$$

with L the length of the fibre in which the interaction takes place and $\Delta\beta = \beta_1 - \beta_2$ the difference in group delays between the two waves. It can be seen that the imposed phase profile depends critically on the group delay difference. If the two signals are exactly velocity matched, $\Delta\beta = 0$, then the magnitude of the interaction is maximised. This can be achieved by ensuring that the signals are of the same wavelength or by arranging for them to have the same magnitude dispersion in the fibre but opposite sign, i.e. +/- D. Generally the two pulses will have different group velocities and propagate at different speeds. The pulses are then said to 'walk off' from one another. Figure 2.1 illustrates the effect of walk off on the induced phase profile for two 6 ps FWHM $sech^2$ pulses propagating through 4 km of fibre. The values of walk off between the two signals are 0, 20 & 40 ps. It can be seen that the exact phase profile can be tailored by the use of appropriate values of pulse width, to control the rise time, and walk off to control the width.

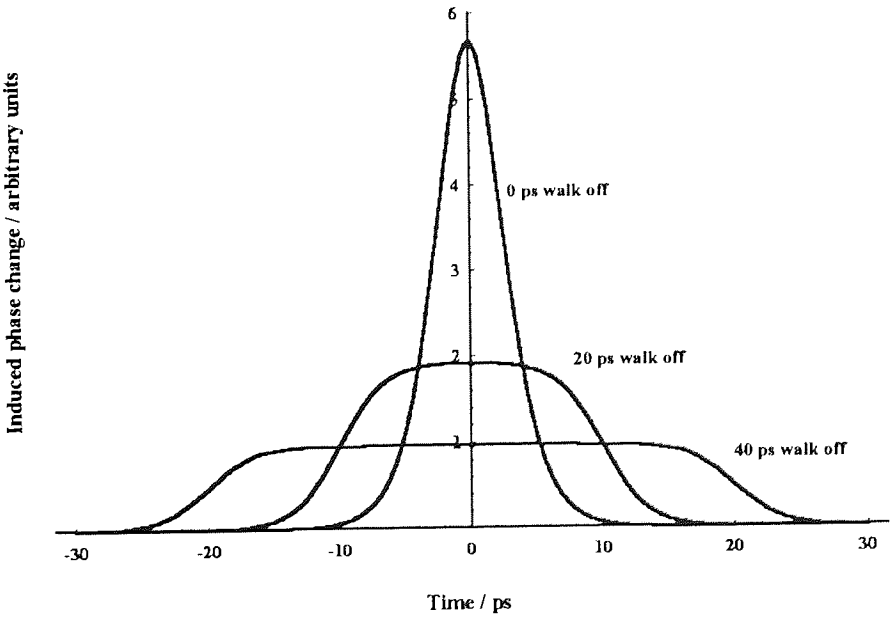

Figure 2.1. Induced phase profile due to XPM for varying degrees of walk off.

2.1.2.3 *Four wave mixing*

A parametric effect related to both SPM and XPM is four wave mixing, FWM, which again results from the third order non-linear polarisation:

$$P = \varepsilon_0 \chi^{(3)} : EEE \tag{2.13}$$

If only one excitation signal field is involved e.g. $E=E_0e^{i\omega t}+ E_0^*e^{-i\omega t}$ the tensor product produces oscillating terms at frequencies ω and 3ω and this process is known as third harmonic generation[21]. When two signal fields are present[22] at frequencies ω_1 and ω_2 the third order term also generates new frequencies at $2\omega_1-\omega_2$ and $2\omega_2-\omega_1$. Thus, the non-linearity forms sidebands at frequencies dependent on the frequency separation of the incident waves. Three excitation fields result in nine new frequency components being formed[23] which have frequencies $\omega_i+\omega_j-\omega_k$ (i,j,k=1,2,3). In partially degenerate FWM where $\omega_1 = \omega_2$ energy from a strong pump signal, ω_1, is transferred to a weak signal ω_3 and the process is called parametric gain[24]. Both harmonic generation and parametric gain have many applications in all optical signal processing.

In order to obtain appreciable FWM in communications fibre it is necessary to phase match the interacting signals[25]. When the signals are perfectly phase matched the relative phase of the optical carriers remains constant throughout the transmission, implying that they have the same velocity. As the phase matching criterion breaks down the efficiency of the FWM reduces. In long haul wavelength division multiplexed, WDM, systems FWM can result in channel cross-talk due to new signals being generated close to channel frequencies impairing system performance[26]. This detrimental effect can be avoided by the use of optical solitons where the fibre non-linearity is balanced by dispersion to effect stable distortion free transmission.

2.1.2.4 *Equation of propagation in monomode optical fibre*

It can be shown that for pulse widths greater than 100 fs, where the optical spectrum is sufficiently narrow to neglect higher order dispersion terms, that the propagation of radiation in monomode optical fibre is governed by the equation[27]:

$$i\frac{dA}{dz} = -\frac{i}{2}\alpha A + \frac{1}{2}\frac{d^2\beta}{d\omega^2}\frac{d^2A}{dT^2} - \gamma|A|^2 A \qquad (2.14)$$

where A is the slowly varying envelope, z is the axis of propagation, $T=t-\frac{d\beta}{d\omega}z$ and γ is the non-linearity coefficient:

$$\gamma = \frac{n_2\omega_0}{cA_{eff}} \qquad (2.15)$$

For the special case of zero fibre loss ($\alpha=0$) equation 2.14 reduces to the non-linear Schrodinger equation[28]:

$$i\frac{dA}{dz} = \frac{1}{2}\frac{d^2\beta}{d\omega^2}\frac{d^2A}{dT^2} - \gamma|A|^2 A \qquad (2.16)$$

The solutions to this apparently simple equation display extraordinary and interesting properties. The propagation behaviour depends critically on whether $\frac{d^2\beta}{d\omega^2}$ is positive or negative, i.e. for silica fibres, whether the wavelength is greater or less than λ_0.

2.1.2.5 Modulation instability

The simplest solution of equation 2.16 for wavelengths greater than λ_0 is that of cw radiation. However, this solution is inherently unstable to perturbations in amplitude or phase. A small variation will grow exponentially with distance and this effect is known as modulation instability[29].

2.1.2.6 Optical solitons

The other solutions to equation 2.16 for wavelengths greater than λ_0, are optical solitons[30]. These pulses propagate either without change of shape, in which case they are fundamental solitons, or have envelopes that vary periodically with distance, higher order solitons. The period over which the higher order soliton shape repeats is known as the soliton period. Solitons field amplitudes take the form of hyperbolic secants and the fundamental soliton is given by:

$$u(z,t) = A\,\mathrm{sec}h\left[\frac{t}{\tau}\right]e^{-\frac{iz}{z_1}} \tag{2.17}$$

which holds provided that:

$$\tau^2 = -\frac{1}{\gamma A^2}\frac{d^2\beta}{dt^2} \tag{2.18}$$

where τ is the sech width of the soliton, and

$$z_1 = -2\tau^2\frac{1}{\frac{d^2\beta}{dt^2}} = \frac{2}{\gamma A^2} \tag{2.19}$$

the peak optical power, $P_{pk} = A^2$, of the soliton is given by:

$$P_{pk} = -\frac{1}{\gamma\tau^2}\frac{d^2\beta}{dt^2} = \frac{\lambda_0^3 DA_{eff}}{(2\pi\tau)^2 cn_2} \tag{2.20}$$

where, D is the dispersion parameter:

$$D = -\left[\frac{2\pi c}{\lambda^2}\right]\frac{d^2\beta}{d\omega^2} \tag{2.21}$$

These solutions can be derived from the inverse scattering method[31] showing that fibre can support optical solitons which balance the effects of non-linearity and dispersion to provide distortionless transmission in a dispersive medium. In principle this result implies that very high bit rate transmission over oceanic distances with many wavelengths is possible without signal degradation. As such optical solitons appear to offer the ultimate solution to ultra-long haul transmission and consequently the technique has received much attention recently world wide. Chapter four is devoted to this topic.

Figure 2.2 details the temporal evolution over one soliton period of N = 1,2 & 3 solitons. The length scale over which higher order solitons repeat is the soliton period, z_o, given by:

$$z_0 = \frac{\pi z_1}{4} = \left(\frac{\pi\tau}{\lambda_0}\right)^2\frac{c}{D} \tag{2.22}$$

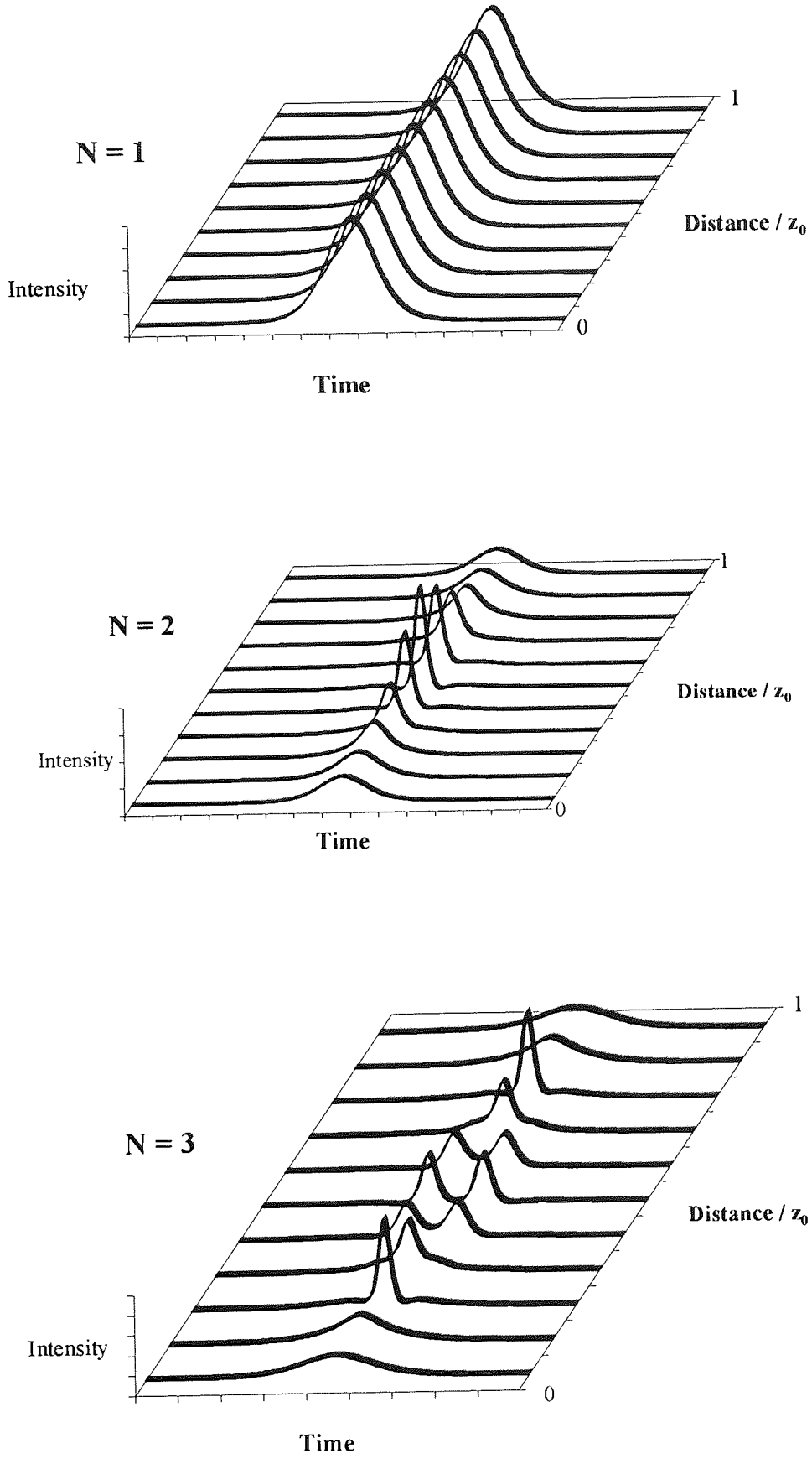

Figure 2.2. Temporal evolution of N = 1,2 &3 solitons over one soliton period

2.1.2.7 *Stimulated Brillouin scattering*

In addition to the non-linearity resulting from the interaction of photons with the electronic response of the medium, non-linearity can exist due to the interaction of photons and phonons. In particular, acoustic waves can induce vibrations in the glass lattice that make up the fibre core resulting in refractive index variations. Photons will be scattered from these inhomogeneities and the process is called Brillouin scattering[32]. Additionally, since the refractive index is dependent on the incident light intensity, lattice vibrations and therefore acoustic waves can be induced by an intense optical signal through electrostriction. Consequently, light from the forward propagating beam, called the pump beam, can provide gain for a backward propagating signal, called the Stokes wave, that is down shifted in frequency by 11 GHz and has a bandwidth of 100 MHz. This process is known as stimulated Brillouin scattering (SBS)[33].

To quantify SBS a threshold value can be determined and this criterion is arbitrarily defined as the input optical pump power, P_{thr}, at which the backward Stokes power P_{stokes} is equal to P_{thr} at the fibre input. It can be shown that[34]:

$$P_{thr} = \frac{21 A_{eff}}{g_b z_{eff}} \tag{2.23}$$

where, g_b is the peak value of the Brillouin gain and is equal to $\sim 5 \times 10^{-11}$ m/W for 1.55 μm communications fibre. In deriving equation 2.23 it has been assumed that there is no pump depletion and that the polarisation of the pump and Stokes wave is maintained along the fibre. For typical fibres with an effective length of 22 km and A_{eff}=50 μm^2 , $P_{thr} \sim 1$ mW and thus can be a serious non-linear degradation to optical communications systems.

2.1.2.8 *Stimulated Raman scattering*

The molecular vibrational modes of the fibre allow a small fraction, $\sim 10^{-6}$, of the incident radiation to be scattered and downshifted in frequency, typically by 13 THz and with a bandwidth of up to 40 THz. This results in power at the pump wavelength being converted into new wavelengths and this is known as spontaneous Raman scattering[35]. For very intense pump waves the downshifted Stokes wave can grow rapidly such that most of the pump energy is converted. This phenomena is known as stimulated Raman scattering[36] (SRS) and can be used for amplification purposes by seeding the process with a low power signal within the SRS spectrum[37].

The Raman threshold is defined in a manner similar to that of SBS, i.e. as the input pump power at which the Stokes power becomes equal to the pump power at the fibre input. From this it may be determined that the critical pump power, P_{cr} is given by[38]:

$$P_{cr} = \frac{16A_{eff}}{g_r Z_{eff}} \tag{2.24}$$

assuming no pump depletion and that the polarisation of the pump and Stokes wave is maintained along the fibre. For typical communications fibre with an effective length of 22 km, A_{eff}=50 μm^2 and g_r=1x10^{-13} m/W the threshold value is ~600 mW, much higher than that for SBS.

2.2 Long haul optical systems

2.2.1 Transmission formats

Most optical communications systems utilise a digital transmission format such that turning the signal on represents a logical 'one' and turning it off represents a logical 'zero'. This process is known as intensity modulation, IM. Installed optical line systems use non return to zero, NRZ, data format in which the coded pulse occupies the entire bit period, i.e. if the next bit has the same value no transition occurs at the end of the time slot. In general two methods of modulation are employed to generate NRZ data, either direct or external. By applying the modulation directly to the bias of the laser, its output may be turned on and off. However, in so doing semiconductor dynamics distort the signal resulting in an enhanced optical spectrum[39]. This deleterious effect may be precluded by operating the laser c.w. and applying the modulation externally. Electro-optic and electro-absorption modulators can produce very close to transform limited NRZ outputs. The alternative data format is return to zero, RZ, in which the signal always returns to the zero level by the end of the time slot. It is characterised by the duty cycle, the ratio of the pulse width to the bit period. Usually RZ sources are externally modulated.

2.2.2 Transmission system performance

System performance is characterised by the bit error ratio (BER), detailing the mean ratio of errors to the total number of bits. Errors occur as a result of impairments from the

transmitter, receiver or the transmission system itself. Contributory factors are noise, jitter, inter-symbol interference and patterning. The standard definition for receiver sensitivity is the optical input power for which a BER of $1x10^{-9}$ is obtained. It is usual to measure this parameter both back to back, i.e. without the transmission link, and also with the system inserted between the transmitter and receiver. Any discrepancy between the two power measurements is called a penalty and results from minor transmission impairments. If it is not possible to obtain a BER of $1x10^{-9}$ by increasing the received optical power the system is said to exhibit an error floor at the best obtainable BER. In this case major transmission impairments have resulted and system performance is not acceptable.

A powerful diagnostic when examining a system output is the 'eye diagram', which is an overlay of all possible states of a sequence. Physically, the eye diagram is derived by triggering an oscilloscope from the system clock. Transmission impairments manifest themselves as changes in the shape of the 'eye' from the ideal case.

2.2.3 Receivers and regenerators

The conversion of intensity modulated optical data into an electrical signal can be simply achieved via direct detection. A *pin* photodiode or avalanche photodiode, APD, envelope detects the incoming optical signal power and emits a photo-current proportional to it. This electrical signal is then amplified to a level sufficient for electronic processing circuitry. The combination of the diode and the low noise amplifier is known as the front end. The bandwidth of the receiver is usually optimised for the modulation format and bit rate used. It should be kept to a minimum to reduce the noise bandwidth but should not induce inter-symbol interference. For NRZ data the optimal filter is one of raised cosine response with a 3 dB bandwidth of 58% of the bit rate[40].

The bandlimited data is split into two paths to allow timing extraction, or clock recovery, and the decision process to take place. Timing extraction is necessary for two reasons: in general data does not have a system clock signal transmitted with it, and secondly, the phase of the incoming data varies as the transmission fibre expands and contracts due to variations in temperature, this is particularly important for transoceanic systems. The decision process involves determining whether each bit is a 'one' or a 'zero'. In general this decision needs to be taken in the middle of the time slot and therefore requires the clock recovery. The combination of the front end, timing extraction and decision process is called the receiver. To form a complete regenerator the output of the receiver is fed to a transmitter,

usually a directly modulated laser, that launches the signal into the next section of the link. Figure 2.3 details schematically the composition of a front end, receiver and regenerator.

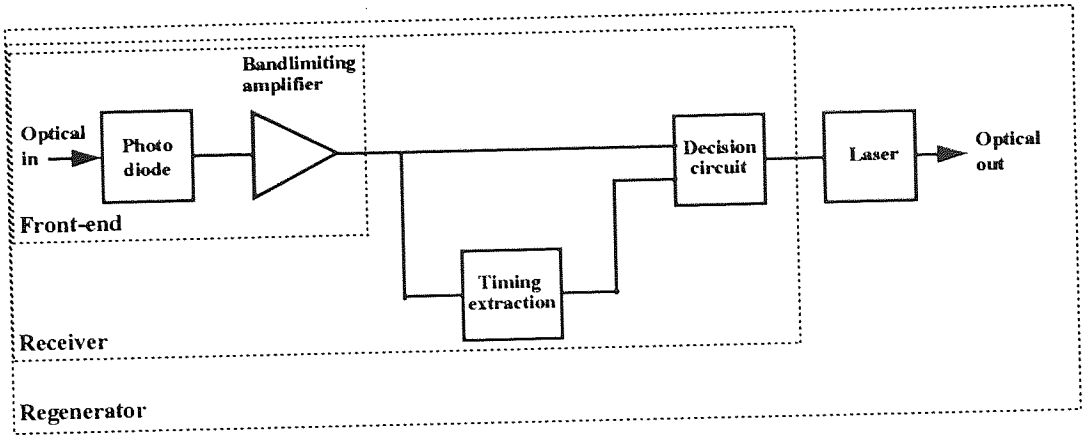

Figure 2.3. Schematic of an opto-electronic regenerator

Receivers are characterised by their sensitivity, the optical power required to provide a BER of $1x10^{-9}$ at the output. In a well designed receiver sensitivity is determined by the ratio of the signal to the noise generated in the front end. This may be determined by[41]:

$$SNR = \frac{P_{si}}{\frac{4kT_eB}{R}} \tag{2.25}$$

where, P_{si} is the mean signal power, k is Boltzmann's constant, T_e is the noise temperature of the front end which is related to noise figure, NF, by: $T_e=290(NF-1)$, B is the electrical bandwidth and R the output impedance of the detector. Due to their inherent gain process the sensitivity of APD receivers is usually around 10 dB better than that of *pin* receivers.

The receiver sensitivity and maximum transmitter launch power set an upper limit to the length of the system. The difference between the receiver sensitivity and launched power is called the power budget and the loss of the link must be less than this to enable 'error free' operation. Usually a 'margin' is allowed to cater for component ageing, etc.

2.2.4 *Optical amplifiers*

Optical amplification may be achieved from the transmission fibre itself by utilising the Brillouin[42] or Raman effects[43], from semiconductor devices[44,45] or from fibre doped with rare earth elements[46]. The preferred choice for application in the 1550 nm window of transmission fibre is the erbium doped fibre amplifier (EDFA). EDFA's offer high gain, low noise, high output power and excellent compatibility with the transmission fibre. In general a semiconductor pump laser at 1480 nm or 980 nm is used to excite the erbium ions in the rare earth doped fibre into a metastable state. An optical signal in the 1550 nm range can effect stimulated emission and become amplified. The major disadvantage with this process is that gain is accompanied by noise. When a signal propagates over a very long system with many amplifiers the noise may accumulate to the point where errors are incurred at the receiver.

As soon as noise is introduced into a system there is a finite probability that a transmission error may occur. If it is assumed that the noise takes the form of Gaussian statistics it is necessary to establish a mean signal to noise ratio of 15.6 dB to obtain a BER of 1×10^{-9}. The mean electrical signal to noise ratio is defined as:

$$SNR = 10\log_{10}\frac{\left[\frac{P_{si}\lambda}{hc}\right]^2}{B\sigma^2} \tag{2.26}$$

and is exactly twice the optical SNR. In equation 2.26; B is the electrical bandwidth of the receiver and σ^2 is the noise variance. The noise variance will in general result from three main sources; shot noise associated with the detection of the signal, receiver thermal noise and beat noise resulting from the interference between the optical signals. In systems that utilise optical amplifiers it is usual to ensure that the noise originating from the amplifier cascade dominates other noise sources. The amplifiers give rise to gain and broadband spontaneous noise. This results in four distinct contributions to the noise variance at the receiver. Signal shot noise: the mean signal power produces a constant signal and associated shot noise. Spontaneous-shot noise: the mean spontaneous noise power produces a constant spontaneous noise current with associated shot noise. Signal-spontaneous beat noise: the signal interferes with spontaneous noise producing intensity variations with a broad bandwidth which are directly converted into current variations. Spontaneous-spontaneous beat noise: spontaneous noise interferes with spontaneous noise at a different wavelength, resulting in intensity variations of a broad bandwidth.

An optical amplifier of gain G produces noise[47], P_{sp}:

$$P_{sp} = 2\left(\frac{hc}{\lambda}\right)(G-1)n_{sp}\delta f \tag{2.27}$$

Where n_{sp} is the population inversion parameter and is related to the amplifiers noise figure: NF = 10 $\log_{10}(2n_{sp})$, and δf is the bandwidth over which the noise is measured. In an N amplifier system the accumulated noise will be approximately:

$$P_{sp} = 2N\left(\frac{hc}{\lambda}\right)(G-1)n_{sp}\delta f \tag{2.28}$$

assuming that the gain of the system equals the loss and that the spontaneous noise spectrum is white. In most systems the two beat noise terms dominate over the others. In a well designed system the signal-spontaneous beat noise term is dominant. This may be achieved by using a narrow band optical filter in front of the receiver to limit the bandwidth over which spontaneous-spontaneous beat noise can contribute. In this case the SNR can be approximated by[48]:

$$SNR = 10\log_{10}\left\{\frac{P_{si}}{4B(G-1)n_{sp}N}\right\} \tag{2.29}$$

Equation 2.29 calculates the average SNR assuming that the signal spontaneous beat noise is distributed equally over the 'ones' and 'zeros', such that the optimum decision threshold is in the centre of the eye diagram. Clearly, in practice this will not be the case since when the signal is a 'zero' this noise term vanishes and spontaneous-spontaneous noise or receiver thermal noise become dominant. Thus, the noise variance for 'ones' and 'zeros' is different and the optimum decision point is moved closer to the 'zeros'.

2.2.5 Dispersion induced inter-symbol interference

An optical signal conveying information has a bandwidth associated with it. The higher the bit rate the wider the spectral width of the signal. On propagation through dispersive fibre the different spectral components arrive at the receiver at different times, resulting in pulse spreading or inter-symbol interference. This impairment can lead to system errors and needs to be limited to an acceptable level. The problem is enhanced in systems using a 'chirped' transmitter such as a directly modulated laser, i.e. where the spectral width

of the signal is greater than the information bandwidth. The pulse broadening, $\Delta\tau_b$, may be determined by[49]:

$$\Delta\tau_b = LD\Delta\lambda \tag{2.30}$$

where $\Delta\lambda$ is the spectral width of the transmitted signal. If it is assumed that the pulse shapes are Gaussian, then the received pulse width, τ_{Rx}, can be evaluated:

$$\tau_{Rx}^2 = \tau_{Tx}^2 + \Delta\tau_b^2 \tag{2.31}$$

where, τ_{Tx} is the transmitted pulse width, for NRZ signals $\tau_{Tx}=1/B$ where B is the bit rate. If the broadening on propagation for NRZ data is not to exceed 10% of the bit period, i.e. $\tau_{Rx(max)}<1.1\ \tau_{Tx}$, a limit is placed on the bit rate transmission distance product:

$$LB < \frac{0.458}{D\Delta\lambda} \tag{2.32}$$

Implying that a transform limited 10 Gbit/s signal operating at 1550 nm on step index fibre with a dispersion of 16 ps/nm/km, is limited by dispersion to a transmission distance of 36.4 km. When designing regenerative systems it is only necessary to ensure that the dispersion limit is not exceeded between each repeater. However, for amplified systems this limit must not be exceeded over the entire length of the link and this is of major significance for transoceanic systems.

2.2.6 Recirculating loops

In designing ultra-long haul optical systems it is relatively easy to calculate the effects of noise accumulation, dispersion and some non-linear effects in isolation. However, in reality optically amplified systems encounter interplay between these impairments that greatly complicates matters. Numerical models may be used to investigate most of these effects, however ultimately the performance of such systems must be determined experimentally. To this end laboratory demonstrators spanning both transatlantic[50] and transpacific[51] distances have been constructed. Although linear cascaded systems of this type are very informative in terms of experimental detail, they require significant capital and manpower investment. Effecting subsequent changes in system components and parameters is again costly and time

consuming. In order to ascertain penalties due to chromatic dispersion, amplifier noise figure and fibre non-linearity, it is possible to use loop configurations in which a small subsegment of a large amplifier chain has its output fed back to its input to enable simulation of very long systems[52]. Such arrangements can consist of relatively few repeaters and fibre spans and thus preclude the prohibitive aspects of ergonomics and economics of a linear cascaded system. They can accurately reflect the performance of a cascaded system and facilitate simple alterations to components and parameters, in particular 'worst case' scenarios are easily established. Additionally, the ultimate limits of system operation can be determined since propagation over longer distances is achieved by allowing the signal to circulate for a longer time. One drawback of using recirculating loops is that it is difficult to determine the effects of component tolerances that would be encountered in a long system.

2.3. Current world status of experimental ultra-long haul transmission systems.

In order to place the work detailed in this thesis in context, this section attempts to outline the current world status of experimental ultra-long haul transmission. Table 2.1 indicates the most significant results available from the open literature (to the authors knowledge).

Much of the early work on ultra-long haul optically amplified systems concentrated on NRZ transmission format. This was compounded by purchasers of systems such as TAT12/13 and TPC-5 opting for this technology. Work detailed in chapter 4 is currently state of the art with 5 Gbit/s data transmitted over 17,600 km. Also detailed in chapter 4 are the subtle deleterious polarisation effects that the system suppliers are now concentrating on reducing on prototype cascaded systems.

Some of the most outstanding results of the past few months have been those described in chapter 3 on 3R regenerators. Using a directly modulated DFB laser and fibre amplifiers in each repeater, 10 Gbit/s data has been transmitted over 400,000 km with a repeater spacing of 160 km. To date no other type of system offers such large repeater spacing or robustness.

The increasing interest in soliton systems has also resulted in some very impressive results. Without transmission control 2.5 Gbit/s data has been transmitted over 17,600 km, see chapter 5, and 20 Gbit/s over 11,500 km by Suzuki et al, though with significantly stronger guiding. The use of transmission control has allowed both the bit rate and propagation distance to be extended significantly. Work undertaken by Mollenauer et al using the passive technique of sliding guiding filters has shown significant promise for transoceanic

systems operating up to 20 Gbit/s. Beyond this the best results have been obtained with synchronous retiming. Chapter 5 details the transmission of 20 Gbit/s data over 125,000 km, the best at this line rate to date, and follows on from the pioneering work of Nakazawa, 10 Gbit/s over 1 Mkm. Additionally, a novel all optical approach to soliton transmission control is demonstrated in chapter 5 that may allow control at ultra-high bit rates.

NRZ: Optically amplified.

Author	Lab	Capacity	Span	Reference	Comments/description:
Widdowson et al	**BTL**	**5 Gbit/s**	**17,600 km**	**Thesis**	**90 km loop with dispersion management.**
Taga et al	KDD	10 Gbit/s	9,000 km	OFC,93 PD1	Straight line using 274 amplifiers
Taga et al	KDD	2x5 Gbit/s	4,550 km	OFC'93 PD4	Straight line IM-DD 2 channel WDM

NRZ: Regenerated.

Widdowson et al	**BTL**	**5 Gbit/s**	**500,000 km**	**Thesis & EL 30, 2056 (1994)**	**3R regenerated system with 205 km span and directly modulated laser**
Widdowson et al	**BTL**	**10 Gbit/s**	**400,000 km**	**Thesis**	**3R regenerated system with 160 km span and directly modulated laser**

Soliton: Without transmission control.

Widdowson et al	**BTL**	**2.5 Gbit/s**	**17,600 km**	**Thesis EL 30, 661 (1994)**	**No soliton control phase locked erbium ring laser source.**
Suzuki et al	KDD	5 Gbit/s	13,000 km	EL 291643(1993)	Electro-absorption modulator source, significantly more guiding than above.
Suzuki et al	KDD	20 Gbit/s	11,500 km	EL 30, 1083(1994)	Alternating amplitude, as above.

Soliton: With transmission control.

Mollenauer et al	AT&T	15 Gbit/s 10 Gbit/s	25,000km 35,000km	OL 19, 704 (1994)	Sliding guiding filters for control + polarisation division multiplexing
Mollenauer et al	AT&T	2x10 Gbit/s	13,000km	OFC'93 PD8	As above
Nakazawa et al	NTT	10 Gbit/s	1 M km	OFC'93 PD7	500 km loop, retiming (amplitude)
Widdowson et al	**BTL**	**20 Gbit/s**	**125,000 km**	**Thesis & EL 30, 1866 (1994)**	**100 km loop, Active retiming, (amplitude)**
Widdowson et al	**BTL**	**2.5 Gbit/s**	**20,000 km**	**Thesis & EL 30, 990 (1994)**	**Soliton control (phase) using all-optical process in fibre**

Table 2.1. Current world status of experimental ultra-long haul transmission.

Chapter 3

3. Opto-electronic regenerators

3.1 Introduction

Imperfections in a transmission medium can distort a signal on propagation. If a communications link is long enough information may be degraded to the point whereby it is lost irretrievably. To enable a system of transoceanic length to operate without errors, the signal must be 'regenerated' in some way at periods along the transmission path. Conventionally this has been achieved by using opto-electronic devices. The pulse degradation suffered in an optical system is primarily due to fibre loss and dispersion. Loss may be overcome by amplification and dispersion by reshaping e.g. a limiting amplifier. On propagation through many such 'regenerators' noise from the amplification process and equalisation errors from the reshaping stage accumulate, placing an upper limit on the transmission distance. To preclude the growth in distortion it is possible to regenerate the pulses back to their original state at each repeater and increase the length of the link. This necessitates a decision being made in the middle of each bit period as to whether a bit is a logic '0' or '1', a process that requires retiming. Repeaters that utilise this technique are known as 3R regenerators from Reshaping, Retiming and Regeneration.

In designing a regenerative system it is necessary to position repeaters at sites along the link prior to the onset of errors. Excessive loss will attenuate the pulses to a level whereby noise generated in the front end of the receiver results in errors occurring in the decision process. A dispersion penalty causes inter-symbol interference (ISI) which can also lead to errors. In addition to the impairments of SNR and ISI, regenerative systems suffer from the accumulation of timing jitter. A clock signal at the line rate must be extracted from the incoming data at each repeater, a process that is always accompanied by the addition of phase noise. Jitter accumulates along the link and can result in errors due to the decision being made at the wrong time.

Jitter emanates from noise and the data pattern. The noise dependence is random in nature and accumulates with '$\sqrt{N}$, where N is the number of regenerators[53]. It can be

decreased both by increasing the optical power incident on the receiver, to improve SNR, and also by reducing the bandwidth of the timing recovery circuit. The pattern dependent jitter is systematic since it is correlated with that produced by the other regenerators in the link, it accumulates with $\sqrt{N}$.

Without recourse to elaborate multiplexing techniques the use of regenerators restricts the system to a fixed bit rate, wavelength and modulation format and, thus, ultimately it is the regenerator that limits the utilisation of the massive potential of the transmission medium. To date commercially 'qualified' opto-electronic regenerators are available up to bit rates of 2.5 Gbit/s. The components that make up the regenerators exist for 10 Gbit/s operation[54] and most functions have been realised in the laboratory at 40 Gbit/s and above, for instance ~100 GHz *pin*[55,56], 40 GHz timing extraction[57], 40 GHz sources[58,59], 40 GHz electronic amplifiers[60] and 40 Gbit/s multiplexers and decision circuits[61]. Thus, the construction of 5 & 10 Gbit/s regenerators is now feasible.

To enhance system reliability the number of repeaters in a link should be kept to a minimum and this implies a large spacing between regenerators. Thus, the power budget is to be maximised by launching as much power as possible and by utilising a sensitive detector. Modern high speed DFB lasers will typically give a mean output power of ~0 dBm and a state of the art receiver at 5 Gbit/s will have a sensitivity of around -30 dBm, allowing a repeater spacing of ~120 km with margin at 1550 nm. By utilising optical amplifiers to boost the transmitted signal and also improve receiver sensitivity this figure can be increased significantly with obvious commercial implications. However, when launching powers in excess of 10 dBm care must be taken to avoid the detrimental effects of non-linear phenomena, in particular inelastic scattering processes and self phase modulation. In this chapter the design of opto-electronic regenerators at both 5 and 10 Gbit/s will be discussed. The use of optical EDFA's to increase the repeater spacing will be demonstrated and their performance tested in a recirculating loop.

3.2.1 5 Gbit/s regenerator configuration

The schematic configuration of the purpose built 5 Gbit/s regenerator[62] used in the transmission experiments is illustrated in Figure 3.1. Data was detected by a 10 GHz *pin* FET receiver and bandlimited by post amplification to 3 GHz. Retiming was performed by a 5 GHz second order phase lock loop[63] (PLL) with a natural frequency, ω_n, 2.5×10^6 rad/s and a damping factor, ζ, of 0.7. To enable the PLL to recover timing information a frequency doubler extracted a spectral component at the line rate from the incoming data[64]. The jitter

incurred as a result of the clock extraction process was below the resolution of the both the sampling oscilloscope, <2 ps rms, and the spectrum analyser used in attempting to measure it (<0.5 ps rms). Regeneration was achieved by a 10 Gbit.s^{-1} D-type flip-flop and subsequent transmission performed by a directly modulated 1557 nm 10 Gbit.s^{-1} DFB laser. The mean launch power from the DFB was 0 dBm and the receiver sensitivity was measured at -21 dBm for a 1x10^{-9} BER and a 2^7-1 PRBS data pattern. The sensitivity obtained is far from state of the art due to the use of a non-optimised commercially available receiver, thus, the repeater spacing could in principle be extended significantly.

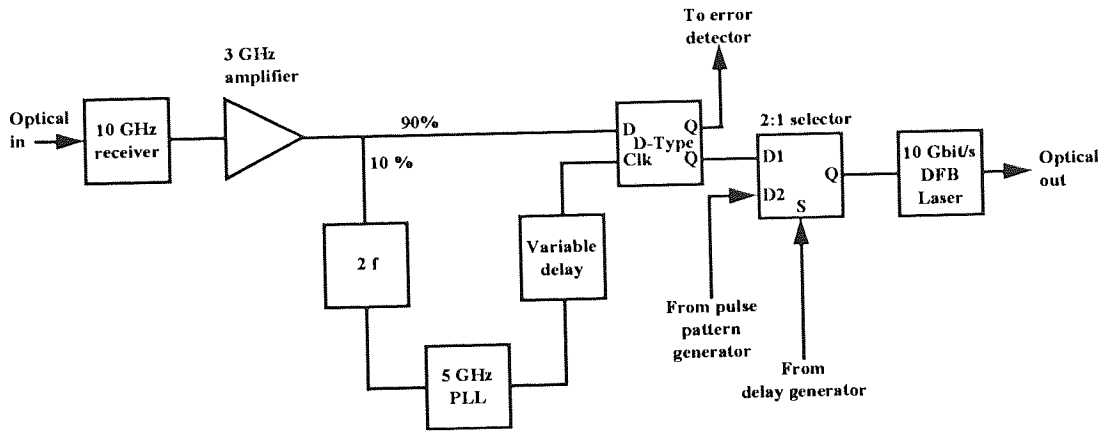

Figure 3.1 5 Gbit/s opto-electronic regenerator schematic configuration.

To reduce the accumulation of systematic pattern dependent jitter the system was configured such that the regenerator transmitted word and word bar on alternate recirculations[65]. Systematic jitter is dependent on the density of the pulses in the pattern and this is affected by finite pulse widths, amplitude to phase conversion[66], etc. If the pattern is inverted at each repeater systematic jitter is cancelled since the density of the pulses is also inverted, thus, pattern dependent jitter is effectively suppressed and jitter should accumulate with a '$\sqrt{N}$ dependence due to random variations.

3.2.2 5 Gbit/s regenerator transmission experiments

The recirculating loop configuration used in the regenerator transmission experiments is shown in Figure 3.2. The 2:1 selector (Figure 2.1) intermittently injected data from the pulse pattern generator into the loop under the control of the delay generator. For the remainder of the measurement cycle the selector allowed the regenerated data from the loop to

pass to the DFB and, thus, recirculate. An error detector was connected to the output of the D-type flip-flop and allowed error ratios to be measured at the end of each measurement period. An optical isolator was spliced to the output of the DFB to minimise reflections that could cause spectral and amplitude instabilities. The transmission medium consisted of 66 km of dispersion shifted fibre, DSF, with a dispersion zero, λ_0, at 1556 nm and a loss of 16.3 dB. Thus, there was a system margin of 4.7 dB per span over the sensitivity point and the measured slope of the BER was 0.7 dB/decade. Thus, 10^7 repeaters, or 660,000,000 km, could be traversed before the theoretical sensitivity point was reached due to SNR. The dispersion at the operating wavelength was - 0.075 ps/nm/km, ensuring that inter-symbol interference was negligible, i.e. 4.95 ps/nm over the span of 66 km.

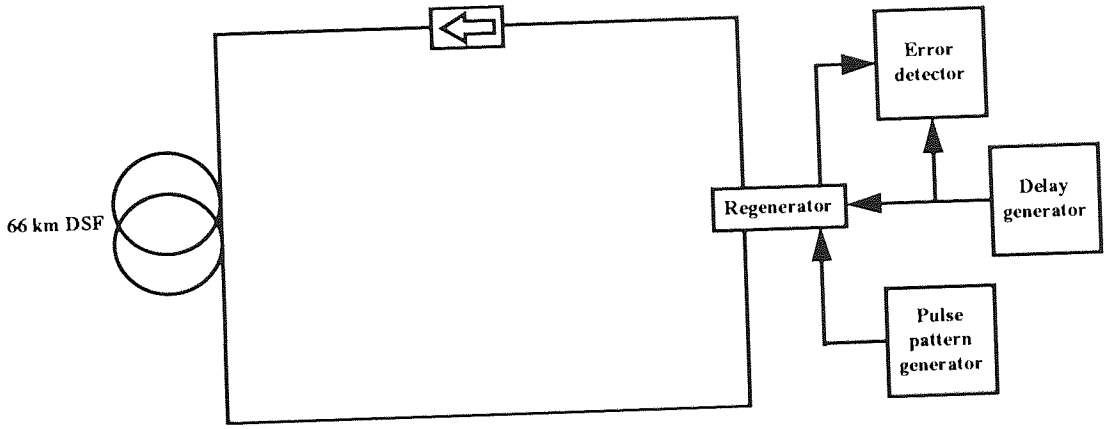

Figure 3.2. Basic recirculating loop configuration for 5 Gbit/s regenerator transmission experiments.

2.2.3 5 Gbit/s regenerator results and discussion

Error free operation (Bit error ratio less than $1x10^{-9}$) in an uncontrolled environment was possible to a distance of 250,000 km, Figure 3.3 details the eye diagram at this distance. Adjusting the polarisation state of the laser output had no measurable effect on the error ratio. Complete and fundamental polarisation insensitivity is a very attractive feature of regenerated systems.

Errors that occurred beyond 250,000 km were artefacts of the loop configuration and not 'real' system errors, see Appendix 1. The jitter that is apparent at the crossings in Figure 3.3 is attributable to this effect and not a true system impairment. Consequently, conclusive evidence as to the noise performance and phase margin of the system could not be ascertained

and also meaningful BER measurements could not be obtained. However, since the transmission distance achievable is far in excess of any practical system, it is of more importance to concentrate on increasing the repeater spacing than to address the loop specific artefacts.

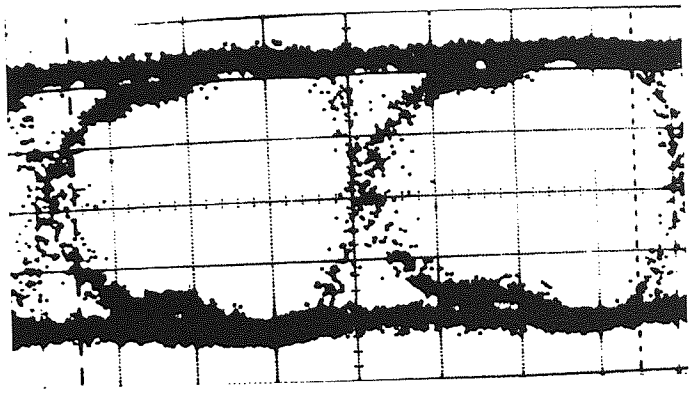

Time (50 ps/Div.)

Figure 3.3. Regenerated 5 Gbit/s eye diagram after transmission over 250,000 km.

By utilising a state of the art receiver with a sensitivity[67] of -31 dBm the repeater spacing could be extended by 40 km to 106 km without impinging on system margin. This figure could be further increased by the use of lower loss DSF, for instance, fibre with a loss of 0.20 dB/km is now available allowing a repeater spacing of 131.5 km. Additionally, optical amplifiers could be used to increase both receiver sensitivity and launch power and this is the topic of the next section.

3.3.1 5 Gbit/s regenerator with optical pre and power amplifiers, experimental

Figure 3.4 details the experimental arrangement used to demonstrate a significant increase in the repeater spacing without reducing system margin. The addition of an erbium power amplifier allowed the launched signal power to be increased to 15.5 dBm and an erbium pre-amplifier with a gain of 20 dB and a noise figure of 5 dB increased the receiver's sensitivity to -39 dBm. A 1 nm bandpass filter was used in front of the receiver to reduce spontaneous-spontaneous beat noise. The 205 km of DSF had a mean λ_0 of 1559 nm and a loss of 47 dB, allowing 7.5 dB of margin per span and a factor of 3 increase in the repeater spacing. The mean fibre dispersion at the operating wavelength was +0.15 ps/nm/km.

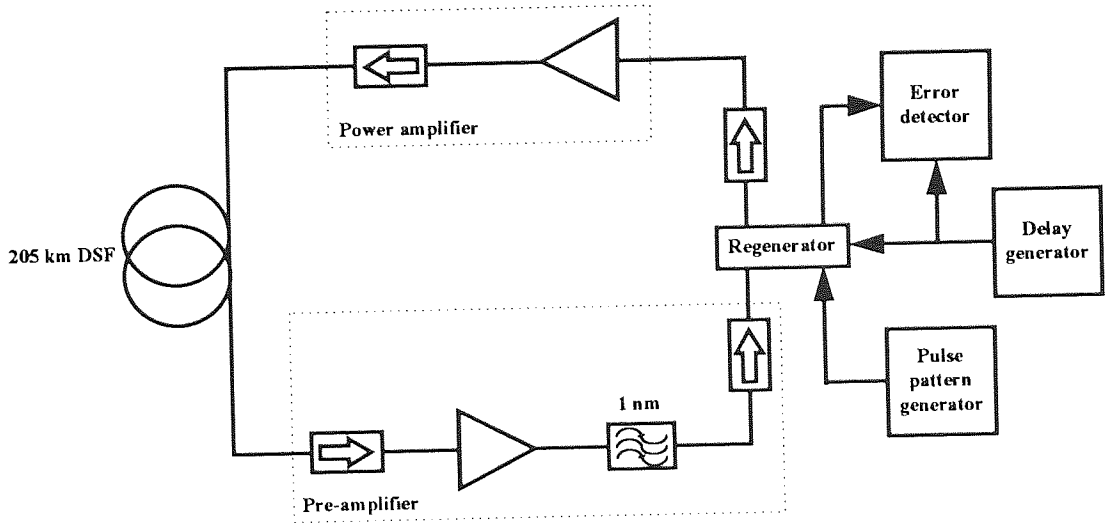

Figure 3.4. Recirculating loop arrangement for opto-electronic regenerator experiments with pre and post amplification.

When launching such high powers into the fibre it is important to ensure that non-linear inelastic scattering processes do not introduce system impairments. In chapter 2 it was indicated that stimulated Brillouin scattering can cause serious detrimental effects with powers greater than around 1 mW. However, in deriving equation 2.23 it has been assumed that the linewidth of the pump beam is very much narrower than the Brillouin linewidth, $\Delta\upsilon_b$. The exact figure for $\Delta\upsilon_b$ varies with fibre design and dopants, but is generally around 100 MHz. Thus the SBS threshold strongly depends on pump linewidth $\Delta\upsilon_L$. Additionally, modulation will broaden the effective linewidth and increase the threshold power. Equation 3.1 details the threshold for a pump beam with finite Lorentzian linewidth intensity modulated at bit rate B[68].

$$P_{thr} = \frac{21A_{eff}}{g_b Z_{eff}} \left[\frac{\Delta\nu_L + \Delta\nu_b}{\Delta\nu_b} \right] \left[\frac{1}{0.5 - 0.25 \frac{B}{\Delta\nu_b} \left(1 - e^{\frac{-\Delta\nu b}{B}} \right)} \right] \tag{3.1}$$

At 5 Gbit/s with a laser of linewidth of 100 MHz and assuming a Brillouin bandwidth of 100 MHz, the threshold power is increased to 10 mW. The mean launch power of 35 mW entering the fibre in this experiment is clearly above this threshold. However, in equation 3.1 it has been assumed that modulation has resulted in a transform limited spectrum, if the source has a frequency chirp the threshold is increased further[69].

Figure 3.5a details the optical spectrum of the directly modulated DFB laser and Figure 3.5b the chirp measured on a time resolved 10 GHz scanning etalon[70]. The wavelength chirp was characterised as 15 GHz peak to peak resulting in a theoretical SBS threshold of 630 mW, assuming $\Delta\upsilon_b$ to be 100 MHz. Thus, spectral imperfections from the DFB laser ensured that stimulated Brillouin scattering effects were negligible and therefore did not cause system degradations. The threshold for stimulated Raman scattering as detailed in chapter 2 is significantly above powers of practical use and it may be concluded that inelastic scattering effects should not impair system performance in this case.

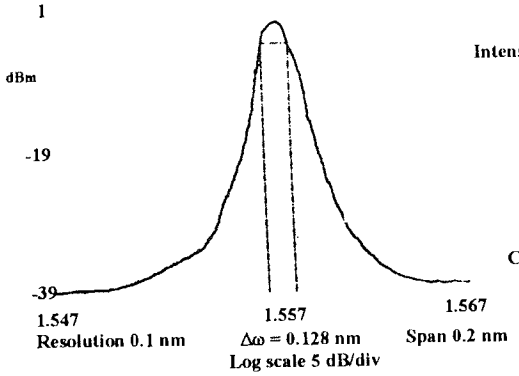

Figure 3.5a. Chirped spectrum from directly modulated DFB laser.

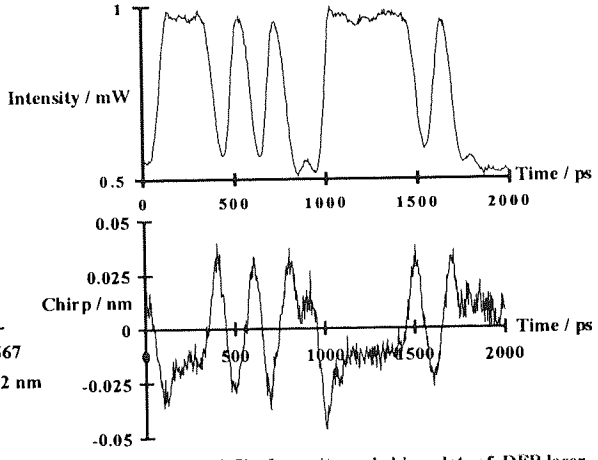

Figure 3.5b. Intensity and chirp plots of DFB laser.

Figure 3.5. Spectral and temporal characteristics of directly modulated DFB laser.

Whilst the large frequency chirp from the DFB helps to reduce SBS it places restrictions on the dispersion value of the fibre that the system may operate over. For this reason it is important for the DFB wavelength to be close to the fibre dispersion zero. In so doing any pulse broadening effects due to non-linear spectral enhancement, e.g. SPM, will also be minimised.

Figure 3.6 details the spectrum at the output of the 205 km of fibre measured on an analyser with a resolution of 0.1 nm. Compared to the spectrum at the fibre input, the deconvolved 3 dB width has increased by only 1.5 GHz.

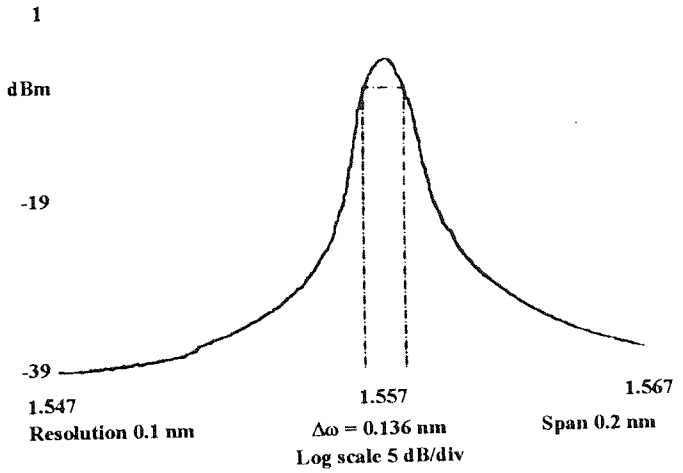

Figure 3.6. Optical spectrum at the output of 205 km of DSF used in the optically enhanced regenerator transmission experiments.

3.3.2 5 Gbit/s regenerator with optical pre and power amplifiers, results and discussion

Error free operation was possible to a distance of 500,000 km before the onset of the loop specific artefact introduced errors at the start of each recirculation precluding the measurement of meaningful BER's, see Appendix 1. The system margin was verified by introducing up to 3 dB of additional attenuation in front of the receiver per span whilst maintaining error free operation. Again adjusting the polarisation state of the signal at the output of the laser had no measurable effect on the error ratio. Extrapolating these results to oceanic distances indicates that considerable margin exists for degradation of each span in the system and this is important when component ageing effects are considered.

Over the transatlantic distance of 6,400 km only 31 repeater housings would be required, considerably less than that of any previous regenerative system that operate at much lower bit rates, for example TAT-9 has ~100 km repeater spacing (~64 repeater housings) and a bit rate of 591.2 Mbit/s. Further increases in repeater spacing could again be achieved with an optimised receiver and lower loss DSF. Also the margin of 7.5 dB may be reduced to around 4 dB giving a repeater spacing of ~260 km requiring only 25 regenerators to span the Atlantic ocean.

3.4 10 Gbit/s regenerator with optical pre and power amplifiers

To cater for the expected growth in demand for capacity it is necessary to increase the system line rate. The 5 Gbit/s regenerator was upgraded to 10 Gbit/s operation by increasing

the bandwidth of the receiver to 6 GHz, changing the PLL VCO for a 10 GHz device and by using a 15 GHz 1557 nm directly modulated DFB laser. Functionally the regenerator and the loop operation was identical to that detailed in the previous sections.

The electrical sensitivity of the receiver was measured as -17 dBm as would be expected from the 3 dB increase in noise bandwidth over the 5 Gbit/s configuration. With the same erbium pre amplifier as used in the previous section, sensitivity was improved to -30 dBm. To cater for the increased spectrum from the transmitter, both information bandwidth and chirp, the 1 nm filter in front of the receiver was replaced by a 6 nm component. Consequently, significantly more spontaneous-spontaneous beat noise was detected and thus impaired sensitivity. As a result of the reduced system power budget the repeater spacing was decreased to 160 km but margin maintained at 7.5 dB.

Error free operation was possible to a distance of 400,000 km before the onset of greatly increased phase noise on the recovered clock due to the loop specific artefact. Again meaningful BER measurements could not be made as a result of this effect, see Appendix 1. The number of regenerators and, therefore, retiming units traversed was ~2,500 almost identical to that of the 5 Gbit/s experiment at 2,440, as expected, see Appendix 1. Increases in repeater spacing could be achieved with an optimised receiver and lower loss fibre. Assuming a receiver sensitivity of - 36 dBm and fibre loss of 0.20 dB/km a distance of 237.5 km could be realised between regenerators with 4 dB of margin per span requiring only 27 repeaters across the Atlantic.

3.5 Conclusions

Error free operation of both 5 & 10 Gbit/s regenerators has been demonstrated over 500,000 and 400,000 km respectively. Further transmission was limited only by an experimental artefact and not 'real' system errors. Erbium doped fibre pre and power amplifiers allowed the repeater spacing to be increased to 205 km for the 5 Gbit/s experiment and 160 km for the 10 Gbit/s case, requiring only 31 and 40 regenerators respectively to span the Atlantic and 44/56 for the Pacific. The use of a directly modulated DFB laser resulted in significant wavelength chirp from the regenerator that increased the Brillouin threshold, and the use of DSF ensured that pulse distortion was maintained at a minimum. These results indicate that over oceanic distances considerable margin for degradation exists per span, ensuring a system of robust nature.

Future work could include the replacement of the erbium amplifiers with semiconductor devices of similar specification. This could greatly reduce the power

consumption and therefore enhance reliability whilst simultaneously reducing the size of the repeater housing. Ultimately it may be feasible to fabricate an optically amplified regenerator on a single substrate. By reducing the power feed, size and number of repeaters it may be possible to install more fibres in the cable for the same cost (whole life). This would then allow more capacity and calls to question the need for amplified systems.

Recently published results[71] indicate that 20 Gbit/s operation is possible with similar repeater spacing to that detailed here, however, to date only single pass experiments have been undertaken and without significant margin. Additionally, evaluation of the power dissipation of a practical regenerator could be undertaken as a step towards assessing the feasibility of system implementation.

Chapter 4

4. Ultra-long haul optically amplified NRZ systems

4.1 Introduction

Point to point optically amplified NRZ communications links spanning transoceanic and transcontinental distances with capacities of many Gbit/s are currently in the final design stages, for example, TAT 12/13 and TPC 5. To enable future system upgradability and increase reliability it is desirable to utilise the concept of the transparent optical pipe, in which the components of the link are limited to optical amplifiers and the transmission fibre itself. Since, the bandwidth of both EDFA's and communications fibre is immense it may be thought that systems comprising of only these components would be almost endlessly upgradable in capacity. Additionally, their apparent transparency immediately lends itself to multiplexing techniques, unlike regenerative systems. However, such links require very careful design since stringent requirements are placed on component parameters and tolerances. To ascertain the viability of the transparent optical pipe concept it is necessary to fully comprehend the accumulated effects of fibre dispersion, non-linearity and amplifier components and characteristics.

If the fibre is considered to be purely linear, good system performance is achieved by ensuring that the signal power is maintained significantly above the noise accumulated along the link, and that the total dispersion is not sufficient to induce a penalty from ISI[72]. Generally, the low loss 1550 nm operating window of dispersion shifted fibre will be used to simultaneously minimise the required gain, and hence ASE generated, and ISI. However, amplifier components introduce polarisation effects that can further deteriorate system performance. Isolators, wavelength division multiplexers and couplers all exhibit a small degree of PDL (~0.1 dB / amplifier) resulting in a SNR at their output that is dependent on the input signal SOP. The erbium fibre, through polarisation dependent gain, provides greater gain to noise components orthogonal to the signal than the signal itself[73]. Over a link of many amplifiers these effects accumulate and can significantly deteriorate the system performance through a greatly impaired SNR[74]. Additionally, polarisation mode dispersion from both the

transmission fibre and amplifier components can result in pulse distortion and ISI[75]. These polarisation effects will vary with time as the signal SOP evolves over the Poincare sphere, resulting in system fades and a time dependent BER[76].

Moreover, the transmission medium in systems of this length can no longer be regarded as purely linear. The weak dependence of the refractive index on the intensity of the signal leads to FWM, and the related phenomena of SPM and XPM. Each of these effects may introduce significant spectral broadening that can cause catastrophic pulse distortion when allied with fibre dispersion[77]. Consequently, the interplay of non-linearity and dispersion greatly complicates system design. Non-linearity is a function of optical power, section length and the number of amplifiers in the link[78]. This imposes an upper limit on the system power level and, therefore, output SNR. For a given path average power the effective non-linearity increases with section length, and optimum performance is obtained with short amplifier spacing, however, from an economics and reliability view point this is undesirable.

In this chapter the effects of fibre and amplifier parameters will be investigated on long haul NRZ system performance. The accumulation of amplifier noise will be determined analytically and the non-linear impairments modelled qualitatively and by numerical modelling, in both cases the results are complemented with extensive experimental results obtained from recirculating loops.

4.2 Linear effects

In order to ascertain a meaningful appreciation of the accumulated effects of ASE and polarisation issues, it is necessary to ensure that the system under question is not dominated by non-linear impairments. Analytically and numerically this is achieved by modelling the system in the linear regime only and greatly simplifies matters. Experimentally, it necessitates a sound understanding of non-linear transmission systems so that their detrimental effects can be minimised. In the discussion that follows it will be assumed that the experimental results are limited by purely linear issues. The techniques for achieving this will be discussed in section 4.3.

4.2.1 Amplifier noise and PDL, theoretical analysis

If non-linear effects are ignored, pulse distortion is minimised by operating a system on the overall dispersion zero. The performance of the system is then governed by the SNR and equation 2.29 can be used to determine the SNR at any point along a system, and the BER

calculated. However, in deriving this equation it has been assumed that the loss and gain in each section are the same for both polarisation states. In practice each amplifier component exhibits some degree of PDL, and consequently, the signal output power varies to a small extent with input polarisation state. In a noiseless system the effect would be a variation in output power with time as the polarisation of the signal evolved. When noise is considered the deleterious effect is compounded, since, there is always a noise component in the low loss polarisation state. It is highly unlikely that the signal will propagate through the low loss state of every component, thus, some of the noise becomes preferentially amplified, reducing SNR[79].

Worst case performance is obtained when the signal receives the lowest gain from every amplifier, whereas the best performance occurs when the signal receives the highest gain. In general the signal gain will lie between these two values.

In attempting to model this effect it is convenient to assume that the signal experiences the highest loss in each PDL element and, hence, the lowest amplifier gain. In so doing the worst possible performance of the system will be considered. The amplifier PDL will have the effect of increasing the noise in the high gain state, while decreasing noise polarised in the low gain state. The spontaneous noise in the following amplifiers will therefore receive a gain approaching the maximum value while the signal receives the minimum. There are three components to consider: the signal, the noise in the high loss state and the noise in the low loss state. Assuming that the amplifiers are operating with fixed total output power control:

Signal power at the i^{th} amplifier $$S_i = Lg_i S_{i-1} \quad (4.1)$$

Noise in low gain state at the i^{th} amplifier $$n_{si} = Lg_i n_{si-1} + k \quad (4.2)$$

Noise in high gain state at the i^{th} amplifier $$n_{pi} = L' g_i n_{pi-1} + k \quad (4.3)$$

Noise power generated by amplifier in one polarisation state $$k = n_{sp}(g_i - 1)\delta f . hc / \lambda \quad (4.4)$$

Saturation $$N = n_{si} + n_{pi} + S_i \quad (4.5)$$

Where,

L loss in high loss state

L' loss in low loss state

g gain of amplifier

n_{sp} amplifier population inversion parameter

δf bandwidth over which the noise is measured

N amplifier saturated output power

The difference between L and L' represents the PDL in each amplifier. As the signal power decreases the gain of the amplifier increases to ensure that the output power remains constant. Given the initial conditions; S_0 = input signal power, $n_{S0} = 0$ and $n_{P0} = 0$ it is possible to use the above equations in an iterative process to calculate the evolution of signal and noise powers. Figure 4.1 illustrates the reduction in signal power over 200 amplifiers for the parameters used in the experiment described in section 4.2.2. i.e. $g_0 = 15$ dB, N = 6 dBm, $n_{sp} = 2.23$, optical bandwidth $\delta f = 6$ nm and $\lambda = 1555$ nm. The PDL values used range from 0 to 0.25 dB per amplifier.

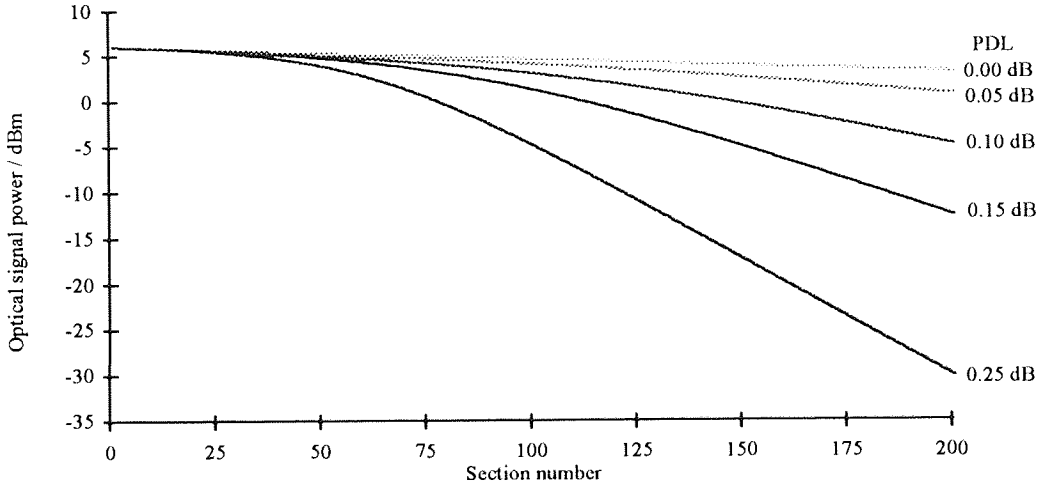

Figure 4.1. Theoretical signal power vs. section number as a function of PDL.

With zero PDL the result is the same as that predicted by equation 2.29. However, as the PDL increases the signal power drops at the expense of increased noise in the orthogonal polarisation state. Figure 4.2 details the evolution of the signal and noise powers for a PDL = 0.15 dB per section.

After ~90 sections the noise power is greater than the signal power, and after ~120 sections the noise in the low loss state is within 1 dB of the saturated output power of the amplifier. Perhaps of more importance is the detected BER obtained from such a system. To calculate the BER it is necessary to determine the spontaneous-spontaneous beat noise variance from both polarisation states and also the signal-spontaneous beat noise variance[80]. The detected SNR is then the signal variance/total noise variance*electrical bandwidth. Figure 4.3 shows the calculated BER against distance for 2.5 Gbit/s operation (electrical bandwidth 1.7 GHz) and a range of PDL values.

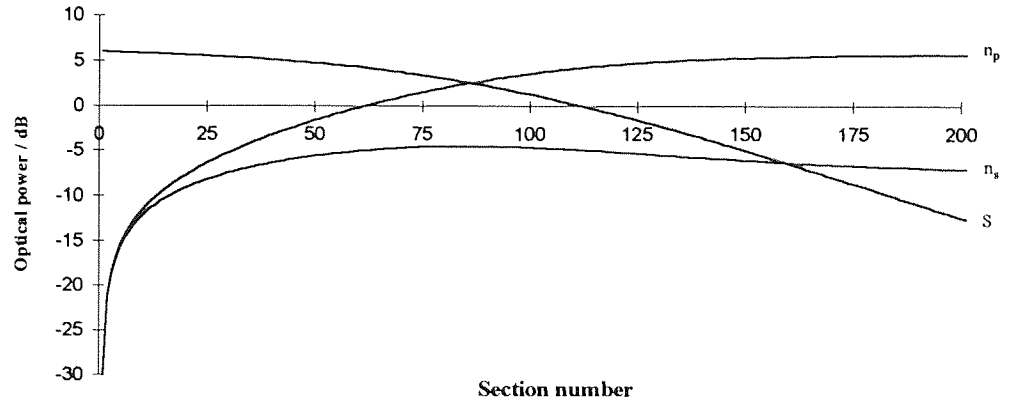

Figure 4.2 Evolution of signal and noise powers for a PDL of 0.15 dB per span.

For a system in which the signal experiences a mean PDL of 0.25 dB per section a $1x10^{-9}$ error ratio is achieved after only ~75 amplifiers. Whereas, for a system with zero PDL the same performance is possible to in excess of 300 spans. Clearly, system performance is strongly dependent on the mean value of PDL, and places very stringent requirements on the components used in the transmission path. It is also worth noting that by aligning the signal to the lowest loss polarisation state the noise in the high loss state suffers greater attenuation. Thus, the total noise build up is less than that from a system with zero PDL. Consequently, performance is improved and for the case of PDL = 0.3 dB per section a BER of $1x10^{-9}$ is obtained after ~500 amplifiers.

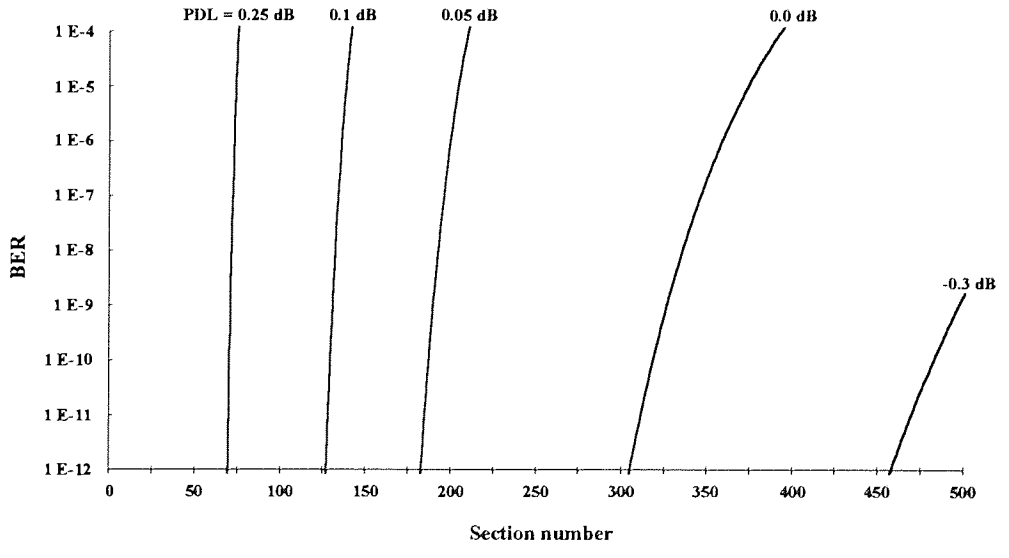

Figure 4.3. BER vs. section number as a function of PDL

From figure 4.2 it can be seen that noise in the low loss polarisation state, orthogonal to the signal, dominates after transmission. On detection the major noise source is the spontaneous-spontaneous beat noise from this polarisation state. By utilising a polariser at the receiver it is possible to remove this noise component from the detection process and improve the SNR. Figure 4.4 shows the improvement achieved by using this technique for the case of PDL = 0.125 dB per section. The transmission distance for which a BER of $1x10^{-9}$ is incurred is increased in excess of 50%.

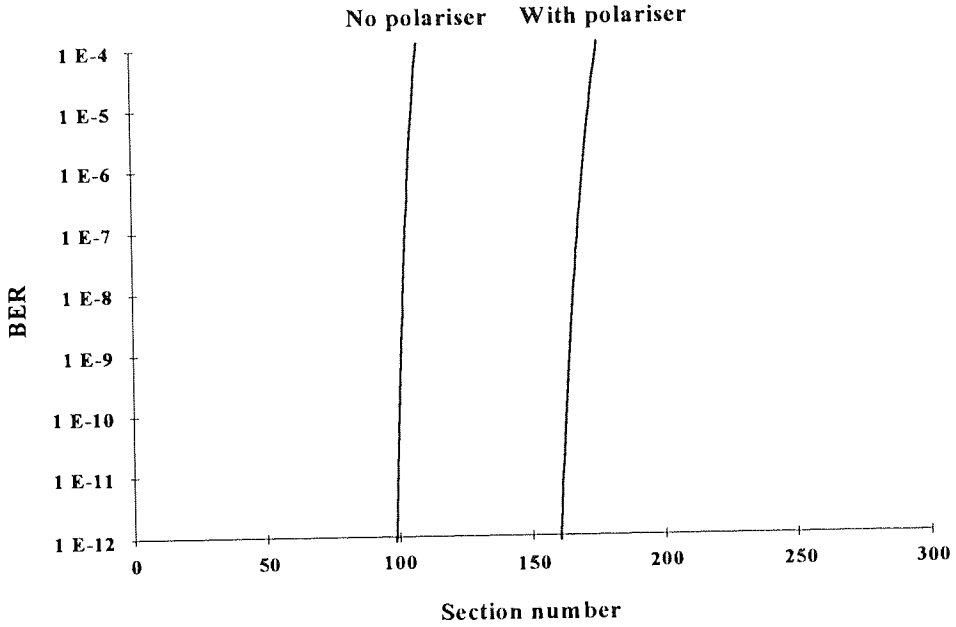

Figure 4.4. Improvement in BER by removing orthogonal noise in a system where the signal lies in the high loss polarisation state.

4.2.2 Amplifier noise and PDL, experimental measurements and comparison with theory

To experimentally determine the effect of ASE and PDL on system performance a single amplifier recirculating loop was constructed and is detailed in figure 4.5. The loop consisted of a contra-directionally pumped EDFA with a saturated output power of 6 dBm, noise figure of 6.5 dB and a gain of 15 dB. An optical isolator with low PMD and PDL ensured unidirectional operation and a 6 nm bandpass filter centred at 1555.5 nm selected the wavelength of operation. The transmission medium consisted of 40 km of fibre with a path average dispersion zero at the operating wavelength. A 3 dB fused fibre coupler allowed data input and output, and a polarisation controller enabled the mean PDL incurred by the signal to be adjusted.

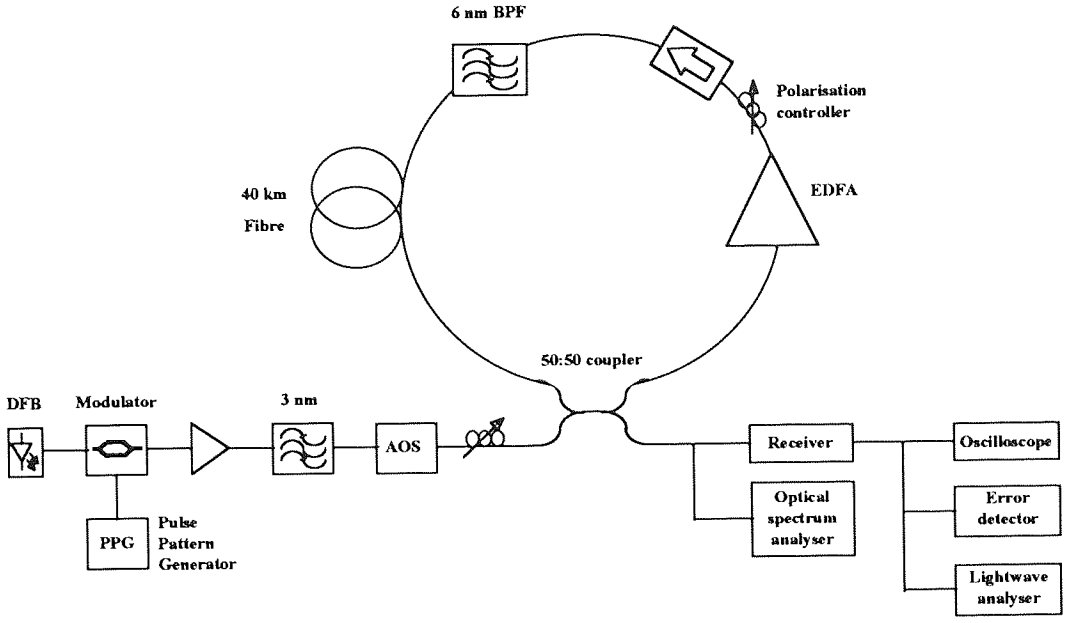

Figure 4.5. Recirculating loop configuration for 2.5 Gbit/s NRZ results.

Data at 2.5 Gbit/s was injected into the loop from a transmitter consisting of a cw DFB laser and a $LiNbO_3$ intensity modulator. An acousto-optic switch gated data into the loop for a period equal to the round trip transit time and a polarisation controller enabled the launched data to be aligned with the recirculating signal. The mean value of signal PDL was adjustable via the two polarisation controllers up to a maximum of 0.3 dB per recirculation.

Figure 4.6a shows the evolution of signal power measured on a H.P. lightwave analyser for four values of PDL. The analyser was set to 0 Hz span and a centre frequency of 19.685 MHz, this being the lowest frequency component in the 2^7-1 PRBS data pattern (2.5 GHz/127). Additionally, higher frequency components were monitored to ensure that fibre effects were not affecting the results, e.g. PMD.

To enable comparison with the experiment figure 4.6b details the evolution of signal power predicted using the theory described in the previous section. It can be seen that the two plots are in excellent agreement, the only minor discrepancy is when the signal is aligned to the low loss state of the loop, (-0.3 dB). In this instance it is highly probable that due to the sustained level of the signal over a very long distance fibre non-linear effects are extracting some power in the experiment. However, it was possible to obtain a BER of $1x10^{-9}$ to 20,000 km and this is in exact agreement with that calculated and illustrated in figure 4.3.

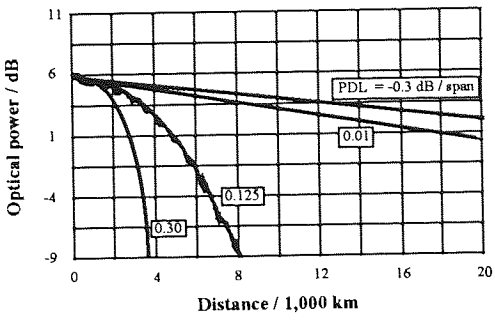

Fig. 4.6a. Experimental

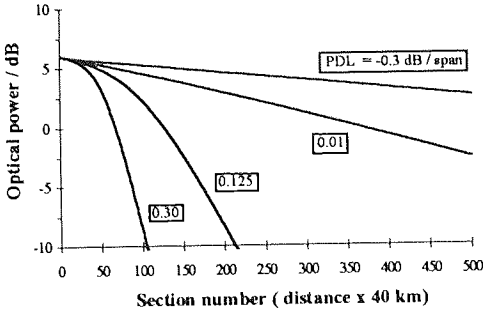

Fig. 4.6b. Theoretical

Figure 4.6. Experimental and theoretical signal power evolution with distance and PDL

For a PDL of 0.01 dB per span this error ratio was achievable to a distance of 15,000 km and for 0.125 dB per span to 4,500 km. Both results are in excellent agreement with theory (figure 4.3). By aligning a polariser to the signal at the receiver it was possible to improve system performance to better than $1x10^{-9}$ BER at 6,000 km for a PDL of 0.125 dB. Again this agrees with that calculated and detailed in figure 4.4. The error ratios measured at 6,000 km are illustrated in figure 4.7.

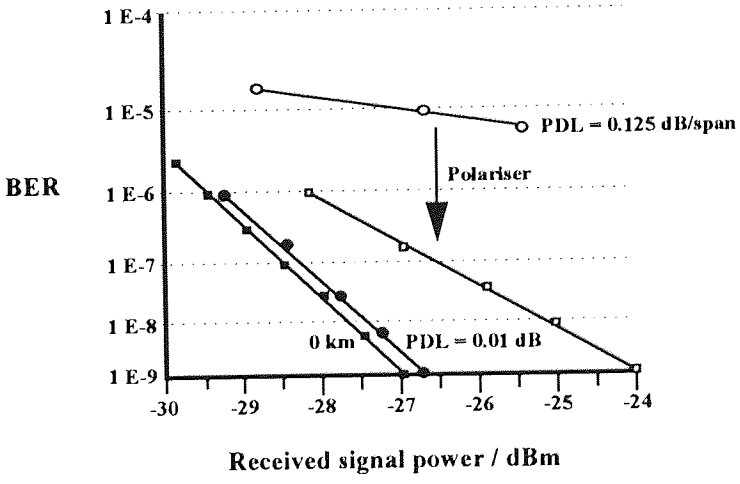

Figure 4.7. System performance at 6,000 km with and without a polariser compensator.

Without a polariser the spontaneous-spontaneous beat noise orthogonal to the signal dominates and results in an error floor at ~$1x10^{-5}$. When this component is removed with a polariser a 3 dB penalty is incurred over the back to back sensitivity at $1x10^{-9}$ BER. For a PDL of 0.01 dB the penalty is only 0.25 dB since the signal has not suffered as much

attenuation. Whilst the use of a polariser has allowed greatly improved error ratios, it is far from an ideal solution. On a practical system an active polarisation controller would be required prior to the polariser to track the signal SOP. Moreover, noise from only one polarisation state is blocked, thus, the SNR of the co-polarised radiation is not improved. Since, the signal power has diminished due to excess attenuation system performance is reduced by the effects of PDL.

4.2.3 Polarisation dependent gain and hole burning

In addition to the issues concerning PDL, long haul EDFA systems suffer from the deleterious effects of polarisation dependent gain[81], PDG, and polarisation hole-burning[82], PHB, in the erbium fibre. Both effects are a result of anisotropy of the erbium ion susceptibility. The erbium ions in the glass host are characterised by a randomly orientated ellipsoid, the shape of which is determined by the strength and alignment of the local field. The excited ions with a major axis of the ellipsoid collinear with that of an incident linearly polarised signal are preferentially stimulated to emit photons. Consequently, in a gain saturated amplifier the gain is slightly lower in the plane of the signal relative to that orthogonal to it and polarisation hole-burning, PHB, occurs. PDG is a related effect that causes higher gain to signals aligned with the linearly polarised pump. As such it behaves like PDL, since co-polarised signals receive preferential gain and improve system performance, whereas, orthogonal signals suffer a reduced gain, resulting in worse SNR. Thus, the mean value for both PDL and PDG over a long link is zero, and it is the variance that is of interest. The effect of PDG may be eradicated by scrambling the pump polarisation to ensure that there is no preferred gain state. PHB, however, is a more serious system impairment since the polarisation state orthogonal to the signal always receives preferential gain. Consequently, it has a non zero mean and always reduces system performance. In order to nullify this effect it is necessary to arrange for equal signal powers to be established in both polarisation states of the erbium fibre. Generally, this is achieved by rotating the signal state of polarisation at a rate greater than the erbium lifetime[83].

The effect of PDG and PHB on system performance can be modelled in a similar way to that described for PDL in section 4.2.1:

Signal power at the i^{th} amplifier $$S_i = Lg_iS_{i-1} \tag{4.6}$$

Noise in low gain state at the i^{th} amplifier $$n_{si} = Lg_in_{si-1} + n_{sp}(g_i - 1)\delta f.hc/\lambda \tag{4.7}$$

Noise in high gain state at the i^{th} amplifier $$n_{pi} = L\alpha g_in_{pi-1} + n_{sp}(\alpha g_i - 1)\delta f.hc/\lambda \tag{4.8}$$

$$N = n_{si} + n_{pi} + S_i \tag{4.9}$$

Where α represents the degree of polarisation sensitivity of the gain of the amplifier.

Figure 4.8 provides a plot of the effect of PDG and PHB on signal power as a function of the number of amplifiers and the degree of polarisation dependence. It can be seen that the effect is almost identical to that caused by PDL plotted in figure 4.1

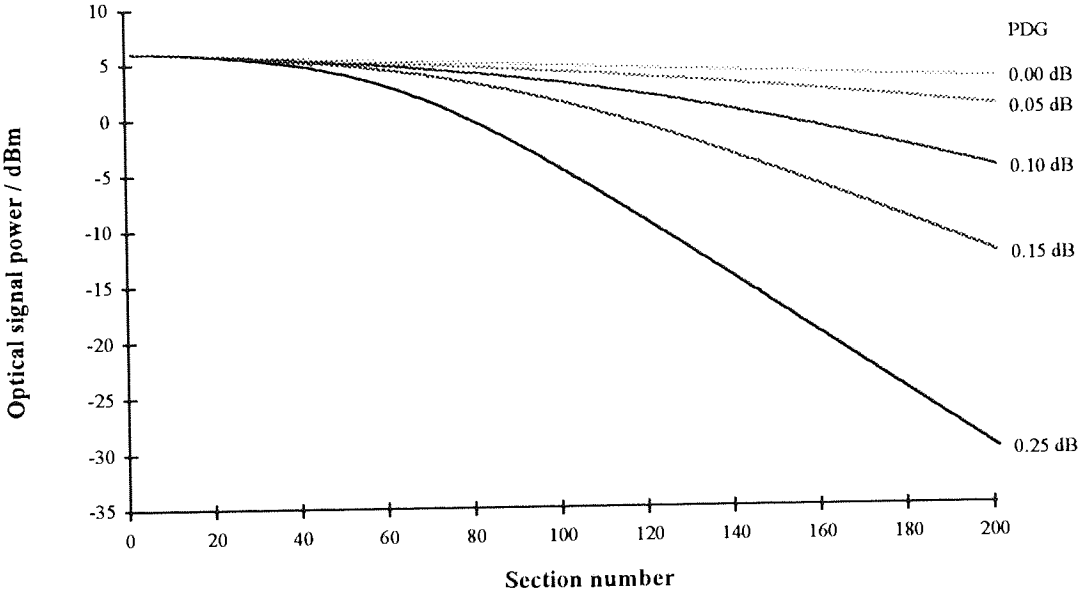

Figure 4.8. Theoretical signal power vs. section number as a function of PDG.

4.2.4 Polarisation scrambling

From the results obtained in the previous sections it is clear that PDL, PDG and PHB can cause severe system impairments on long haul EDFA links. It was also indicated that the erbium effects can be greatly reduced by rotating the polarisation state of the signal at a rate in excess of the erbium lifetime, ~10 ms. Consequently, polarisation scramblers have been constructed that operate at frequencies of a few kHz[84]. However, when these devices are used on systems containing elements with PDL they sweep through both the maximum and minimum loss at the rate of scrambling. This results in the signal attaining an amplitude modulation. This may be suppressed by scrambling at a frequency that is filtered by the concatenated response of the erbium amplifier chain e.g. ~2.5 kHz. Complete suppression of the a.m. is very difficult and, thus, these scramblers offer only minor improvement to system performance. An alternative approach is to scramble the signal at a frequency that is above

the line rate[85]. In so doing each bit sweeps through the entire range of PDL values, ensuring that the worst case performance is not obtained for any bit. Thus, high speed polarisation scrambling offers the advantage of reducing the effect of PDL in addition to PDG and PHB.

Previously, high speed polarisation scramblers have been realised with fast $LiNbO_3$ phase modulators. The signal is impressed into the modulator with a linear polarisation at 45° to the principal axis of the crystal. These devices need to be driven by high speed, high power RF amplifiers which are both costly and a reliability issue as indeed is the modulator itself. Figure 4.9 details a novel alternative approach to high speed polarisation scrambling.

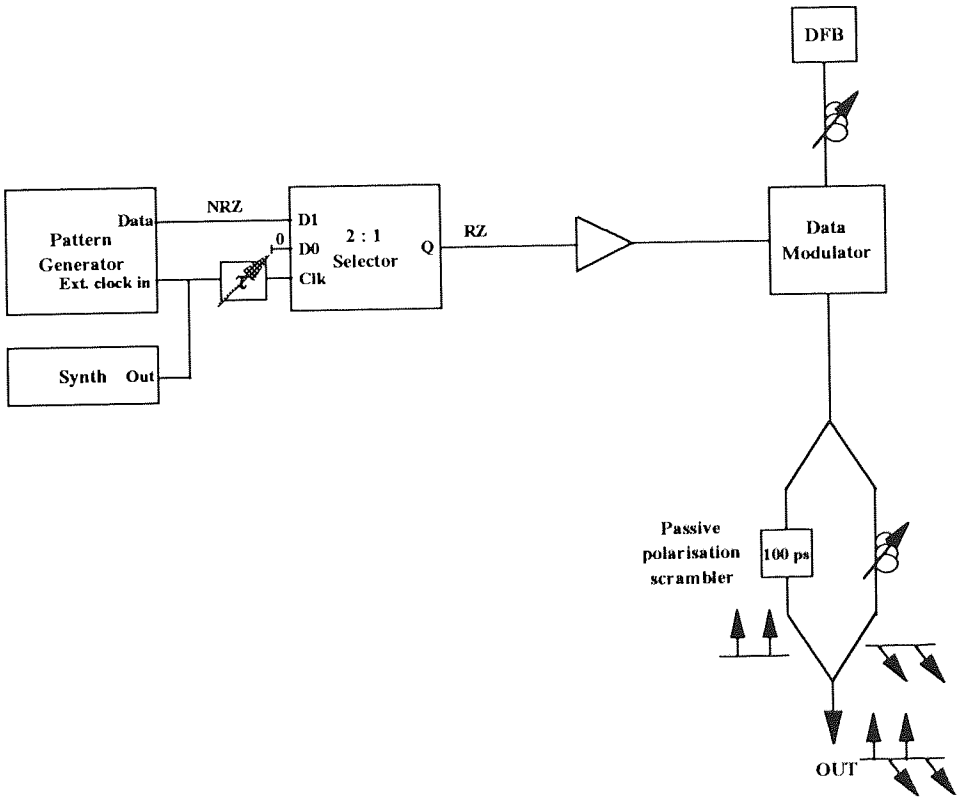

Figure 4.9. High speed passive polarisation scrambler.

Optically the scrambler is passive and only a commercial high speed 2:1 selector chip is required in addition to the normal NRZ transmitter electronics. RZ data with a FWHM of half the bit period (in this case 100 ps) is generated by the 2:1 selector and impressed upon the data modulator. The resultant optical signal is split and the two halves recombined with one half delayed by 100 ps and in orthogonal polarisation state relative to the other half. The prototype scrambler was constructed using fused fibre couplers, a fibre delay and polarisation controller and was thus susceptible to environmental changes. However, the technique is

ideally suited to planar silicon integration, which would ensure long term stability. Figure 4.10a shows the resultant eye diagram at 5 Gbit/s detected on a 32 GHz *pin*. It can be seen that there is some distortion to the eye where the orthogonal pulses overlap (falling edge of one pulse overlapping with leading edge of the next pulse due to finite and differing rise/fall times). It is imperative that the two pulse trains are orthogonal since any overlap in the same polarisation state will interfere. Figure 4.10b details the eye when band-limited to 3 GHz and shows that the distortions detected by the high speed *pin* are filtered by the equalised receiver.

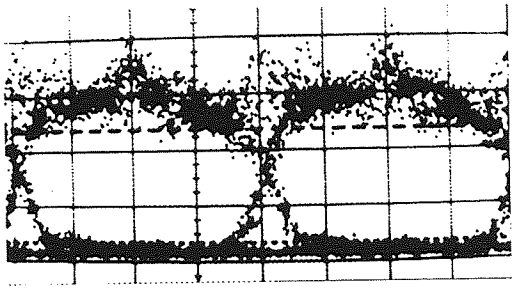

Fig. 4.10a. Eye detected on 32 GHz *pin*

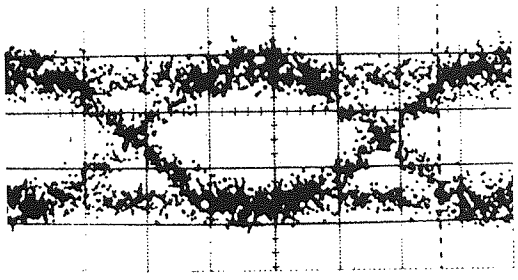

Fig. 4.10b. 3 GHz bandlimited eye

Figure 4.10. Eye diagrams from passive high speed polarisation scrambler.

Recirculating loops are not the ideal test facility for low speed polarisation scramblers. Each loop amplifier is liable to see random signal state of polarisation from one recirculation to the next. Consequently, there is an inherent scrambling effect with frequency dependent upon the reciprocal of the loop transit time. The effectiveness of scrambling will vary with time since the rate of polarisation change is random, or temperature driven, not systematic as would be expected from a modulator. Thus, when low speed scramblers are used in a recirculating loop very little benefit is observed. However, loops can be used to measure the effectiveness of high speed scramblers.

A recirculating loop was constructed to assess the passive scrambler. To accurately simulate TAT 12/13 a filter was not included in the transmission path and, thus, it was necessary to ensure that the gain peak of the amplifiers accurately matched the dispersion map. With the components available the dispersion zero of the 45 km spans of fibre was too close to the amplifier's gain peak and, therefore operating wavelength. This resulted in enhanced four wave mixing and associated spectral broadening, see section 4.3. Consequently, system performance was significantly impaired.

Figure 4.11 details the variation in Q at 6,300 km at the TAT 12 line rate of 5 Gbit/s over a ~2 hour period.

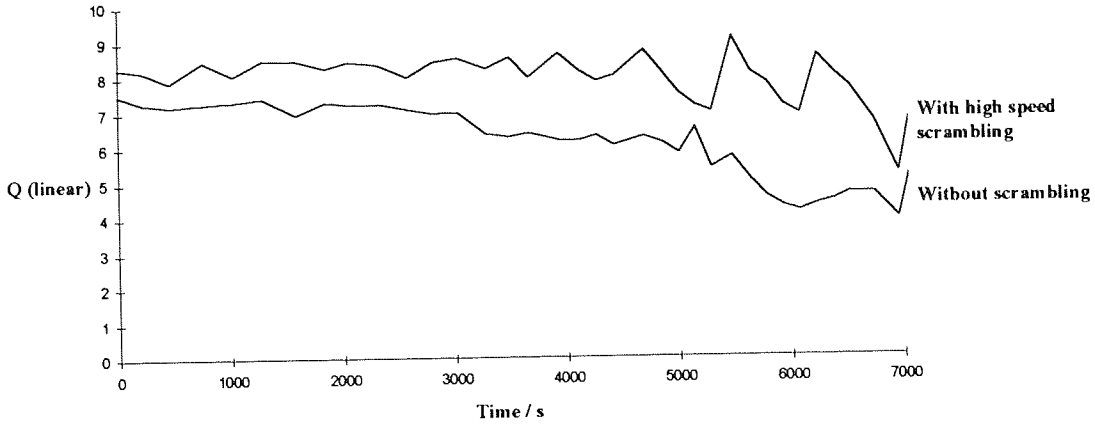

Figure 4.11. Q variation with time, with and without high speed polarisation scrambling.

The mean Q was 6.6 and the standard deviation was 1.0. From this graph it is readily apparent that system performance is variable with time due to the evolution of signal state of polarisation. Also plotted on Fig. 411 are the results obtained with the passive high speed scrambler. The mean Q is much improved at 8.03 and the standard deviation reduced to 0.361. Clearly, there is a significant improvement in system performance and further tests need to be undertaken on a more optimised transmission path.

4.2.4.1. Alternative implementations of the high speed passive polarisation scrambler

RZ data in the original proposal for the passive polarisation scrambler was derived by a high speed 2:1 selector. In practice alternate optical sources may prove to be a more desirable option. Mode locked lasers[86] and gain switched DFBs[87] are frequently used to generate RZ pulses for soliton transmission. They can generate short pulses (5 - 50 ps) that may be subsequently modulated with data prior to the polarisation scrambler. Additionally, electro-absorption modulators[88], EAM, can be used to externally modulate a DFB with either NRZ or RZ data dependent on the characteristics of the electrical drive. Indeed it is possible to utilise an EAM to generate the RZ pulses and also superimpose the data at the same time[89]. This approach may well turn out to be the most practical due to the reduction in the component count (no 2:1 selector).

High birefringence fibre (hi-bi fibre) is designed to have a large differential group delay, DGD, (~1 ps/m). It can be used to realise the optical delay and scramble the polarisation simultaneously as detailed in figure 4.12.

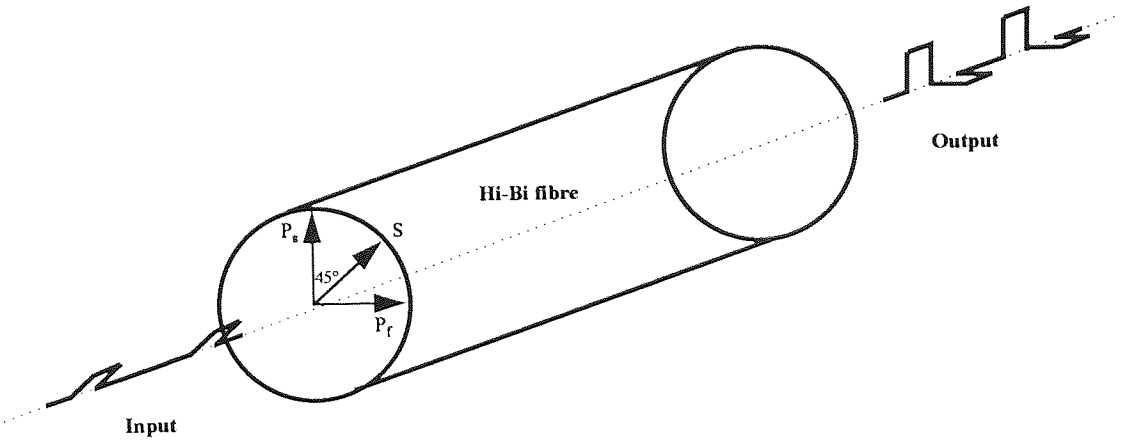

Figure 4.12. Alternate realisation of passive high speed polarisation scrambler using high birefringence fibre.

The RZ data signal is impressed into the hi-bi fibre in a linear state of polarisation at 45° to the principal axes. The signal contains equal power in both the fast axis, P_f and the slow axis, P_s. The length of the hi-bi fibre is arranged such that the total DGD is equal to the required delay (half a bit period). This configuration avoids the problems associated with the interferometric technique in terms of stability and obviates the use of planar silicon technology.

4.2.5 Polarisation Mode Dispersion

The two degenerate orthogonal modes in single mode optical fibre propagate with very slightly different velocities[90]. Consequently, a signal with power in both modes experiences a differential group delay (DGD) that results in pulse broadening. Random changes in the environment of a fibre cause variations to the temperature and stress that the fibre experiences[91,92]. Thus, the DGD becomes a randomly varying function of time, generally described by Maxwellian statistics[93], and the state of polarisation at any point along the fibre will also vary randomly with time.

If a length of fibre produces a spread in arrival times of ΔT, the statistical nature of the PMD suggests that the expected spread in arrival times after N such lengths would be $\Delta T\sqrt{N}$. However, the greatest system impairments will occur when the DGD drifts into the tail of the Maxwellian distribution and when the principal states are occupied with the equal power. Thus, it is the performance of the system under these conditions that is of most interest. The ability to accurately control the state of polarisation in a recirculating loop[94,95] enables the worst case scenarios for PMD to be easily investigated and the system

performance under these conditions ascertained. Figure 4.13 details the loop used to conduct such an experiment.

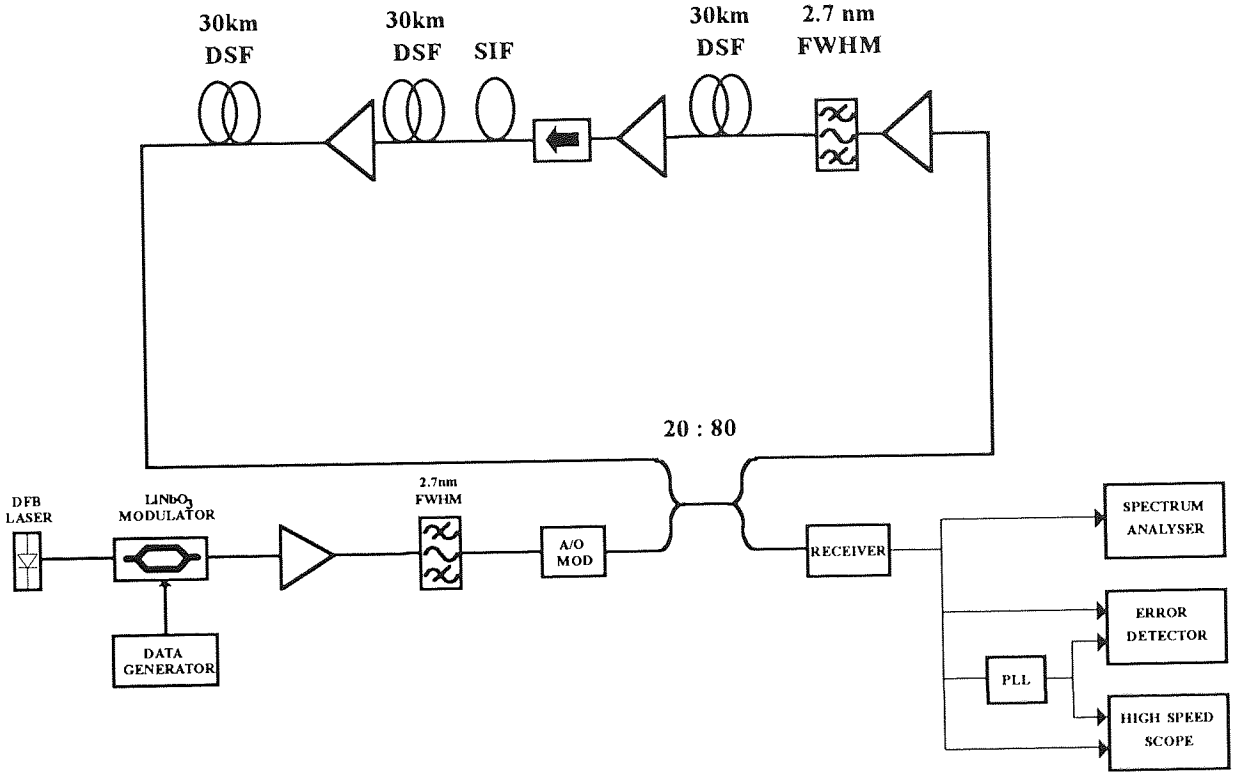

Figure 4.13. Recirculating loop arrangement used in PMD experiment.

In order to improve the noise performance of the system over that illustrated in figure 4.5 a 20 : 80 coupler was used with a loss of 1 dB to recirculating data. Additionally, the loss of the isolator, filter and coupler were shared between the three amplifiers resulting in ~1 dB per section of excess loss over that of the fibre.

When the signal state of polarisation was adjusted to simultaneously minimise the effects of PDL and PMD an error ratio of $1x10^{-9}$ was achieved to a distance of 17,600 km for a 5 Gbit/s 2^7-1 PRBS data pattern and the received pulse train showed no degradation due to pulse distortion as illustrated in figure 4.14.

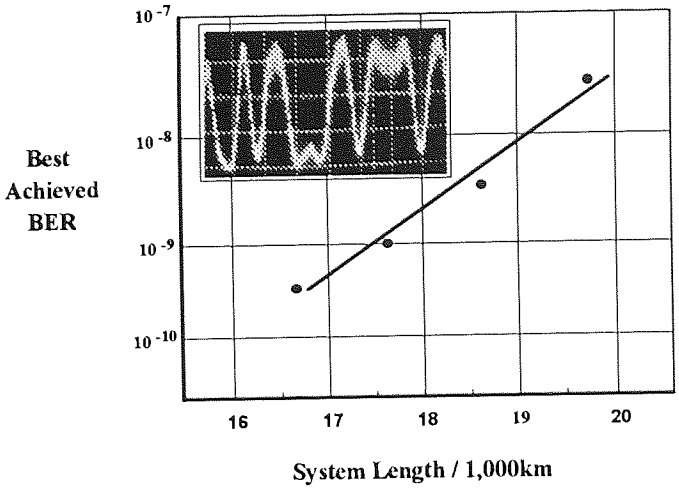

Figure 4.14. BER vs. distance at 5 Gbit/s, inset 17,600 km pulse pattern.

The loop polarisation controllers were then configured such that the PMD of the fibre, 0.032 ps/km, was encountered by the signal on every recirculation and that the principal states contained equal power. This resulted in signal cancellation of the 10 GHz component of the two polarisation states every 3,140 km and this is shown figure 4.15. Under these conditions an error floor of $>1x10^{-4}$ was incurred at 6,000 km and figure 4.16 details the received pulse pattern.

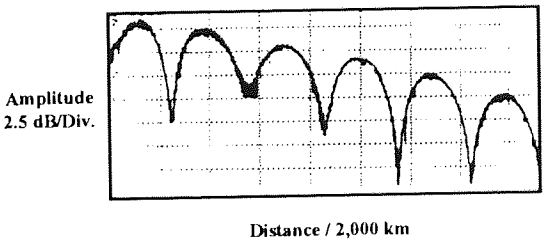

Figure 4.15. Evolution of 10 GHz component

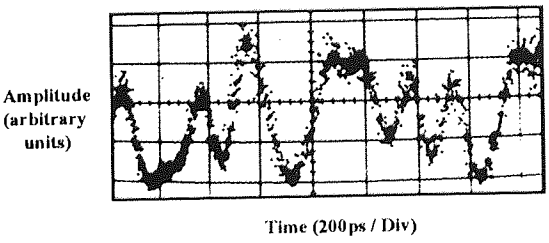

Figure 4.16. Pulse pattern at 6,000 km.

Since the loop configuration enables the signal to encounter the same PMD on every recirculation the accumulation of DGD grows with N rather than $\sqrt{N}$ expected in an uncontrolled system. Consequently, in this case the PMD is expressed in ps/km. The pulse broadening incurred is therefore, 6000 x 0.032 = 192 ps. Assuming Gaussian statistics this results in an expected pulse width of $(200^2 + 192^2)^{½} = 277$ ps, which is in excellent agreement with that measured experimentally. Whilst this represents a worst case scenario, the long term evolution of system polarisation for such an amplified link is likely to ensure that PMD penalties similar to this are incurred at some time.

4.3 Non-linear effects

From the previous section it is clear that optically amplified NRZ systems can suffer greatly impaired performance from polarisation effects. To maintain acceptable system performance it is necessary to utilise state of the art components in the transmission line, and also to perform some form of scrambling at the transmitter. In addition to these detrimental effects non-linearity can also cause severe pulse distortion resulting in very poor system performance. In this section the effects of various non-linear phenomena on optically amplified NRZ systems will be discussed and experimentally investigated.

4.3.1 Self phase modulation (SPM)

Self phase modulation results from the intensity dependence of the refractive index of the fibre. As the signal power increases, the refractive index also increases, and thus the instantaneous phase of the pulse is varied. The magnitude of this phase shift can be determined from equation 2.8. Since, a rate of change of phase is equivalent to frequency, spectral broadening occurs when the signal power varies, e.g. the rising and falling edges of NRZ pulses. If dispersion is ignored this may not adversely affect system performance, since, all wavelengths propagate at the same velocity. However, in a dispersive regime, the new frequencies generated will propagate at different velocities, and consequently, arrive at the receiver at different times. Thus, the detected pulse shape will be different from that transmitted[96,97,98]. On the rising edge of the pulse SPM results in a red shift and the falling edge a blue shift. In normal dispersion the red shifted leading edge propagates with higher velocity than the rest of the pulse, and the blue shifted trailing edge with lower velocity[99]. Thus pulse broadening results and can severely limit system performance. In anomalous dispersion the red shifted leading edge propagates more slowly and the blue shifted trailing edge more quickly, consequently pulse compression can result. Equation 4.10 can be used to calculate the broadening suffered by initially unchirped Gaussian pulses on propagation[100].

$$b = \left[1 \pm \sqrt{2}\phi_{max}\frac{z}{L_D} + \left(1 + \frac{4}{3\sqrt{3}}\phi_{max}^{2}\right)\frac{z^2}{L_D^{2}} \right]^{0.5} \qquad (4.10)$$

Where, L_D is the dispersion length; $L_D = \frac{To^2}{|\beta_2|}$ (4.11)

To is the Gaussian pulse width and β_2 the GVD parameter.

and $\phi_{max} = \gamma P_o Z_{eff}$ (4.12)

The sign in front of the second term in equation 4.10 determines whether the dispersion is normal (+) or anomalous (-). To obtain an approximate expression for the broadening incurred along a many amplifier link the effective length, z_{eff}, needs to be scaled with z/z_o, where z_o is the repeater spacing. Figure 4.17 details the broadening with distance for both normal and anomalous dispersive regimes and also for the case of no SPM. The parameters used are taken from one of the experiments described in section 4.4: D=1 ps/nm/km, z_o=40 km, bit rate = 2.5 Gbit/s, pulse rise time=fall time =0.25 bit period, λ=1550 nm, $n_2 = 3.2\text{x}10^{-20}$ m/W, A_{eff}=50 μm^2.

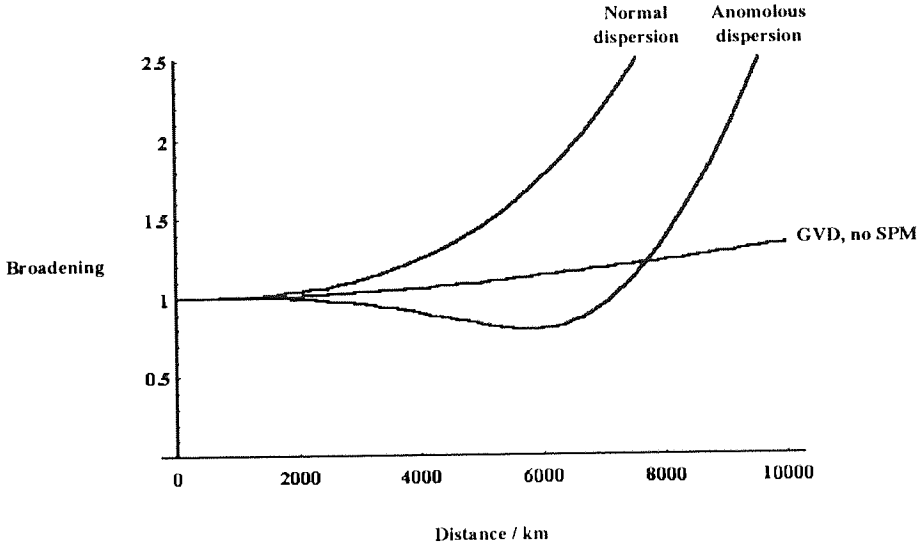

Figure 4.17. Variation in pulse width with propagation distance due to GVD and SPM.

With zero SPM, dispersion results in pulse broadening with distance due to the spectral width of the information signal. Ultimately this will lead to inter-symbol-interference and result in errors. In normal dispersion the effects of SPM induce broadening at much shorter distances due to the sign of the non-linear chirp. However, in the anomalous regime the effects of SPM chirp and dispersion are opposite and initial pulse compression results[101]. Ultimately the enhanced spectrum is sufficient to induce broadening with dispersion.

To obtain an indication as to the validity of this equation it is used to model some early work conducted prior to the registration of this PhD[102]. Experimentally 400 ps pulses were injected into a recirculating loop and their pulse width measured against distance for various powers. In this simple experiment the loop gain was 0.996 and therefore power was

lost on transmission, this effect is taken into account in the model. Figure 4.18 reproduces the experimental results and also those predicted by the model for an anomalous dispersion of 1.7 ps/nm/km.

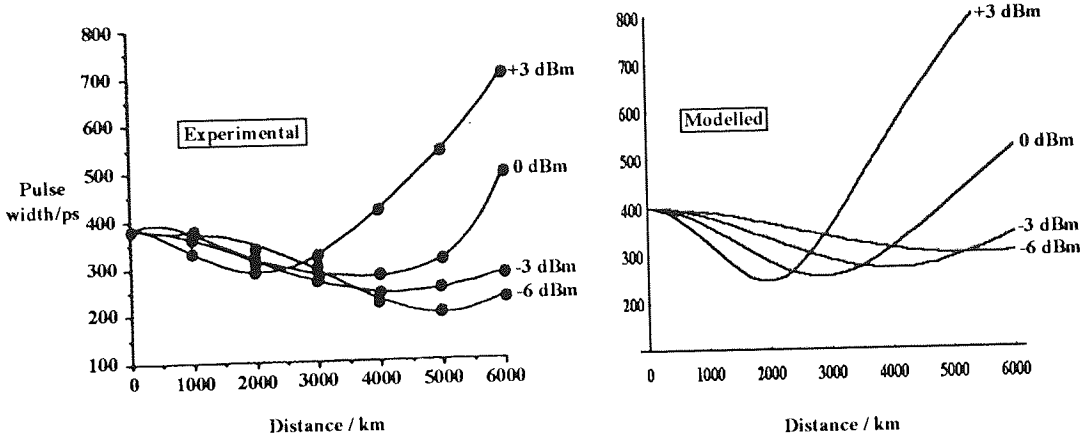

Figure 4.18. Experimental and theoretical results for pulse width evolution with power.

It can be seen that the two plots are in good agreement, indicating that this simple model may be useful for obtaining an insight into transmission performance of systems limited by GVD and SPM. If it is assumed that the maximum distance that error free data can be transmitted is that which allows restoration of the pulse width, it can be shown from equation 4.10 that:

$$z_{max} = 0.806 L_D \tag{4.13}$$

and that the required peak power to achieve this is:

$$P_{max} = \frac{1.139}{\gamma z_{eff}} \tag{4.14}$$

Thus, the longest distance that can be propagated before broadening occurs is $0.806L_D$, however, to ensure that the received data is error free the signal to noise ratio must also be adequate.

Figure 4.19 illustrates the power required to restore the pulse width at any given distance and also that to provide 3 dB of margin over the BER = $1x10^{-9}$ point due to SNR. The parameters are the same as those used previously with an amplifier of noise figure 6.5 dB

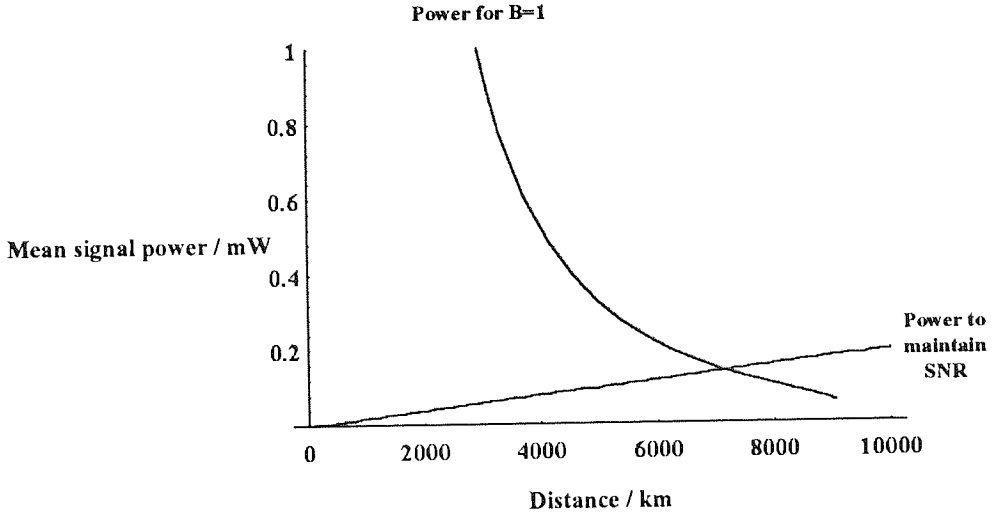

Figure 4.19. Theoretical power required to restore pulse width and that needed to obtain adequate SNR.

Thus, the furthest error free distance is achieved at the point of intersection. It should be noted that the curve for P_{max} has a maximum value of 0.806 L_D, and if this point occurs prior to intersection this is the best permissible transmission distance. Thus for a given dispersion we can plot the maximum transmission distance against bit rate. For the parameters cited above Figure 4.20 illustrates bit rate vs. distance for both D=0.1 & 1 ps/nm/km.

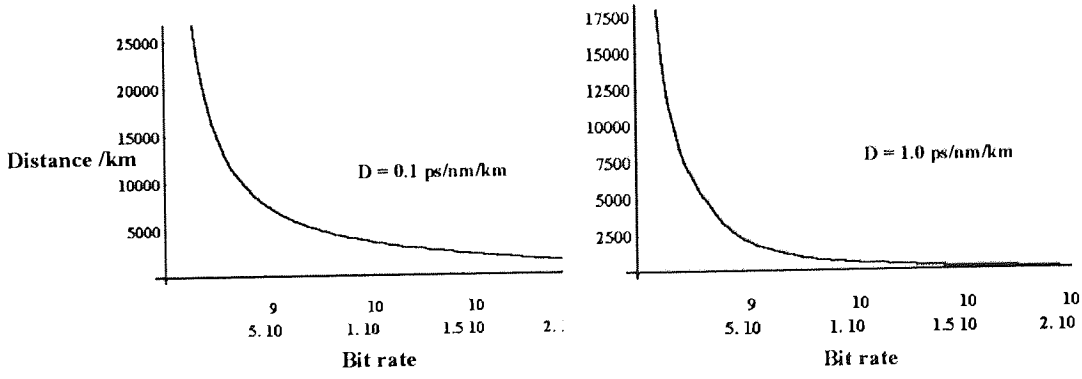

Figure 4.20. Theoretical bit rate vs. maximum transmission distance for D=0.1 & 1.0 ps/nm/km.

This suggests that the best possible transmission performance at 2.5 Gbit/s is ~6,800 km for a dispersion of 1 ps/nm/km and 15,600 km at 0.1 ps/nm/km. At 5 Gbit/s with D = 0.1 ps/nm/km a distance of 7,700 km should be obtainable. These plots illustrate the importance

of operating at very low levels of dispersion in order to ensure minimum pulse distortion due to SPM. Ideally, the system operating wavelength should be chosen to be on the dispersion zero of the fibre.

4.3.2 Four wave mixing (FWM)

Co-propagating signals with wavelengths close to the fibre dispersion zero are velocity and phase matched over very long lengths[103]. As a result substantial exchange of energy between different wavelengths is induced due to enhanced four wave mixing[104]. In particular a strong signal will act as a pump for weak spontaneous emission generated by the line amplifiers and noise will grow at the expense of the signal[105]. This results in a large increase in the optical bandwidth. However, since the noise components propagate at the same group velocity the integrity of the signal is not necessarily lost.

It can be shown that the non-linear power generated by a single fibre link due to four wave mixing is given by[106]:

$$P_{ijk}(L) = \left[\frac{1024\pi^6 36\chi_{1111}^{3^2}}{n^4\lambda^2 c^2 A_{eff}}\right] P_i P_j P_k \frac{(1-e^{-\alpha L})^2}{\alpha^2}\left(\frac{\alpha^2}{\alpha^2+\Delta\beta^2}\right)\left[1+\frac{4e^{-\alpha L}\sin^2\left(\frac{\Delta\beta L}{2}\right)}{\left(1-e^{-\alpha L}\right)^2}\right] \qquad (4.15)$$

where, P_i, P_j and P_k are the powers in three co-propagating signals and the propagation constant difference $\Delta\beta$:

$$\Delta\beta = \left(\frac{2\pi\lambda_k^2}{c}\right)\Delta f_{ij}\Delta f_{jk}\left[2D+\left(\frac{\lambda_k^2}{2c}\right)\left(\Delta f_{ik}-\Delta f_{jk}\right)\left\{\frac{dD(\lambda_k)}{d\lambda}\right\}\right] \qquad (4.16)$$

with $\Delta f_{mn}=|f_m-f_n|$ where m,n=i,j,k. In general FWM problems are solved by numerical integration.

To illustrate the detrimental effects of FWM to operation on the fibre dispersion zero the results of some numerical simulations will be discussed. The modelling is performed by numerical integration of the scalar non-linear wave equation using a split step fourier technique[107]. Figure 4.21 shows the 2.5 Gbit/s 16 bit pulse pattern that is to be input to the simulated system. Both optical and electrical bandlimited (raised cosine with 3 dB cut off at 1.8 GHz) pulse patterns are shown in addition to the eye diagram and the optical spectrum.

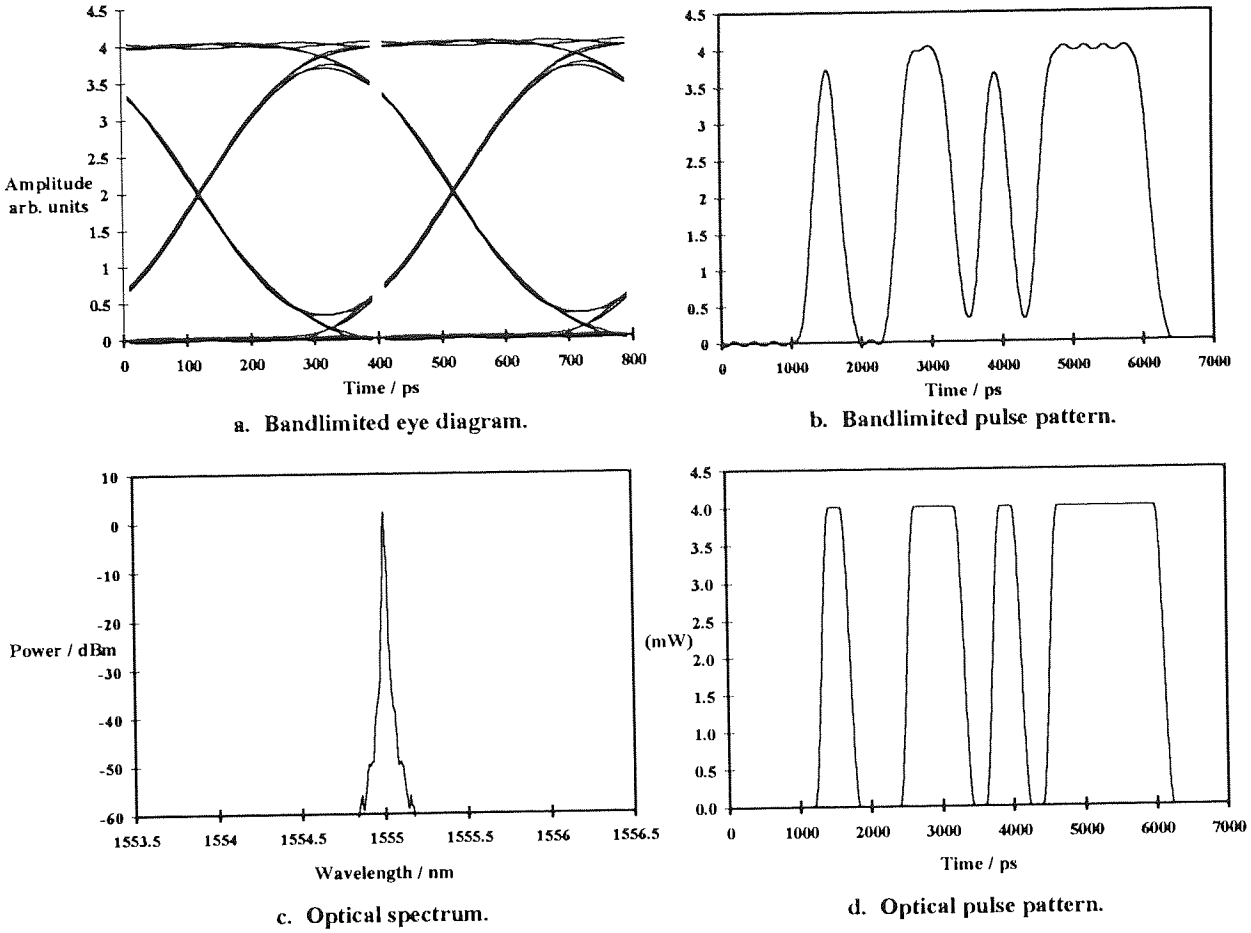

Figure 4.21. Input to simulated system, detailing bandlimited eye diagram and pulse pattern, optical spectrum and pulse pattern.

Figure 4.22 provides the same information only this time at the output of a simulated 10,000 km system operated on the dispersion zero. The amplifier spacing is 40 km, the noise figure 5 dB, Kerr coefficient 2.66×10^{-20} m^2/W, effective area 64 μm^2 and peak signal power 4 mW. The optical spectrum reveals that essentially all of the energy from the signal has been converted in to broad band noise and the optical pulse envelope is extremely noisy. The filtering process at the receiver considerably improves matters but severe eye closure is still apparent.

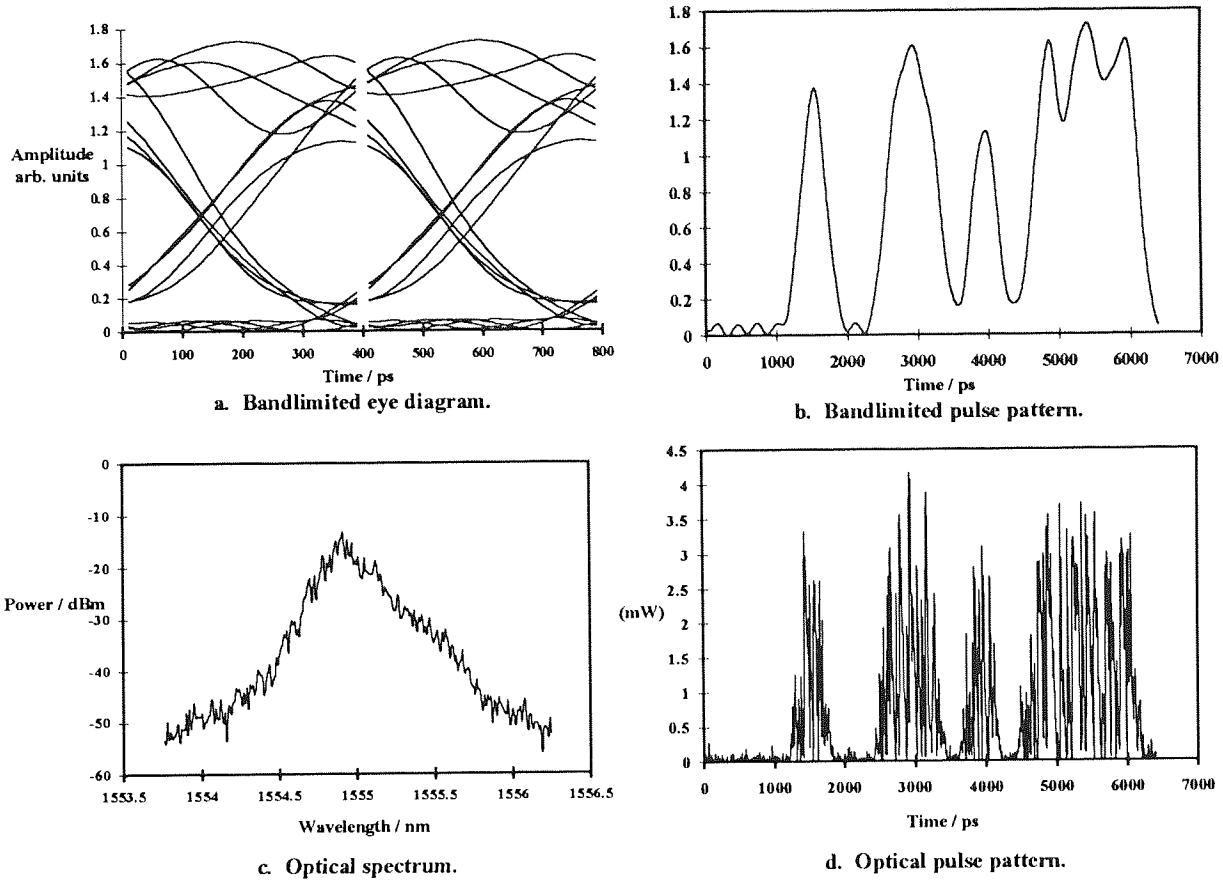

Figure 4.22. Bandlimited eye diagram and pulse pattern and optical spectrum and pulse pattern at the output from a simulated 10,000 km link with D = 0.

Figure 4.23 details the results from effectively the same simulation only this time without non-linearity, i.e. $n_2 = 0$. There is no noticeable pulse broadening in the optical spectrum which is distorted due to the accumulation of background ASE only. Moreover, both the eye diagram and the pulse pattern are only impaired by the addition of noise.

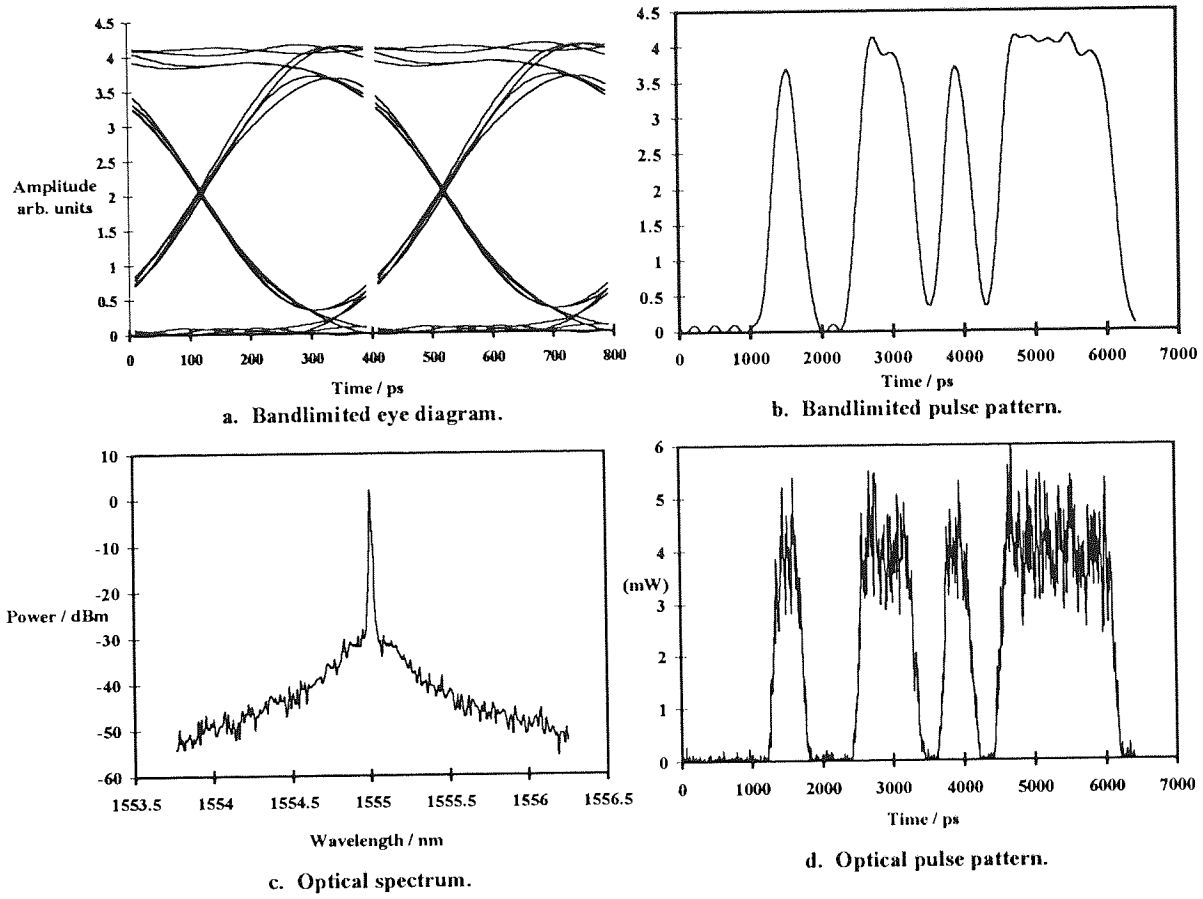

Figure 4.23. Bandlimited eye diagram and pulse pattern and optical spectrum and pulse pattern at the output from a simulated 10,000 km link with D = 0 with $n_2 = 0$.

Figure 4.24 details the results from a simulation with the amplifier noise suppressed, i.e. $n_{sp}=0$ and $n_2=2.66\text{x}10^{-20}$m/W. As would be expected the optical spectrum has some new low level frequencies generated due to spectral broadening from SPM. The temporal plots reveal that pulse compression has occurred on isolated ones due to the interaction of second order group velocity dispersion and SPM induced wavelength chirp[108]. This is also apparent on the eye diagram as a lowering of the cross over point.

Clearly, the impairments and eye closure apparent from Figure 4.22 is not the linear superposition of those detailed in Figures 4.23 and 4.24, and some non-linear process is responsible. Since, the signal wavelength is placed on the fibre dispersion zero there is significant synchronism between it and the ASE components at similar wavelengths. Consequently, the signal acts as a pump for the weak spontaneous emission resulting in the noise to grow at the expense of the signal due to enhanced four wave mixing.

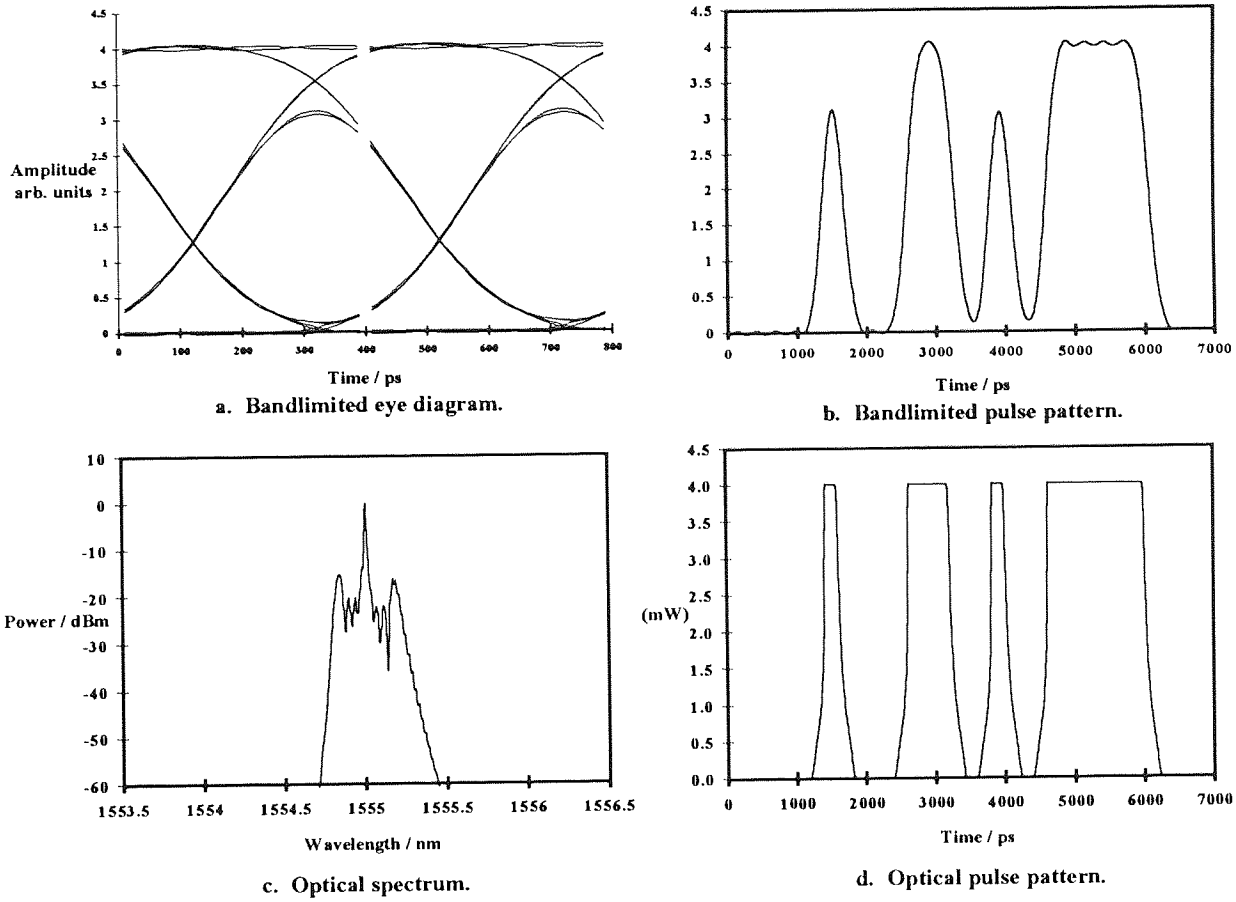

Figure 4.24. Bandlimited eye diagram and pulse pattern and optical spectrum and pulse pattern at the output from a simulated 10,000 km link with D = 0 with n_{sp}=0.

Figure 4.25 details the output from a simulation of a single amplifier recirculating loop experiment discussed in section 4.4. The peak power input to the fibre is 8 mW at a wavelength on the path average λ_0 of the 40 km of fibre that consists of the following links:

Link	Length / km	λ_0 / nm
1	6.5	1558.6
2	6.53	1559.2
3	6.57	1551.6
4	6.53	1551.3
5	5.56	1550.9
6	6.5	1556.1

Table 4.1. Composition of the loop fibre used to illustrate the effects of FWM on D=0.

The optical spectrum has significantly broadened and temporally the isolated pulses have narrowed. This results in the single 'ones' only attaining half of the amplitude of a string of 'ones' after detection by the band-limiting receiver. Thus, the eye diagram suffers closure with the optimum decision point moved very close to the 'zero' level.

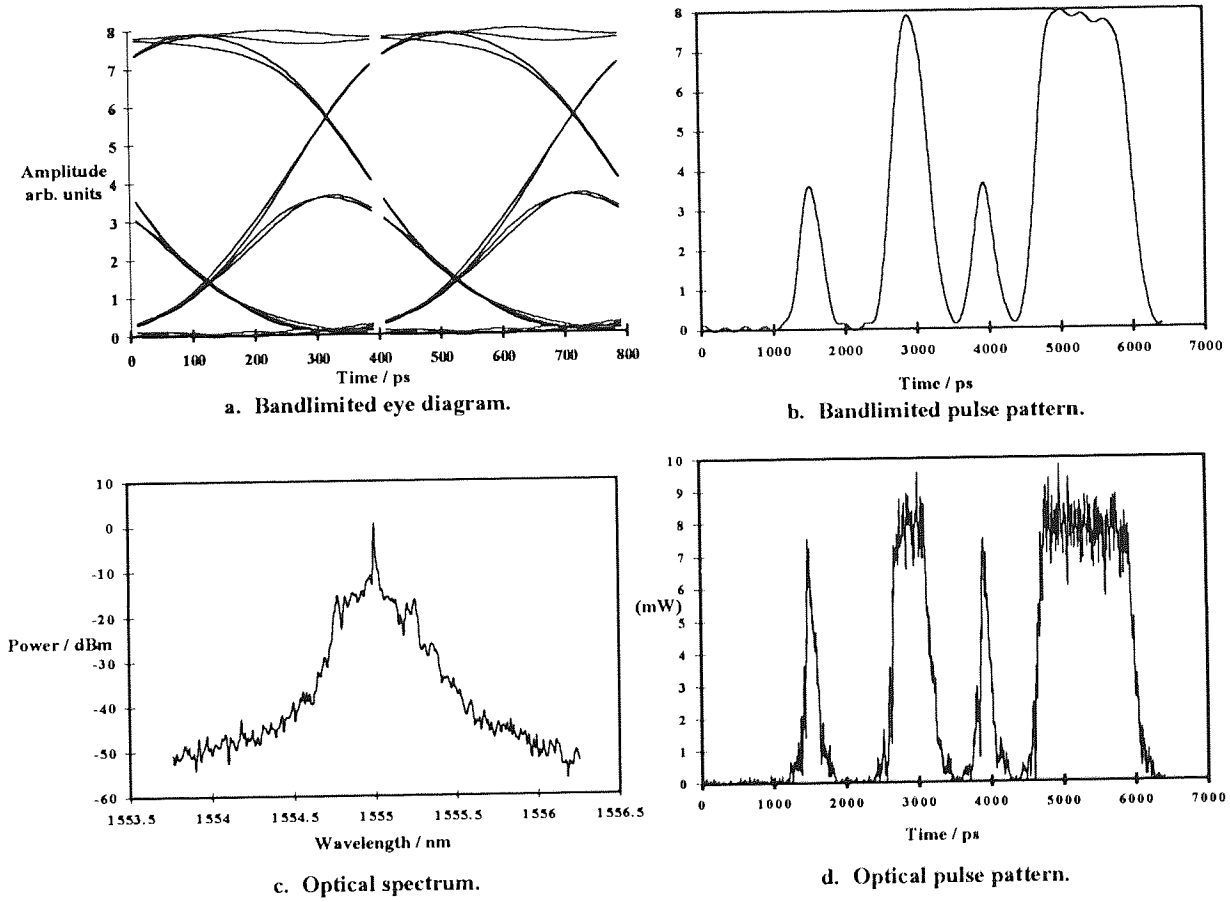

a. Bandlimited eye diagram.

b. Bandlimited pulse pattern.

c. Optical spectrum.

d. Optical pulse pattern.

Figure 4.25. Bandlimited eye diagram and pulse pattern and optical spectrum and pulse pattern at the output from a simulation of experiment in section 4.4.

From this and the previous sections it is apparent that to minimise the effects of SPM and GVD it is desirable to operate on the dispersion zero, however, in so doing enhanced four wave mixing results in data corruption. In section 4.4 dispersion maps will be used experimentally to simultaneously minimise the effects of SPM, GVD and FWM in ultra-long haul optically amplified NRZ systems.

4.3.3 Stimulated Brillouin scattering (SBS)

To accommodate the accumulated effects of SBS over a multi-amplifier system equation 3.1 can be modified to reduce the threshold power with the number of repeaters in the link. In practice each span would contribute the same amount of backwards propagating stokes waves which would be blocked by the isolator in the amplifier. Thus we can simulate the effect on a long haul system by scaling with log(N), where N is the number of amplifiers in the link. For a Lorentzian profile pump signal:

$$P_{thr} = \frac{21A_{eff}}{g_b z_{eff}} \left[\frac{\Delta\nu_L + \Delta\nu_b}{\Delta\nu_b} \right] \left[\frac{1}{0.5 - 0.25 \frac{B}{\Delta\nu_b} \left(1 - e^{\frac{-\Delta\nu b}{B}} \right)} \right] \left[\frac{1}{1 + \log\left(1 + \frac{z}{z_o} \right)} \right] \tag{4.17}$$

and for a Gaussian profile:

$$P_{thr} = \frac{21A_{eff}}{g_b z_{eff}} \left[\frac{\Delta\nu_L^{\,2} + \Delta\nu_b^2}{\Delta\nu_b^2} \right] \left[\frac{1}{0.5 - 0.25 \frac{B}{\Delta\nu_b} \left(1 - e^{\frac{-\Delta\nu b}{B}} \right)} \right] \left[\frac{1}{1 + \log\left(1 + \frac{z}{z_o} \right)} \right] \tag{4.18}$$

The threshold power for both profiles is illustrated in figure 4.26 assuming the same parameters as those used in section 4.1.1.

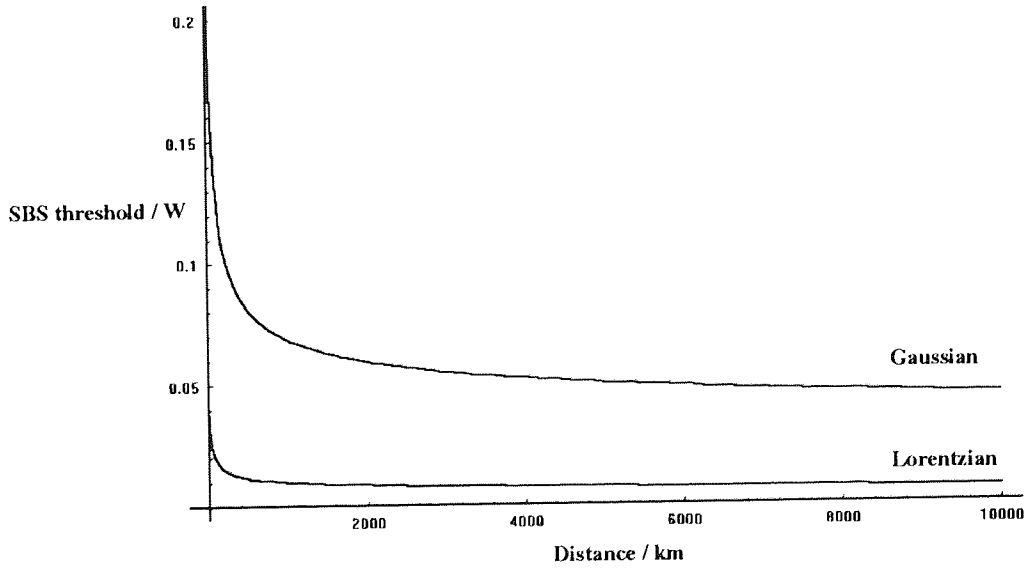

Figure 4.26. Evolution of SBS threshold with distance for Lorentzian and Gaussian profiles.

It should be noted however that spectral broadening associated with SPM and FWM as the signal propagates down the link has been neglected from this plot. These effects will not only enhance the spectrum, and therefore increase the threshold power, but also alter its profile and for this reason both Lorentzian and Gaussian results are provided. However, from the results obtained it would seem that SBS will not be a major impairment since both SPM and FWM would causes severe degradation at much lower power levels.

4.3.4 Stimulated Raman scattering (SRS)

Since, the Raman bandwidth is many THz wide[109] its effect is not reduced with modulation or source chirp as is the case for SBS. However, over an amplified link the Stokes wave will generally be outside the bandwidth of the cascaded system and can therefore be considered as just an additional loss term, with the new noise components filtered out. Thus, the effective threshold for a many amplifier link can be approximated by:

$$P_{cr} = \frac{16 A_{eff}}{g_r Z_{eff}} \left[\frac{1}{1 + \log\left(1 + \frac{z}{z_o}\right)} \right] \tag{4.19}$$

Figure 4.27 details the evolution of Raman threshold power with distance for the parameters used previously. It can be seen that SRS is not likely to cause significant system impairments at the power levels that will allow good performance due to the effects of SPM and FWM.

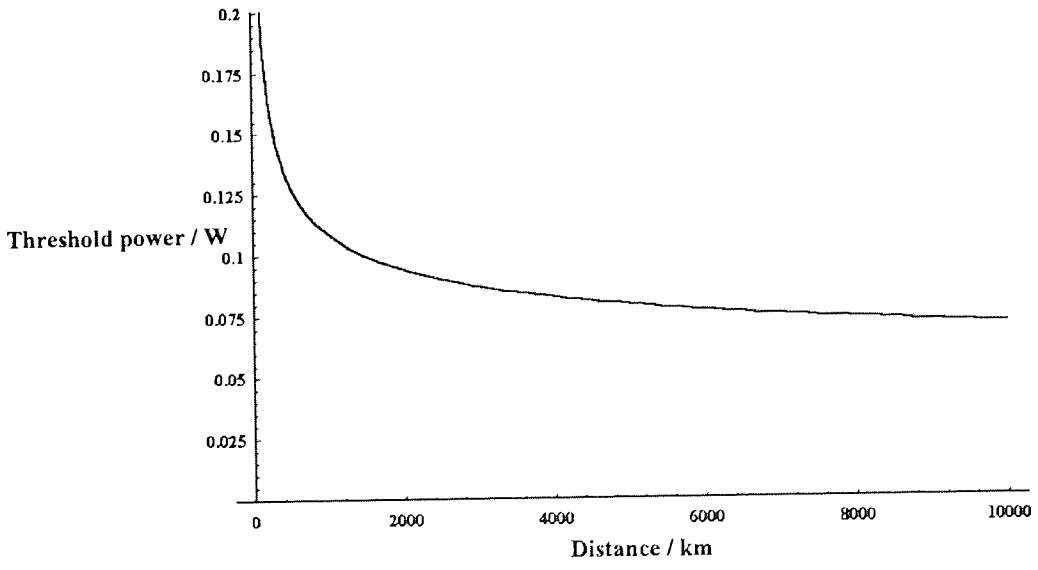

Figure 4.27. Evolution of Raman threshold power with distance.

4.4. Experimental results.

Experimentally the effects of fibre dispersion, non-linearity and amplifier noise on system performance have been investigated with a recirculating loop similar to that detailed in figure 4.5. The amplifier spacing and component characteristics used were representative of those expected to be found in ultra-long haul systems. The isolator ensured unidirectional operation, thus minimising optical reflections, and would normally be associated with the amplifier. It is unlikely that a cascaded system would utilise bandpass filters due to potential long term drift problems. However, to allow assessment of system performance over a range of operating wavelengths, and therefore dispersion values, a 2.7 nm tuneable filter was included in the loop (not 6 nm as indicated in figure 4.5). A low chirp source was realised by using a cw DBF laser externally modulated by a lithium niobate Mach-Zehnder interferometer.

4.4.1. 2.5 Gbit/s results.

Figure 4.28 is a plot of measured BER vs. path average fibre dispersion at 6,000 and 10,000 km for a mean input power to the transmission fibre of 3 dBm.

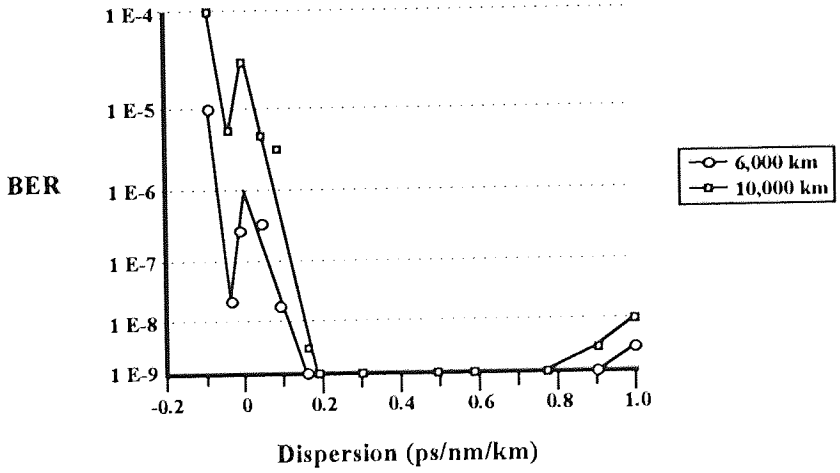

Figure 4.28. 2.5 Gbit/s BER vs. path average dispersion at 6,000 and 10,000 km.

On the short wavelength side of λ_o the pulses broadened due to both chromatic dispersion and the chirp induced by SPM, as discussed in section 4.3.1. This resulted in significant distortion and ISI and error free operation (BER $<1x10^{-9}$) was not obtained. Increasing the power level enhanced the spectral broadening from SPM and system

performance deteriorated. These detrimental effects reduced as the operating wavelength approached λ_o since pulse broadening from dispersion decreased.

However, at wavelengths very close to λ_o enhanced phase matching between the signal and ASE resulted in power being extracted from the signal into new noise frequencies due to FWM, as discussed in section 4.3.2. This effect was compounded with higher power levels and figure 4.29a shows the pulse pattern after 10,000 km of transmission when operating on λ_o for a mean power of 6 dBm input to the fibre.

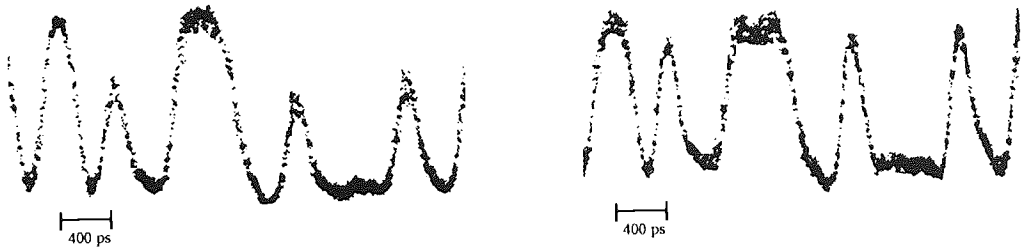

Fig. 4.29a Effects of FWM at 10,000 km 4.29b Optimum dispersion

Figure 4.29. Effect of operating dispersion value on pulse distortion.

Isolated '1's are noticeably attenuated due to the combined effects of spectral broadening by FWM & SPM and second order dispersion. Indeed in this case the optical spectrum had broadened to 0.5 nm and shifted by 0.75 nm to a shorter wavelength. After only 1,000 km of transmission no power was detected at the transmit wavelength and, consequently, the received data was significantly errored. Figure 4.29a is in excellent agreement with that simulated and detailed in figure 4.25

As the operating wavelength was increased phase matching reduced and the detrimental effects of FWM eased. In this regime it was possible to utilise pulse compression obtained from SPM in anomalous dispersion to offset to some extent the broadening resulting from chromatic dispersion. Experimentally at a dispersion of 0.1 ps/nm/km a BER of $1x10^{-9}$ was obtained to a distance of 16,000 km and this is in excellent agreement with that predicted from the theory detailed in section 4.1.1, which implied transmission was possible to a distance of 15,600 km. The measured penalties were only 0.2 dB and 0.8 dB at 6,000 and 10,000 km respectively and figure 4.29b details the pulse pattern at 10,000 km showing no signs of pulse distortion. At 6,000 km it was possible to obtain error free operation over a 10 nm wavelength window as detailed in figure 4.28. However, when the signal power entering the fibre was increased to 6 dBm the resultant spectral broadening and its interaction

with fibre dispersion restricted error free operation to only a very limited wavelength range of less than 1 nm. This clearly illustrates the importance of achieving the necessary balance between non-linearity and dispersion for NRZ systems of this length.

As the signal wavelength was increased dispersion dominated and pulse broadening occurred even at low power levels where no spectral broadening was apparent. Thus error free operation was not possible for high values of dispersion. Where system operation was marginal it was possible to limit spectral broadening by reducing the signal power and a trade off occurred between signal to noise ratio and pulse distortion. Indeed, error free operation was possible to a distance of 6,200 km at 1 ps/nm/km dispersion for a mean power entering the fibre of 1.5 dBm. This is in excellent agreement with the theory presented in section 4.3.1 which predicts that a distance of 6,800 km should be possible.

4.4.2. 5 Gbit/s results.

Increasing the bit rate of a system requires an increase in the receiver bandwidth and, therefore, detected noise. Consequently, it is necessary to increase the signal power to maintain the SNR. However, in so doing non-linear effects are enhanced resulting in the possibility of increased pulse broadening in a decreased bit period. Thus, it is usually necessary to reduce the signal level and this further impinges on system SNR. Figure 4.30 shows the system performance at 6,200 km as function of fibre dispersion for 5 Gbit/s data and a mean power level entering the fibre of 3 dBm.

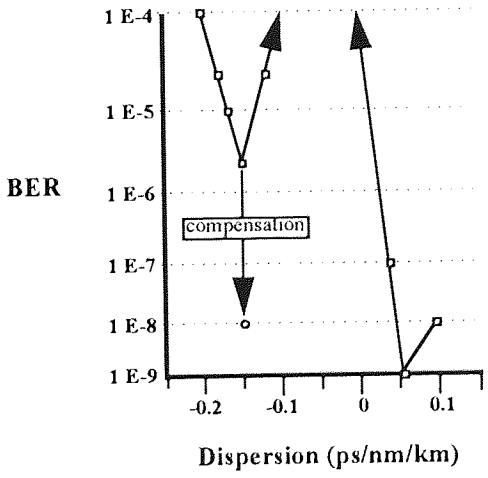

Figure 4.30. 5 Gbit/s BER vs. path average fibre dispersion at 6,000 km.

It can be seen that the same trends that were observed at 2.5 Gbit/s are followed only with much tighter restrictions on allowable pulse distortion. Again the error ratio improved as the operating wavelength approached minimum dispersion until phase matching induced FWM. On the short wavelength side of λ_o it was possible to use 25 km of step index fibre at the receiver to compensate for the dispersion of the link and, therefore, reduce pulse broadening as illustrated in the diagram. On the long wavelength side of the dispersion zero a BER of $1x10^{-9}$ was obtained at a dispersion of 0.06 ps/nm/km.

To improve performance further it is necessary to operate on the system λ_o but ensure that phase matching dose not occur over long distances. This may be achieved by adding a phase perturbation into the transmission path. For example, by inserting relatively short lengths of step index fibre with a dispersion of around 17 ps/nm/km and operating at the path average λ_o it is possible to ensure that the signal does not propagate with enhanced FWM in any fibre. The net dispersion over the entire length of the link is zero so the effects of SPM are also minimised. Figure 4.31 shows the system performance against path average dispersion obtained by utilising this technique.

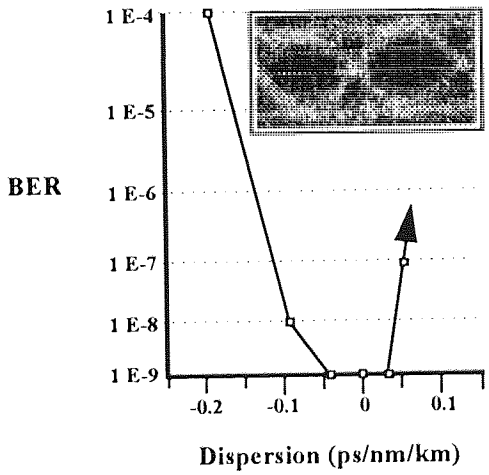

Figure 4.31. 5 Gbit/s vs. fibre dispersion at 6,000 km with dispersion management.

The insertion of 385 m of step index fibre into the loop allowed propagation over 9,000 km before a BER of $1x10^{-9}$ was encountered. FWM was reduced to the extent that no spectral broadening could be measured on a conventional spectrum analyser with a resolution of 0.1 nm. Inset in figure 4.31 is the detected eye at 9,000 km. There were no signs of pulse distortion implying that improving the noise performance of the system would allow transmission to greater distances.

Modifying the experiment to that illustrated in figure 4.13 allowed the noise penalty from the fibre coupler and filter to be reduced from 4 dB/span to 1 dB/span. Error free transmission was extended to 17,600 km as would be expected from the 3 dB improvement in SNR and this is detailed in figure 4.14. This result implies that non-linearity was not limiting the system, since, further propagation would significantly enhance such effects. When the signal SOP was adjusted such that the PDL was 0.03 dB/span and the PMD was negligible a BER of $5x10^{-8}$ was obtained at 6,000 km, implying that some form of high speed polarisation scrambling would be necessary to maintain acceptable long term system performance.

4.4.3. 10 Gbit/s results.

Operation at higher bit rates again necessitates an increase in the receiver bandwidth, reducing the SNR and also the allowable pulse distortion. Figure 4.32 details the detected pulse pattern at 0 km and 9,000 km for 10 Gbit/s data with a mean power of 3 dBm input to the fibre. The signal wavelength was such that the path average dispersion was very slightly positive.

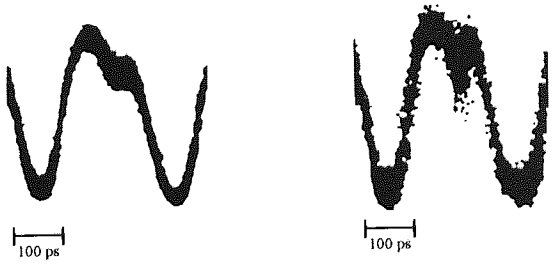

4.32 a 4.32 b

Figure 4.32. Transmitted pulse (a) and that after 10,000 km of transmission (b), showing modulation instability.

As the speed of operation of $LiNb0_3$ modulators increases so does the required drive voltage. High speed, high output power 10 Gbit/s electrical amplifiers are currently state of the art and the performance is not as well controlled as those at much lower bit rates. Consequently, imperfections can result in patterning of the data and this can be seen in Figure 4.32a. In particular, some of the 'one' levels suffered ringing and droop.

A perfect 'one' may be regarded as a solution to the non-linear Schrodinger equation governing propagation in the fibre i.e. pseudo c.w. However, when perturbations occur in the anomalous dispersion regime the solution is unstable and the perturbation grows exponentially

with distance. Consequently, the imperfect transmitted data suffered enhanced pulse distortion with propagation due to modulation instability and error free operation was limited to a distance of 6,000 km. In order to improve on this result it would be necessary to launch data with significantly less pulse distortion, placing stringent requirements on the high speed electronics. At higher bit rates such devices are not commercially available.

If the SNR limited result of 5 Gbit/s error free to 17,600 km is extrapolated to 10 Gbit/s the maximum transmission distance attainable is only ~9,000 km, assuming no additional non-linear impairments. Thus, for the transpacific span a BER of $1x10^{-9}$ would just be possible but only with the signal state of polarisation optimised.

4.5 Conclusions

To utilise optically amplified NRZ transmission systems at high bit rates over transoceanic spans requires careful control of the system dispersion and operating power levels. Appropriate dispersion management schemes have allowed the detrimental effects of non-linearity to be reduced and 5 Gbit/s data to be transmitted 17,600 km error free. However, this result was obtained by optimising the signal SOP such that minimal PMD and PDL were encountered. A practical system would require the use of a polarisation scrambler at the transmitter and very careful control of the fibre's PMD at the manufacturing stage.

At 10 Gbit/s error free performance was only obtainable to a distance of 6,000 km. The increased bandwidth of the receiver allowed pulse distortion from non-linear effects to be transmitted through to the error detector. The use of an optimised transmitter may permit transmission to 9,000 km before impinging upon the SNR limit. Further increases in performance would require the use of lower noise figure amplifiers and possibly 980 nm pumping. Amplifiers with a 3 dB noise figure would allow the transpacific route to be traversed with 3 dB of 'margin'. However, upgrading beyond 10 Gbit/s looks unlikely.

Thus, the idea of the bit rate independent transparent optical pipe is not realisable with ultra-long haul optically amplified NRZ systems. Further, since dispersion management schemes are required to allow acceptable performance at 5 Gbit/s and above, wavelength division multiplexing is not an option. With the added impairments of PDL, PMD, PHB and PDG system performance is further impaired and fluctuates with time. Multiplexing in polarisation is also precluded by these effects. In the limit of the transmission of very high bit rates over ultra-long distances it may be necessary to regenerate the signal at points along the span to ensure acceptable performance levels. Alternatively, it is possible to use non-linearity to balance dispersion by transmitting solitons as data bits and this is the topic of the next chapter.

Chapter 5

5. Ultra-long haul soliton transmission

5.1. Introduction

The propagation of radiation inside a monomode optical fibre is governed by the non-linear Schrodinger equation, the stable solutions of which are its eigen-functions, commonly known as optical solitons[110]. Solitons arise as a balance between the phase shifts induced by the fibre non-linearity and dispersion. The ability of solitons to maintain their temporal and spectral profile on propagation suggests that they may be ideally suited to ultra-long haul transmission. However, fibre loss is accompanied by pulse broadening and necessitates use of the 'average soliton model'[111]. To ensure stable propagation with discrete amplifiers the induced phase shift in each section should be small, requiring the amplifier spacing to be much less than the soliton period. The average dispersion is then balanced by the average non-linear phase shift by launching a power such that the mean value over a single link is equal to the ideal soliton power for an identical, but lossless fibre. For broad pulses the average soliton model is easily realised in practice. However, as the bit rate is increased the pulse width must be reduced and this decreases the soliton period for a given value of dispersion. As a result the amplifier spacing must also reduce, adversely affecting system design.

In addition to impairing system performance in terms of SNR, ASE from the transmission line amplifiers gives rise to the Gordon-Haus effect[112]. Noise at wavelengths close to that of the soliton induce random shifts in the carrier frequency and this interacts with fibre dispersion to produce a random timing jitter whose variance is given by:

$$\left\langle \delta t^2 \right\rangle = \frac{(G-1)\mu h n_2 D L_{sys}^3}{9\tau A_{eff} L_{amp}} \qquad (5.1)$$

Where L_{sys} is the overall length of the system, L_{amp} the spacing between amplifiers and τ the pulse width FWHM. In order to maintain an acceptable BER the rms jitter must be kept small compared to the bit interval. This places restrictions on the noise figure of the amplifiers, fibre dispersion and pulse width. Figure 5.1 details the eye diagrams obtained after a simulated 6,000 km system both with and without ASE for the parameters; D = 1 ps/nm/km, pulse width 20 ps, amplifier spacing 40 km, noise figure 7 dB.

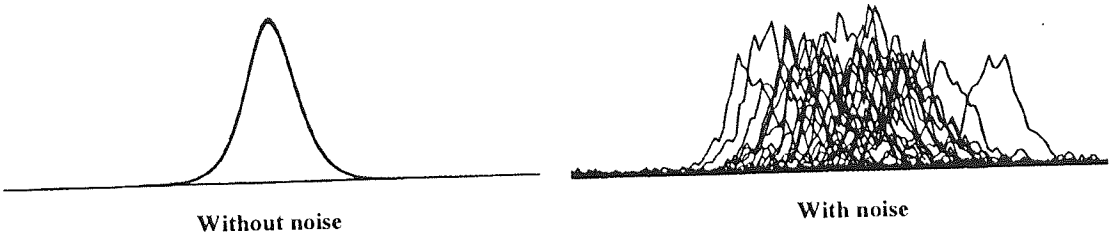

Without noise

With noise

Figure 5.1. Simulated eye diagrams at 6,000 km without and with ASE to illustrate the effect of Gordon-Haus jitter.

A further source of timing jitter is the acousto-optic effect[113] arising from an interaction between the signal and the transmission medium itself. Large transverse gradients of radiation intensity from a signal pulse in the fibre can lead to electrostrictional excitation of acoustic waves. These waves propagate radially out of the core until an impedance change is encountered, such as the core cladding boundary. A fraction of the energy is reflected back modifying the refractive index of the core, thus, acting on the optical signal resulting in temporal shifts whose variance is given by:

$$\left\langle \delta t^2 \right\rangle = \frac{\alpha \lambda^8 A_{eff} D^4 R L_{sys}}{\tau^2} \tag{5.2}$$

where, R is the bit rate and α a constant of proportionality. In order to minimise the effects of both Gordon-Haus jitter and the acousto-optic effect it is necessary to reduce the dispersion value of the transmission fibre and increase the soliton pulse width.

Power in the tail of a soliton induces a change in the refractive index of the fibre at the point of neighbouring pulses. This can lead to adjacent solitons periodically attracting, if they are of the same phase, or repelling, if they are of the opposite phase, and is called soliton-soliton interaction[114]. The period over which the solitons collapse is given approximately by:

$$z_p = z_0 e^{\frac{T}{2\tau}} \tag{5.3}$$

where, T is the bit period. In a transmission system this effect can lead to system errors as pulses coalesce and temporally shift in their time slot. To avoid such problems the power in the tail of the pulses must be minimised and this requires narrow pulses. However, the use of short pulses enhances timing jitter from both Gordon-Haus and acousto-optic effects and a compromise clearly exists. To ensure that soliton-soliton interactions do not induce transmission errors it is usual to apply the inequality:

$$L_{sys} < \frac{z_p}{4} \tag{5.4}$$

Figure 5.2 illustrates the effect on transmission of two initially in phase solitons.

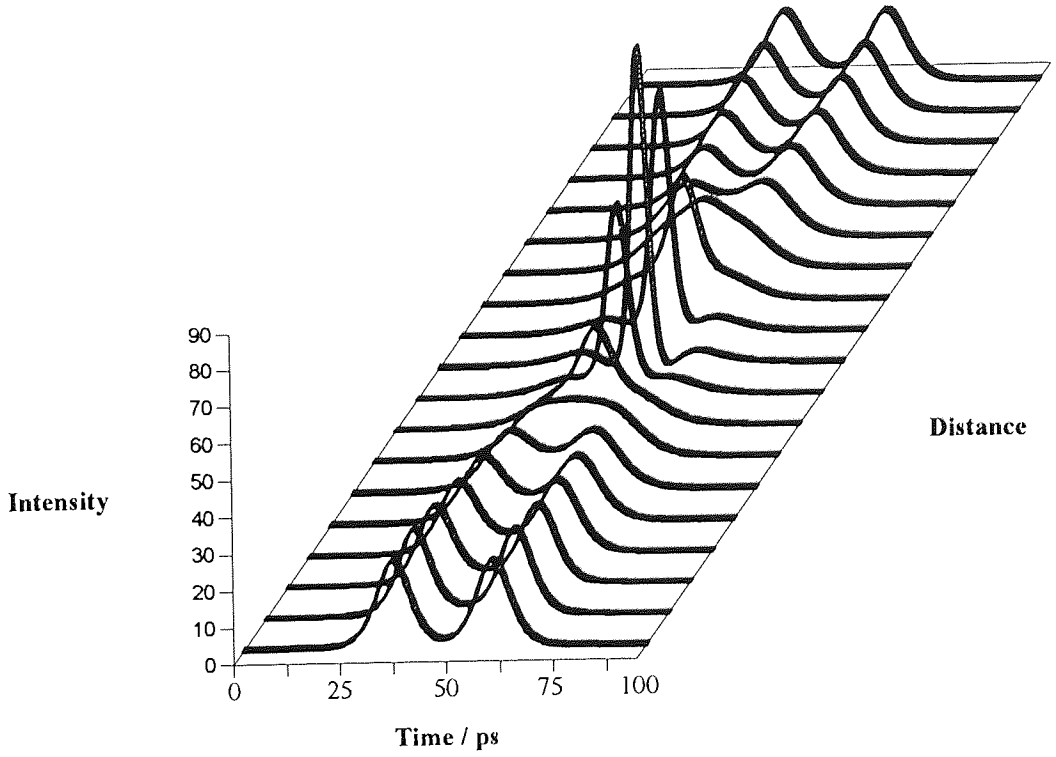

Figure 5.2. Interaction between two initially in phase solitons, showing period collapse.

For sufficiently short solitons the optical spectra may overlap with the Raman scattering gain spectrum resulting in the peak of the pulse pumping its own wings, inducing a

continuous downshift in the average frequency. This phenomena is called soliton self frequency shift[115] and can lead to the data stream being attenuated by the filtering action of the transmission path on propagation.

In the limit of transmitting very high bit rates over ultra-long distances the impairments detailed above imply that some form of soliton transmission control is required to stabilise the accumulation of jitter and noise and to reduce the deleterious effects of soliton-soliton interactions. In general soliton control significantly increases the complexity of the transmission path, and in some cases results in a form of soliton regenerator. In this chapter soliton transmission both with and without control will be discussed. The performance of systems without control is experimentally evaluated and the feasibility of upgrading in both time and polarisation domains assessed. To allow higher speed operation over oceanic distances two forms of transmission control are experimentally examined. Retiming by periodic synchronous modulation in both amplitude and phase domains is investigated. In the case of phase modulation transmission control a new all optical technique known as soliton shepherding is demonstrated for the first time.

5.2. Soliton propagation without transmission control

From a practical view point it is desirable to utilise a simple transmission path architecture without recourse to narrow band optical filters or high speed electronics. However, propagation without transmission control requires the soliton source to be extremely stable in terms of pulse width, amplitude noise, timing jitter and wavelength jitter. Additionally, transform limited pulses of $sech^2$ intensity profile with a time bandwidth product of 0.315 should ideally be realised within the transmitter. In practice meeting all of these requirements is very difficult and a variety of soliton sources have been proposed and experimentally tested. Arguably the most promising candidate in terms of pulse quality is the mode locked erbium fibre ring laser (MLEFRL)[116]. However, it is also the most difficult to stabilise, since, very high harmonics of the cavity fundamental are normally used at frequencies of interest to communications.

Pulses within a MLEFRL may experience soliton shaping effects in the fibre cavity. The energy shed during this process is converted in to pulses by mode locking at a later stage. Thus, it is possible to generate pure solitons without a dispersive tail. However, as already mentioned fibre lasers are highly susceptible to the environment and require stabilisation.

5.2.1. *Phase locked erbium fibre ring laser*

Previous stabilisation schemes[117,118] controlled the length of the fibre cavity such that the round trip time was an integer number of bit periods. In general this necessitated thermal or mechanical stretching of the laser cavity. Where direct control of the fibre length is employed this process invariably perturbed the signal state of polarisation and resulted in wavelength jitter, since, an integer number of beat lengths were required to fit in the laser. Additionally, these control techniques were slow to respond and prone to overshooting. Consequently, the laser was infrequently perfectly mode locked.

In order to obtain pure soliton pulses from the MLEFRL over extended periods a new control scheme has been devised[119]. Unlike other ring laser stabilisation techniques the cavity fibre is left completely unperturbed with only the phase of the rf drive adjusted with a phase lock loop (PLL) to track cavity length variations. One of the advantages of this scheme is that since the fibre is unaffected by the control, stability in terms of polarisation, and therefore wavelength, is much improved. Additionally, the technique is capable of tracking high speed (100's kHz) variations as well as thermal drifts, a major limitation of the fibre stretch type of control.

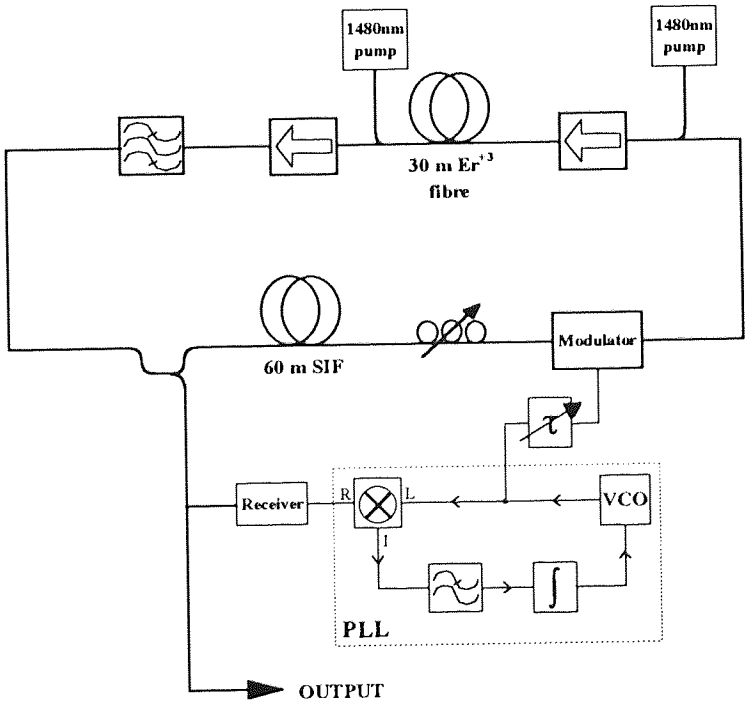

Figure 5.3. Schematic of phase locked erbium fibre ring laser.

Figure 5.3 details the configuration of the phase locked erbium fibre ring laser (PLEFRL). The active medium consisted of 30 m of erbium doped fibre bi-directionally pumped with 1480 nm semiconductor diodes. Mode locking was performed by a $LiNbO_3$ amplitude modulator with a 3 dB bandwidth of ~ 8 GHz. Isolators with very low polarisation dependent loss and polarisation mode dispersion were placed either side of the erbium fibre to minimise reflections and ensure unidirectional operation. The cavity included 60 m of step index fibre with a peak optical power close to the fundamental soliton power. A tuneable 1 nm FWHM filter selected the wavelength of operation and ensured that the pulse widths produced were suitable for long haul transmission (~20 ps). The laser output was detected by a 2.5 Gbit.s^{-1} receiver which fed a 2.5 GHz electronic PLL. The PLL modulated the laser via an adjustable delay that corrected for arbitrary phase. The parameters of the PLEFRL were; natural frequency, $\omega_n = 4 \times 10^6$ rad.s^{-1} and damping factor, $\zeta = 0.7$.

The laser was mode locked at 2.5 GHz and the pulse width adjusted to 23 ps FWHM via the electrical drive to the modulator. A mark - space ratio of better than 1:17 ensured that soliton-soliton interactions were negligible when performing transmission experiments. The time bandwidth product, $\Delta\tau\Delta\nu$, was measured as 0.32, resulting in transform limited sech^2 pulses. The measured pulse to pulse timing jitter was below the resolution of the instrument used (~ 2 ps).

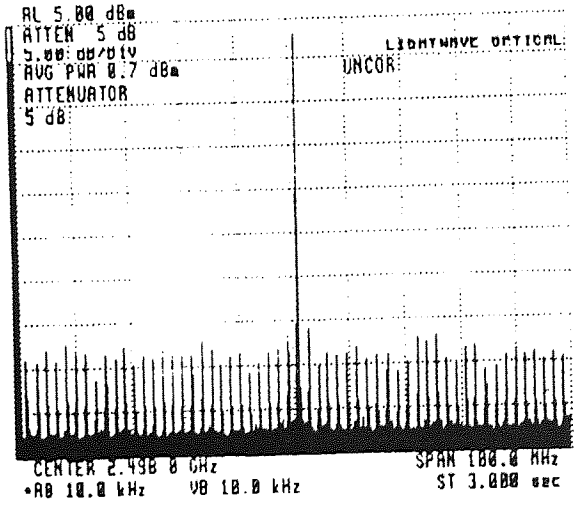

Figure 5.4. R.F. spectrum of PLEFRL showing 35 dB suppression of cavity modes to dominant 2.5 GHz mode.

Figure 5.4 shows the RF spectrum illustrating 35 dB suppression of the cavity modes relative to the dominant 2.5 GHz mode. The long term stability of the source allowed its use

on a day to day basis without need for adjustment and no sporadic noise bursts were observed. Additionally, the laser cavity was heated from 20 to 40 °C without loss of mode locking.

5.2.2 Single channel soliton transmission without control

Accurate measurement of all of the parameters that are important for a soliton source is difficult, and ultimately, it is the transmission performance that determines its suitability. Figure 5.5 details the configuration of the recirculating loop used in the transmission experiments to assess three lasers. The soliton sources used were 1) the PLEFRL, 2) mode-locked semiconductor laser (MLSL) and 3) an electro-absorption modulator (EAM) externally modulating a cw DFB laser.

The MLSL generated ~25 ps pulses with $\Delta\tau\Delta\nu$ = ~0.4, assuming a Gaussian profile, and was therefore not transform limited. In operation the laser was moderately complex in alignment of the external grating (required to allow wavelength tuneability). The EAM was the simplest source in terms of operation, since no adjustment was required once configured. The particular device used produced ~50 ps pulses with $\Delta\tau\Delta\nu$ ~0.44 implying that the source was not transform limited, assuming sech profile.

The pulse train from the lasers was externally modulated with a 2^7-1 PRBS data pattern using a balanced symmetrically driven lithium niobate Mach-Zehnder interferometer to yield a low chirp source. An acousto-optic switch gated the injection of data into the loop for a period equal to the round trip time (480 μs). The loop consisted of three 33 km spans of Corning dispersion shifted fibre with a mean dispersion zero, λ_o, of 1548.6 nm and an average slope of 0.075 $ps.nm^{-2}.km^{-1}$. An isolator with very low PDL (<0.1 dB) and PMD (<1 ps) was used to aid stability and a 3 nm FWHM bandpass filter to select the wavelength of operation whilst providing negligible guiding action (theoretically less than 10% improvement in transmission distance[120]). Data was injected into the loop and coupled out to the receiver via a 20 : 80 fused fibre coupler. The loss of each span was compensated by a 7.5 dB gain EDFA, contra-directionally pumped by a 1480 nm semiconductor laser. The measured noise figures under these conditions were 4.8 dB. The receiver comprised a 1.7 GHz *pin* FET front end and a cascade of wide bandwidth external electrical amplifiers to boost the signal to a level suitable for a bit error ratio detector.

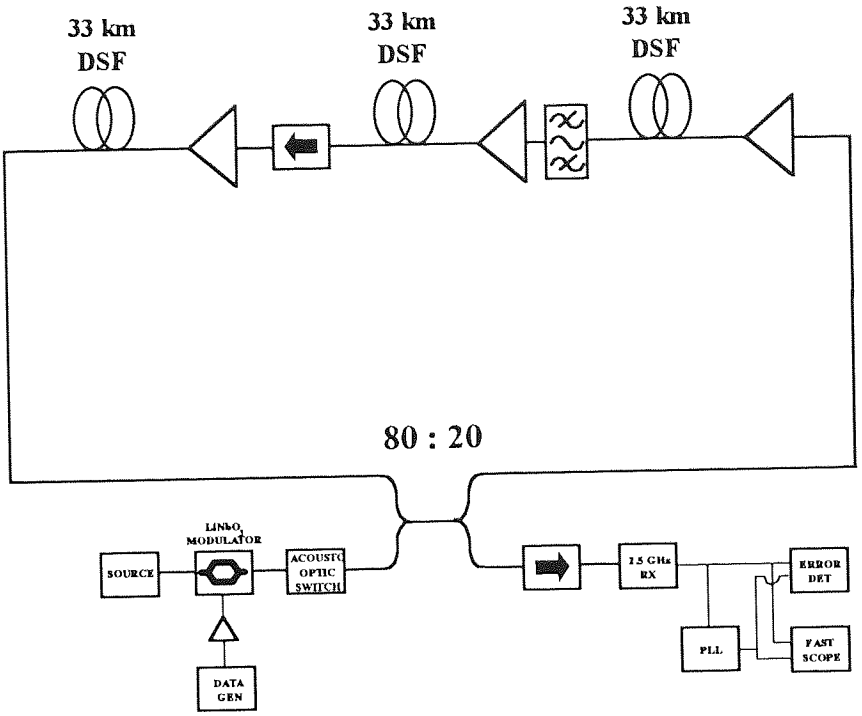

Figure 5.5. Recirculating loop configuration for transmission experiments without control.

For each of the sources in the transmission experiments the path average fibre dispersion at the operating wavelength was ~0.6 $ps.nm^{-1}.km^{-1}$ but adjusted to find the optimum performance. Figure 5.6a details the best achieved error ratios for the three lasers at 2.5 Gbit/s and figure 5.6b the evolution of power in the 2.5 GHz component of the soliton pulse stream with distance.

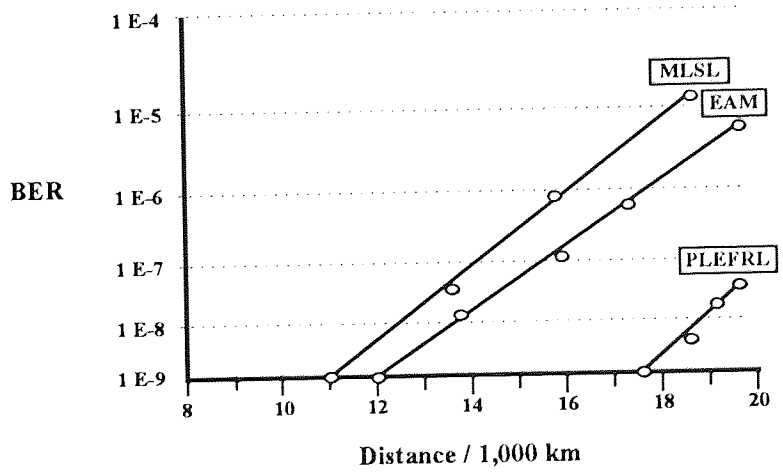

Fig. 5.6a 2.5 Gbit/s BER vs distance for three soliton sources

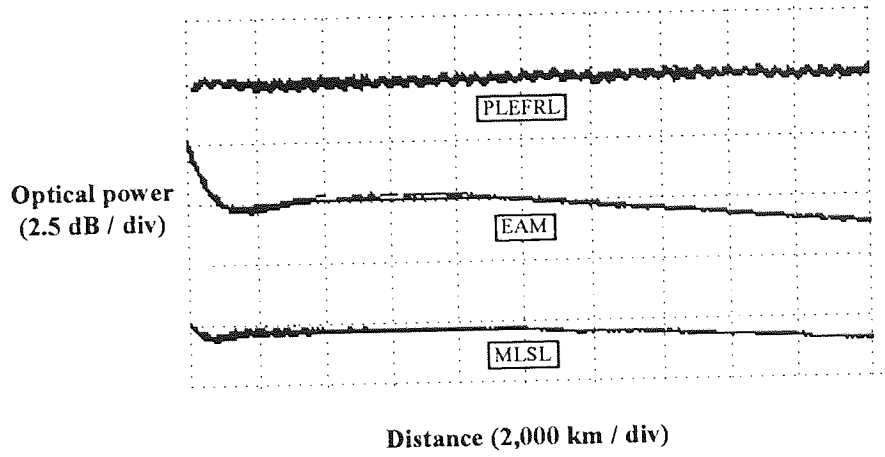

Figure 5.6b. Evolution of power in 2.5 GHz Spectral component

Figure 5.6. BER and transmission performance of three soliton sources.

From Figure 5.6b there is clear evidence of energy shedding over the first few hundred km as the chirped Gaussian like pulses of the MLSL ($\Delta\tau\Delta\upsilon$ = 0.4) evolved into solitons resulting in dispersive wave radiation, DWR, leaving a dispersive tail. Subsequent transmission was limited due to this tail acting as medium for enhanced soliton-soliton interactions resulting in increased jitter and lead to a roll off in amplitude of the 2.5 GHz component beyond 10,000 km. Indeed error free operation was only achieved to a distance of 11,000 km as against a theoretical maximum of 18,000 km for the transmission of pure solitons.

The EAM produced pulses of 50 ps duration as opposed to ~23 ps for the other two sources. Consequently, transmission performance was limited by signal to noise ratio. However, by increasing the pump power to the loop amplifiers it was possible to obtain adiabatic pulse compression on propagation and improve system performance. Again figure 5.6b illustrates the evolution of power with distance and clearly shows an initial 3 dB drop in amplitude as the pulses shed energy to form solitons from the original chirped profile ($\Delta\tau\Delta\upsilon$ = 0.44). On subsequent propagation the pulses compressed and developed a noticeable dispersive tail and error free transmission was limited to 12,000 km and this is in line with that expected theoretically.

Propagation of pulses from the PLEFRL resulted in a drop in amplitude of the 2.5 GHz component of <2 dB after 20,000 km of transmission and this was primarily due to the accumulation of timing jitter. Error free performance was possible to a distance of 17,600 km and is in very close agreement with analytic theory (18,000 km), suggesting that the system

was optimised since it was limited by both signal to noise ratio and Gordon - Haus jitter. This result represents an improvement on the best reported to date at this bit rate even with the use of fixed guiding filters[121]. In this case only a broad band (3 nm) filter has been used every 100 km to select the transmission path gain peak. This implies, for the first time, that soliton transmission with significant margin over global distances is possible with a very simple transmission path architecture.

It can therefore be concluded that source impairments do not limit the propagation of pulses generated by the PLEFRL. Thus, for the ultimate in transmission performance, without utilising soliton control, it is important to launch pulses that are very close to pure solitons.

In achieving these results the PLEFRL proved to be extremely stable in terms of pulse width, amplitude noise, timing jitter and wavelength jitter resulting in a soliton transmission system that did not require either narrow band optical filters or retiming modulators to span transoceanic distances with significant system margin. However, if the bit rate is to be increased to 5 Gbit/s analytic theory indicates that it is difficult to operate over 10,000 km with any margin. To increase the aggregate capacity it therefore seems sensible to utilise the extra degrees of freedom offered by wavelength, time and polarisation.

5.2.3.1 Polarisation division multiplexing

Polarisation division multiplexing (PDM) as proposed by Evangelides el at[122] offers the potential of doubling the capacity of a system with virtually no degradation in system performance. Demultiplexing a PDM signal may be achieved with polarisers provided that the two channels remain largely orthogonal on propagation. The advantage of this technique is that it offers greater immunity to timing jitter and soliton-soliton interactions than OTDM, since the bit period is twice as large. However, theoretical work to date has assumed that there is no polarisation dependent loss in the transmission path and, therefore, the two soliton data streams remain orthogonal. When a signal propagates through a PDL element the vector component of the electric field in the low loss polarisation state experiences less attenuation than the component orthogonal to it. This has the effect of rotating the field very slightly towards the lower loss polarisation state. Thus, in a PDM system both channels will be 'guided' towards the same state of polarisation. Consequently, orthogonality is lost and demultiplexing with simple polarisers may not be possible. Indeed in the limit an OTDM demultiplexer would be required , therefore, losing some of the advantages offered by PDM in terms of Gordon-Haus jitter and soliton-soliton interaction tolerance.

5.2.3.2 Polarisation guiding theory

The direction of an electrical field is rotated by a PDL element. Two initially orthogonal fields are rotated towards each other causing a reduction in the angle β between them. Figure 5.7 details the attraction of the two channels when passed through a PDL element of 0.165 dB. β is varied from 0 to π/2 radians and the angle from the low loss axis of the PDL element varied from 0 to 2π radians. When β = 0 the two co-polarised signals neither attract nor repel as would be expected. When β = π/2, as is the case for PDM, the two signals always attract, unless they are perfectly aligned with the two principal axes of the PDL element. Consequently, orthogonality will be lost on propagation down a transmission path containing any components with PDL.

The mean attraction over all of space is zero and in general β will follow a random walk. However, of greatest interest is the worst case scenario since at some point in time it is likely the polarisation state will tend to this.

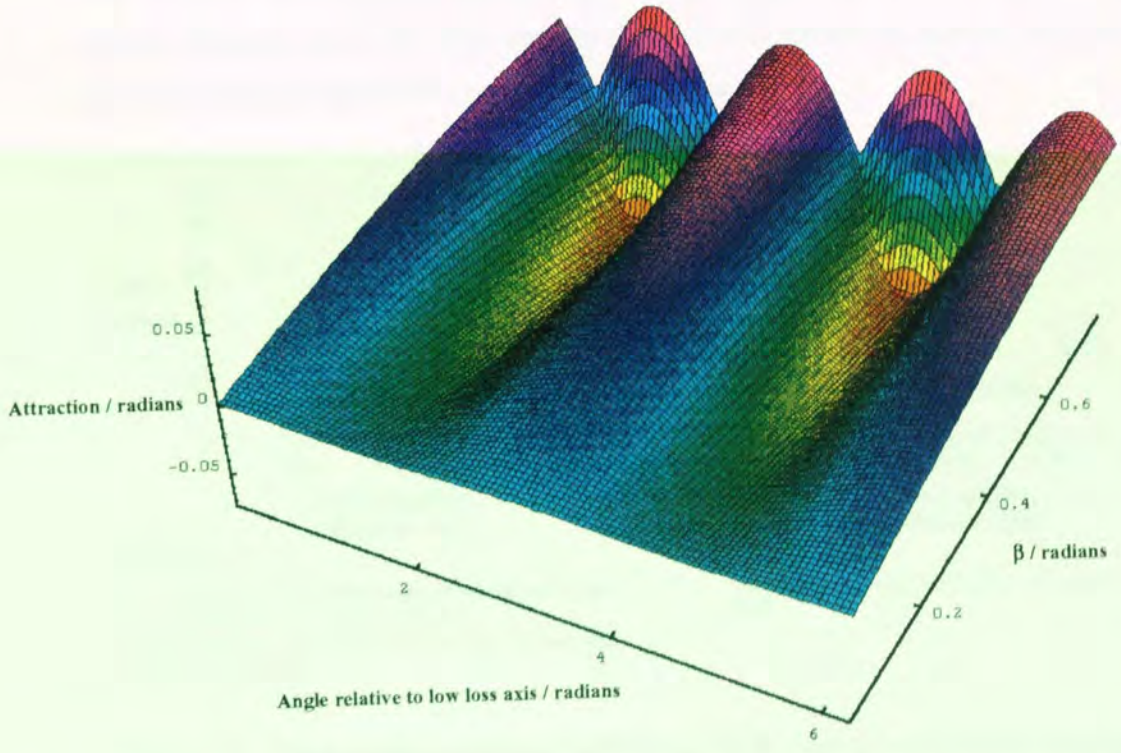

Figure 5.7. Polarisation rotation showing attraction with relative angle, β, and angle to low loss axis for PDL = 0.165 dB.

Assuming all i PDL elements of the transmission path are aligned with the low loss axis bisecting the two fields, then by summing the rotations of the fields caused by every element it can be shown that:

$$\beta = \frac{\pi}{2} - 2\tan^{-1}\tanh\left[\frac{i.\ln 10}{40} PDL(dB)\right] \qquad (5.5)$$

Figure 5.8a. details this curve for PDL = 0.165 dB to allow comparison with the experiment discussed in the next section. Figure 5.8b. shows the theoretical variation of total power of the two fields measured both parallel and orthogonal to the low loss state. In a real system the PDL elements will be randomly oriented to the incoming signal polarisation. Since there is no preferred direction, the mean relative rotation of the fields will be zero, however, there will be a significant standard deviation about this mean caused by the random walk effect. The second curve of Figure 5.8a shows the 6σ condition, corresponding to an error ratio of $1x10^{-9}$, for a system with elements having a mean PDL of 0.165 dB[123]. Clearly random alignment cannot be relied upon to eliminate the polarisation guiding effect and the use of polarisers for demultiplexing could lead to errors.

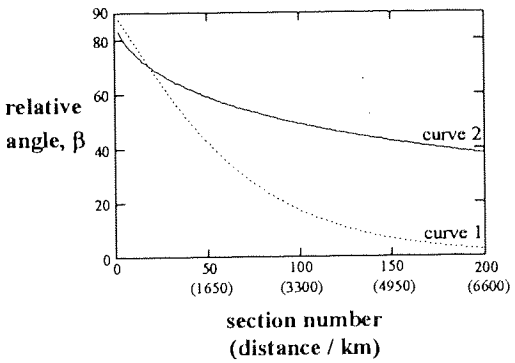

Figure 5.8a.

Curve 1: Systematic variation of β assuming all low loss states aligned at 45° to launch field vectors. PDL = 0.165 dB

Curve 2: 6 σ variation of β allowing PDL elements to be randomly oriented. PDL = 0.165 dB.

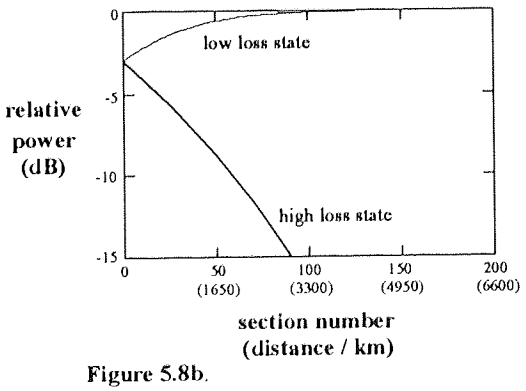

Figure 5.8b.

Theoretical power in high loss and low loss polarisation states

Figure 5.8. Theoretical evolution of relative angle, β, and signal power due to PDL.

5.2.3.3. Polarisation guiding experimental

The experimental configuration is illustrated in figure 5.9. Details of the soliton source and recirculating loop transmission path can be found in section 5.2.1 and 5.2.2

respectively. The ring laser pulse stream was modulated with a 2^7-1 PRBS pattern and bit interleaved to form a 2 x 2.5 Gbit.s^{-1} PDM/OTDM transmitted signal. At the receiver timing extraction was performed on the entire 5 Gbit.s^{-1} data stream, therefore removing start up ambiguities that occur from a demultiplexed recovered clock[124]. The data was optically time division demultiplexed to 2.5 Gbit.s^{-1} via a 20 GHz $LiNbO_3$ modulator, providing a 170 ps acceptance window to soliton jitter. A polariser with 30 dB extinction was situated in front of the demultiplexer to ensure that solitons from only one polarisation state were detected. The channel on which the bit error ratio was measured varied randomly on every loop cycle, ensuring that the BER was valid for the entire 5 Gbit.s^{-1} data stream. The mean transmission fibre dispersion at the operating wavelength was 0.5 ps.nm^{-1}.km^{-1} and the mean PDL per section was 0.165 dB. Polarisation controllers within loop allowed accurate control of the signal SOP's. In particular, the eigenstate that corresponded to the signal experiencing the same polarisation state on every recirculation could be found. The transmitter data stream was then configured such that both signal SOP's were at 45° to the low loss state of the loop.

Figure 5.10 details the evolution of power in the 5 GHz spectral component of the pulses in both the low loss and high loss eigenstates of the loop. With the polariser aligned to the low loss state an increase in power of 3 dB is observed as the two 2.5 Gbit/s channels rotate from initial orthogonality to being coincident in the low loss state at 3,000 km. With further transmission the spectral component diminishes due to the accumulation of timing jitter. Power in the high loss state falls rapidly as the signal rotates into the low loss SOP. Figure 5.10 is in excellent agreement with the theoretical plot given in figure 5.8b in which timing jitter is not included.

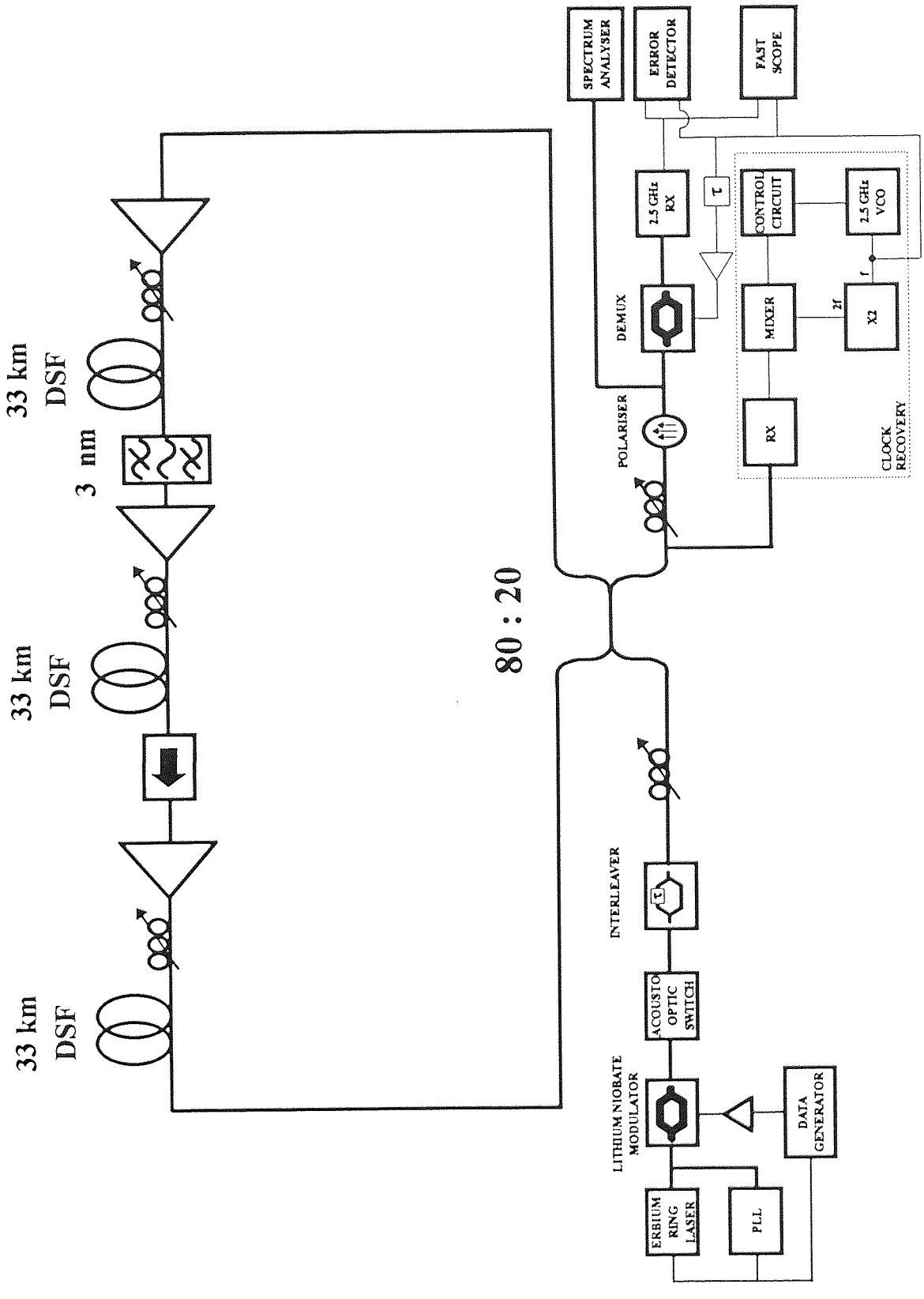

Figure 5.9. Recirculating loop configuration for PDM experiments.

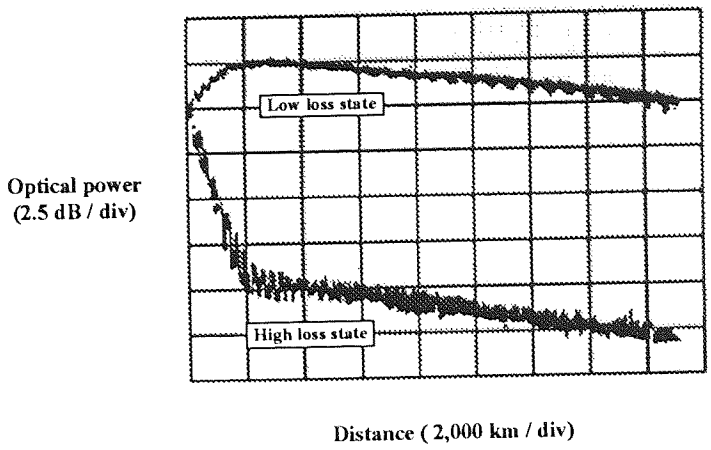

Figure 5.10. Evolution of power in 5 GHz component in low and high loss polarisation states when launching a PDM signal.

Figure 5.11 shows the pulse pattern detected through the polariser after 1,000 km of transmission with the polarisation at the receiver adjusted such that maximum signal power was obtained from one of the channels (channel 1). It can be seen that channel 2 is no longer orthogonal, 66% of its power is in the same polarisation state as channel 1.

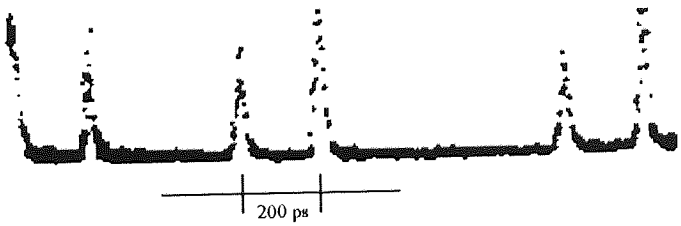

Figure 5.11. PDM pulse pattern at 1,000 km detected through a polariser.

To ascertain the validity of the data, BER measurements were performed on both channels after the signal had passed through the polariser. Error free operation was possible to a distance of 11,000 km where a 1×10^{-9} BER was measured, this compares well with other work in which significantly stronger wavelength guiding was utilised[125]. Further transmission resulted in errors due to soliton timing jitter. It is thought that this was due to the combined effects of Gordon-Haus jitter and soliton-soliton interaction. Since no transmission control is utilised, Gordon-Haus jitter builds rapidly over the first few 1000's km and results in the possibility of adjacent solitons being jittered much closer together. Also over this distance the two channels rotate into the same polarisation state. Consequently, on subsequent

transmission far stronger interaction forces are experienced than would be expected for unperturbed solitons. Figure 5.12 shows the received pulse pattern at 15,600 km revealing soliton-soliton attraction on adjacent 'l's with isolated 'l's appearing to be unaffected. To reduce the interaction forces one of the channels was disconnected at the transmitter and BER measurements performed on the other through the OTDM demultiplexer. Error free operation was possible to a distance of 15,600 km which is in agreement with analytic theory as being the Gordon-Haus limit for this system. Thus, it was concluded that soliton-soliton interaction was limiting the maximum transmission distance in the two channel experiment.

Figure 5.12. Bandlimited pulse pattern at 15,600 km showing soliton-soliton interaction on adjacent ones.

For long haul systems with significant PDL it may not be possible to accurately demultiplex PDM channels with polarisers and OTDM techniques must be used. Consequently, the allowed acceptance window is decreased making the system less tolerant to jitter. However, launching PDM signals reduces soliton-soliton interactions up to the point where the channels are co-aligned and some benefit is realised.

5.2.4. Optical time division multiplexing

For a given capacity OTDM allows the receiver bandwidth to be reduced over that of a non-multiplexed system and thus gives an advantage in terms of signal to noise ratio. Additionally, optical gates such as the non-linear loop mirror[126,127] allow switching windows that pass almost the entire bit period. Thus, a soliton can be jittered to the extremes of its time slot and still be passed through to the electrical detector. The band-limiting effect of the receiver will integrate the jittered pulse such that it can be detected without an error occurring. In contrast, a receiver not using OTDM will again integrate the same pulse but this time into

both its time slot and the one next to it, incurring an error. These advantages suggest that it may be possible to utilise OTDM to increase the aggregate line rate of a transmission system.

The experiment detailed in the previous section utilised an OTDM demultiplexer and PDM/OTDM transmitter. The results obtained indicate that part of the advantages offered by OTDM are negated by the combined effects of Gordon-Haus jitter and soliton-soliton interactions. In order to span oceanic distances at very high aggregate capacities multiplexing in time and/or polarisation alone is not sufficient. One option would be to multiplex many wavelengths, requiring gain flattening techniques for the optical amplifiers. Another is to use soliton transmission control at periods along the link and this is the topic of the next section.

5.3. Soliton transmission with control

To allow very high bit rate transmission over global distances various soliton control schemes have been proposed and some experimentally verified. All of the techniques rely on limiting degrees of freedom of the soliton. In particular, control of the temporal and/or spectral perturbations has to be realised. The remainder of this chapter will discuss the advantages and disadvantages of transmission control via spectral filtering and then move on to concentrate on the experimental investigation of various soliton retiming schemes. In particular synchronous modulation of amplitude is utilised and for the first time the use of phase modulation is practically demonstrated by an all optical technique in the transmission fibre itself.

5.3.1. Soliton control in the frequency domain

The major limitation to ultra-long haul soliton transmission is the accumulation of timing jitter, as detailed in section 5.1. It has been shown that the mean square pulse position fluctuations increase with the cube of distance for the Gordon-Haus effect[128], equation 5.1, and with the fourth power of distance for the acousto-optic effect[129], equation 5.2. However, if the extent to which the soliton's centre wavelength can be perturbed is limited the temporal fluctuations will also be reduced. One way of achieving this is to place narrow band optical filters with a centre wavelength equal to that of the unperturbed soliton at periods along the transmission path[130]. Wavelengths away from the centre of the pass-band will be attenuated more than those at the centre when a soliton propagates though the filter. Consequently, the average wavelength of the soliton is 'guided' towards the unperturbed value, reducing the accumulation of timing jitter. For the Gordon-Haus effect the mean square fluctuations of

frequency reach a steady state level and the mean square position fluctuations increase only linearly[131]. The mean square pulse position variations for the acousto-optic effect are damped such that they increase with the square of distance. Additionally, by utilising multi-peaked guiding filters such as etalons it is possible to control all channels of a WDM link simultaneously[132] and this is clearly an advantage of the technique. Moreover, since only optical filters are required the approach is passive.

However, in order to maintain the fundamental soliton amplitude, energy that has been attenuated by the guiding filters must be compensated for by excess gain from the line amplifiers. To reduce temporal jitter further it is necessary to use 'stronger' guiding filters (narrower band) resulting in greater attenuation of the solitons from each filter. The associated increase in excess gain is accompanied by the generation of more ASE at the filter gain peak and ultimately the system becomes noise limited. Clearly a compromise exists between adequate guiding to minimise timing errors and adequate signal to noise ratio to minimise energy fluctuations. Mollenauer et al[133] found that the filter producing the minimum error ratio was just strong enough to reduce the standard deviation in timing jitter by approximately half at the transpacific distance.

This technique has been used to considerable effect in propagating 20 Gbit/s data over 11,500 km[134], far in excess of the Gordon-Haus limit. In order to achieve this alternating-amplitude solitons were used to reduce soliton-soliton interactions[135,136]. However, even this result does not allow sufficient system margin over the transpacific distance and an improved control technique is required.

The accumulation of ASE down the transmission line can be greatly reduced by slightly offsetting the centre wavelength of each guiding filter. The non-linear nature of the soliton pulses enables new spectral components to be generated that allows them to follow the shift in gain peak of the system but noise from amplifiers earlier in the link will be attenuated by subsequent filtering. In so doing the transmission path becomes substantially opaque to noise while remaining transparent to the data. Consequently it is possible to utilise much stronger guiding and thus enhance the reduction in timing jitter accumulation. The technique is known as 'sliding frequency guiding filter' soliton control[137]. Another advantage of the scheme is that if imperfect $sech^2$ pulses are transmitted into the link the dispersive wave radiation will tend to be left with the ASE, thus, reducing the restrictions placed on the soliton source. Sliding guiding soliton control has allowed 10 Gbit/s data to be transmitted over 35,000 km and 15 Gbit/s over 25,000 km[138] (both 2 channel PDM), single channel 20 Gbit/s over 14,000 km[139] and 2x10 Gbit/s WDM over 13,000 km[140]. Again the approach is optically passive and this is desirable.

Recent work suggests that in practically realisable systems the technique is limited to around 20 Gbit/s for each channel over oceanic distances by the effects of soliton-soliton interactions and the soliton period[141]. Also, from a systems implementation point of view the use of narrow band filters at every amplifier, with different centre wavelengths, is not desirable in terms of reliability and maintenance. In light of this and the excellent work undertaken by others already the use of guiding filters alone is not investigated experimentally in this thesis. Instead two options for synchronous retiming of solitons will be discussed that allow both very high speed operation and ultra-long haul propagation.

5.3.2. Soliton control by synchronous amplitude modulation

It has been theoretically[142] shown and experimentally verified[143] that virtually unlimited transmission is possible by using soliton controls in the time and frequency domains. Synchronous modulation of amplitude allows retiming of the soliton pulse position, correcting for temporal jitter, removal of the effects of soliton-soliton interaction and suppression of the accumulation of ASE. The amplitude modulator is driven by a sine wave derived from a recovered clock signal and timed such that the solitons pass through the peak of transmission. A pulse experiencing temporal jitter, from the Gordon-Haus effect, acousto-optic effect or soliton-soliton interactions, will be attenuated more on one edge than the other. Consequently, the centre of gravity of the pulse is pulled back towards the middle of the time slot, in close analogy with guiding filters. The attenuation suffered by the soliton is compensated for by excess gain from the amplifiers. Any ASE components away from the centre of the time slot will also be attenuated. With dispersion all wavelengths, other than the soliton wavelength, will walk through the bit period suffering attenuation on propagation through the retiming units and thus noise accumulation is suppressed.

A particularly attractive approach to the transmission of very high capacity data is the use of optical time division multiplexing (OTDM), to allow increases in the aggregate line rate, allied with soliton propagation. However, in addition to the accumulation of timing jitter and amplitude noise when transmitted over ultra-long distances, further difficulties arise as the aggregate data rate is increased since it becomes necessary to reduce the pulse width and thus the soliton period. To ensure applicability of the average soliton model the amplifier spacing should also be decreased and this adversely affects system design in terms of economics and reliability. Source imperfections can result in dispersive wave radiation coupling closely spaced adjacent solitons thus enhancing soliton-soliton interactions and timing jitter. However, by applying a small degree of synchronous amplitude modulation at periods along

the transmission path it is not only possible to stabilise the energy and temporal position of the solitons but also to increase the repeater spacing over that normally required[144] and simultaneously ease the requirements placed upon the soliton source. These benefits are illustrated and used to good effect in this section to demonstrate for the first time the transmission of 20 Gbit/s data over global distances.

5.3.2.1. 20 Gbit/s experimental soliton transmission with amplitude control

Figure 5.13 details the recirculating loop configuration used in the transmission experiments. 10 GHz pulses from a harmonically mode locked external cavity semiconductor laser were modulated with a 2^7-1 PRBS data stream by a $LiNbO_3$ Mach-Zehnder interferometer and compressed down to 6 ps in a 300 m length of dispersion compensating fibre (DCF). The resultant signal was passively interleaved into a co-polarised 20 Gbit/s data stream and gated into the loop via an acousto-optic switch and a 80:20 fused fibre coupler. Transmission control was achieved by a 1 nm bandpass filter and a 26 GHz GaAs amplitude modulator which incorporated a 30 dB extinction polariser that necessitated the use of a polarisation controller within the loop. The round trip loss was compensated by four erbium doped fibre amplifiers with noise figures ~5 dB. At the receiver timing recovery was performed by a 20 GHz electronic phase locked loop (PLL). The PLL voltage controlled oscillator (VCO) operated at 10 GHz and was used to drive the error detector and the $LiNbO_3$ demultiplexer. The output of the VCO was also used to drive a microwave frequency doubler to derive a phase locked 20 GHz reference that fed the loop retiming modulator. Note that it was essential to perform timing extraction at the full line rate since the component at the base rate of 10 GHz was negligible, especially under transmission control.

5.3.2.2. 20 Gbit/s soliton transmission with amplitude control results and discussion

With transmission control disabled error free operation, BER < $1x10^{-9}$, was limited to a distance of 2,000 km by the accumulation of timing jitter. The path average fibre dispersion at the operating wavelength was 0.33 ps/nm/km and the time bandwidth product of the source was 0.6. When retiming was utilised the data stream propagated a distance of 125,000 km error free. Figure 5.14a details the 20 Gbit/s eye diagram detected on a 20 GHz *pin* and also the demultiplexed bandlimited eye. Further transmission was limited only by the state of signal polarisation drifting out of alignment with the polariser during the elongated measurement cycle.

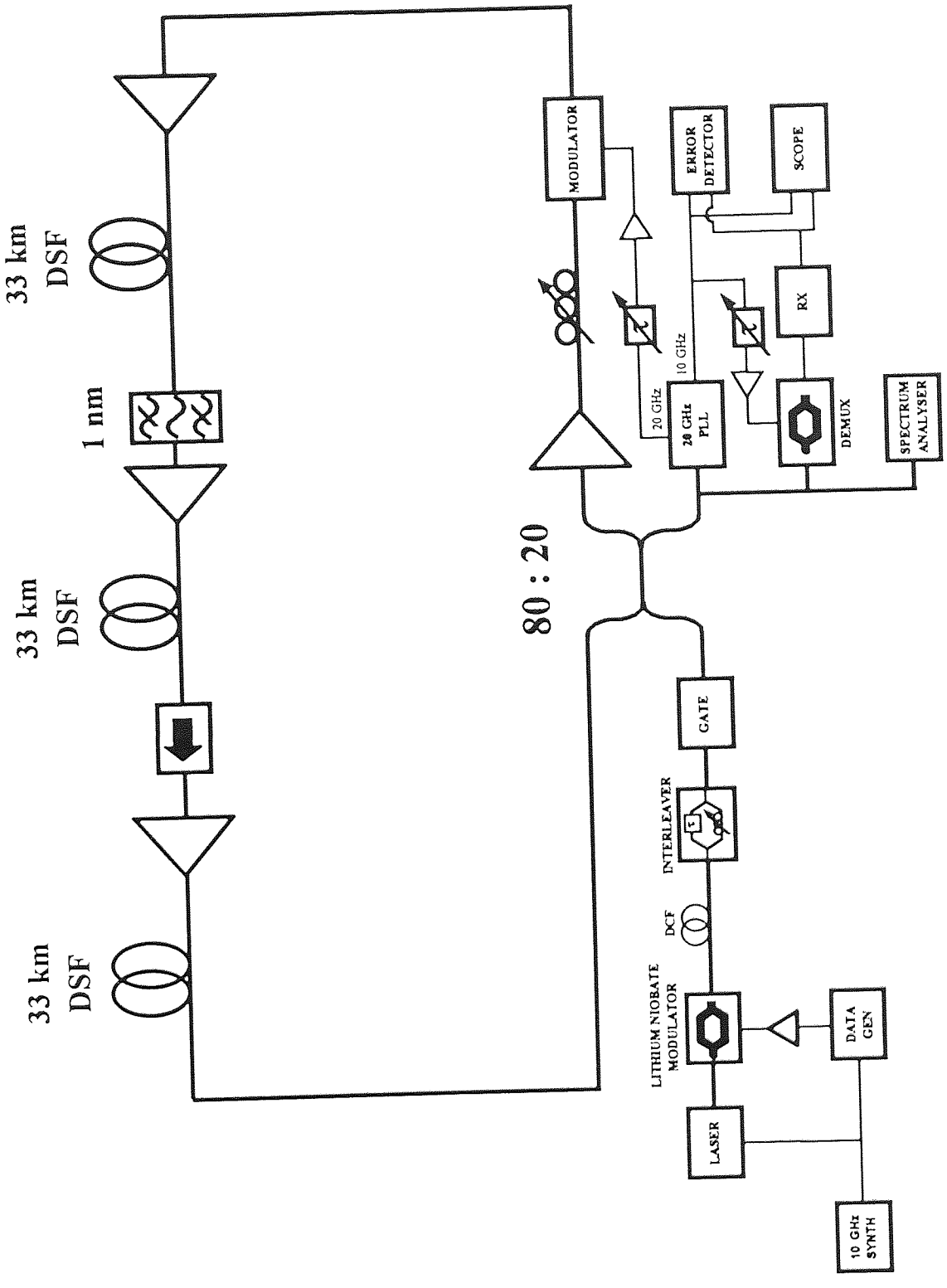

Figure 5.13. Recirculating loop configuration with amplitude modulation control.

The $V\pi$ of the transmission control modulator was in excess of 25 V and the 20 GHz sine wave applied to stabilise the transmission had a peak to peak value of 1.4 V, indicating that the degree of optical modulation required was very small. The pulse width of the recirculating solitons was measured on an auto-correlator to be 6 ps giving a mark-space ratio of 1:8. Indeed, pulses of greater width than this have been successfully utilised in the transmission of 40 Gbit/s data[145], suggesting that this system could easily support an upgrade in capacity via a further stage of OTDM.

The ratio of the soliton period, z_o, to the amplifier spacing, z_A, was only 1.3 resulting in resonances occurring in the spectrum of the solitons. Variation in loop pump power allowed the width of the propagating solitons, t_p (FWHM), to be adjusted from 8 ps to 5 ps, and this also varied the amplitude of the sidebands in the spectrum. However, the spectral position of these resonances, $\delta\nu_n$ (Hz), did not vary significantly with pulse width as predicted by theory[146]:

$$\delta\nu_n = \pm\frac{1}{2\pi t_p}\sqrt{1+8n\frac{z_0}{z_A}} \tag{4.6}$$

noting that $z_o \alpha t_p^2$ and that n is the sideband order.

For the values applicable to this experiment the first sideband is predicted to be 0.65 nm away from the peak. Experimentally it was measured to be 0.6 nm and is depicted in figure 5.14b which was measured on an analyser with a resolution of 0.1 nm. Clearly, the use of synchronous transmission control has allowed stable propagation even when the soliton period approached the amplifier spacing.

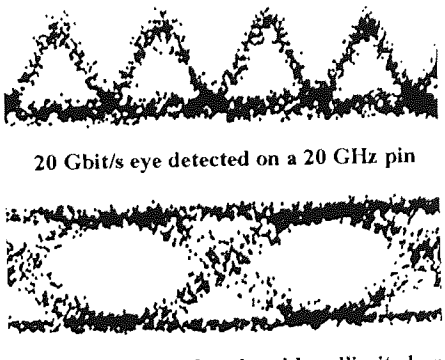

20 Gbit/s eye detected on a 20 GHz pin

10 Gbit/s demultiplexed and bandlimited eye

Fig. 5.14a. 125,000 km eye diagrams.

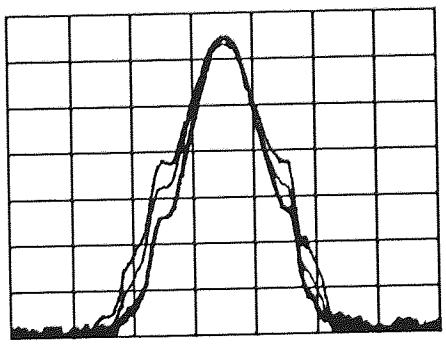

Fig. 5.14b. Optical spectra of propagating solitons for pulse widths of 5, 6.5 & 8 ps

Figure 5.14. Transmission results of 20 Gbit/s solitons at 125,000 km, 20 Gbit/s and 10 Gbit/s eye diagrams and optical spectra for pulse widths of 5, 6.5 and 8 ps.

5.3.2.3. Summary

The application of OTDM and soliton control in enabling error free operation of 20 Gbit/s data over global distances has been demonstrated. Additionally, the technique has allowed the soliton period to approach the amplifier spacing and this is desirable from a system design view point, particularly at very high data rates. The pulse width used was 6 ps thus enabling a possible upgrade to 40 Gbit/s via an additional stage of OTDM. Suppression of the residual frequency component at the base rate due to the retiming process necessitated clock recovery to be performed at the full line rate.

5.3.3. Soliton control by synchronous phase modulation

Theoretical studies[147] have indicated that soliton control by synchronous modulation in phase is capable of providing superior suppression of Gordon-Haus jitter than that of amplitude modulation. In such a system optical filters and phase modulators driven by a recovered clock are placed at periods along the transmission path. The modulator is configured such that solitons arriving at the correct time experience no net phase shift. However, those that are temporally jittered experience a net phase modulation. On propagation through subsequent soliton supporting fibre the imposed phase shifts are used to correct for the original temporal jitter.

The transfer function of an electro-optic phase modulator is given by:

$$u_{out} = u_{in} e^{i\Phi \cos w_m t} \tag{5.7}$$

where, Φ is the peak phase excursion and ω_m the angular drive frequency of the modulator. It was shown[60] that the expected timing variance for an ensemble of solitons in such a system is given by:

$$\left\langle T^2(z) \right\rangle = \frac{\beta_2 \left\langle \sigma^2 \right\rangle}{8\alpha_{m2}\gamma} \left[1 + \frac{\gamma}{\kappa^2} e^{-2\gamma z} \left(\frac{2\alpha_{m2}\beta_2}{\gamma} - \tfrac{1}{2}(\gamma + \kappa) e^{2\kappa z} - \tfrac{1}{2}(\gamma - \kappa) e^{-2\kappa z} \right) \right] \tag{5.8}$$

where, $\beta_2 = \delta^2\beta/\delta\omega^2$ dispersion, $\sigma = n_{sp}(G\text{-}1)$ noise spectral density, $\alpha_{m2} = \Phi\omega_m{}^2/2l_m$ modulator chirp parameter, l_m is the modulator spacing, $\gamma = 2/3\Omega^2 l_f \tau^2$, with Ω the bandwidth of the optical filter and l_f the filter spacing, $\kappa^2 = \gamma^2 - 2\alpha_{m2}\beta_2$.

Figure 5.15 details the accumulation of Gordon-Haus jitter with distance for a system with pulse width 20 ps, amplifier, filter and modulator spacing of 30 km, n_{sp} = 1.5, filter bandwidth of 1.2 nm and peak phase excursion of 1 mrad at 5 GHz. Also shown in the diagram is the unconstrained case whereby neither guiding filters nor phase modulation is utilised and the case for a system with just the filter acting as the control mechanism.

Further work has highlighted the potential of the technique in suppressing soliton-soliton interactions[148]. Thus it would seem that synchronous phase modulation may be a particularly attractive approach to soliton transmission control.

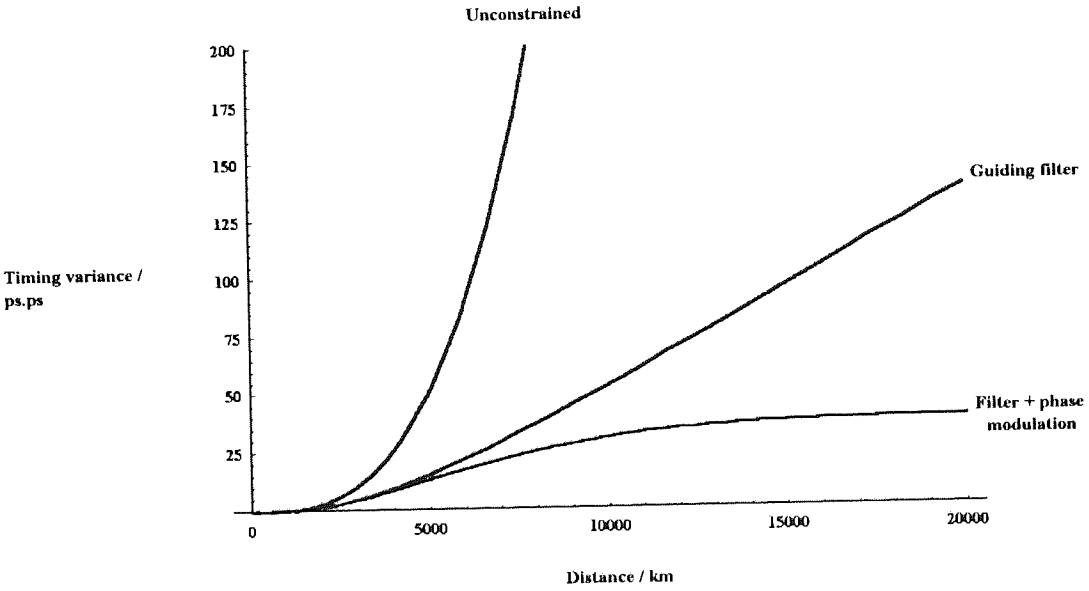

Figure 5.15. Jitter accumulation for uncontrolled system, filtered and filtered + phase modulation.

5.3.4. All optical transmission control: Soliton shepherding

The previous sections have demonstrated the effectiveness of using both amplitude and phase modulation in the control of soliton transmission. However, if these techniques are to be employed at much higher bit rates very high speed modulators and associated electronics are required at periods down the system. In many cases these components do not yet exist and the reliability of such devices is a serious issue. In this section a particularly elegant active technique[149] is demonstrated for the first time whereby non-linear interaction in length of optical fibre allows a clock signal to retime (shepherd) the soliton data. Since, modulation is

provided by non-linear processes in the transmission fibre itself ultra-high speed operation should be realisable. Indeed, all optical clock extraction has been previously demonstrated at 40 Gbit/s[150].

5.3.4.1 The soliton shepherding technique

Schematically the soliton shepherding concept is illustrated in figure 5.16. By temporally overlapping a clock and soliton data stream in a non-linear medium a phase profile ($\Delta\phi(t)$) is imposed on the solitons by the clock pulses. Owing to the particle like nature of the soliton, the imposed phase modulation is distributed over the whole pulse resulting in a net shift in carrier frequency. The sign and magnitude of this shift depend on the position of the soliton relative to the clock pulse. If this effect is combined with an appropriate sign and magnitude of fibre dispersion, D, the imposed frequency shifts can be converted into suitable time delays to correct for the original temporal misplacement. Hence, we 'shepherd' the soliton towards the centre of the time slot as defined by the clock pulse.

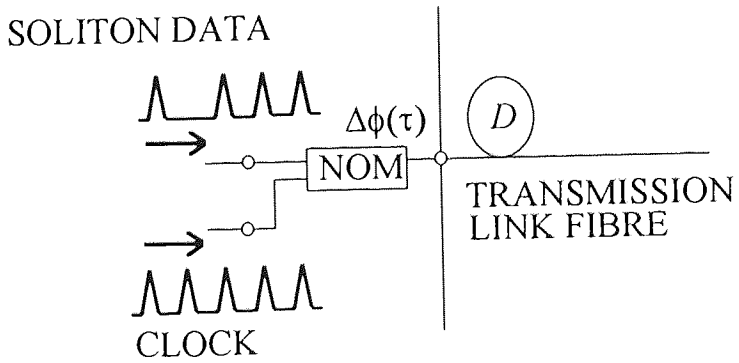

Figure 5.16. The soliton shepherd concept.

In order to keep the transmission path optically passive it is desirable to utilise the non-linear properties of the optical fibre to realise the phase modulation. In this case cross phase modulation (XPM) is used and the shape of the imposed phase profile depends on the width of the clock pulse and the group delay difference between the signal and clock (walk-off). XPM in conjunction with soliton supporting dispersion present within the transmission link act together to temporally guide the soliton bits.

5.3.4.2. *Soliton shepherding experimental*

The recirculating loop configuration used in the soliton shepherding experiments is shown in figure 5.17.

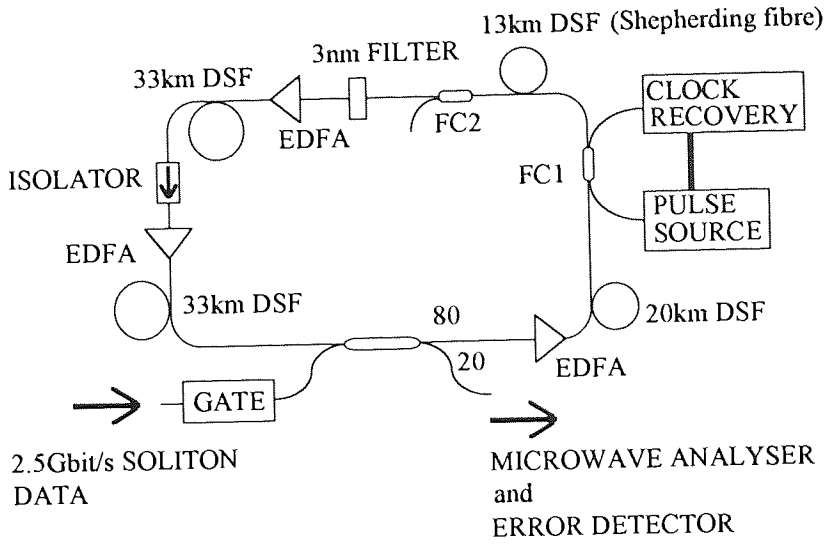

Figure 5.17. Recirculating loop configuration for soliton shepherding experiment.

The soliton source was the PLEFRL detailed in section 5.2.1, producing 23 ps FWHM pulses at 1562 nm. The retiming pulses were derived from a 2.5 GHz PLL clock recovery circuit used to externally modulate ($LiNbO_3$) a cw DFB laser. The resulting 50 ps duration pulses where tuned to a wavelength of 1538 nm in order to closely match the group delay difference between the signal and clock pulses co-propagating in a 13 km length of the loop transmission fibre. The clock pulses were launched into and out of the shepherding fibre via fused fibre couplers FC1 and FC2 respectively. The path average dispersion of the loop at the signal wavelength was 1 ps/nm/km giving rise to a theoretical accumulated timing jitter of 22 ps rms at 9,000 km resulting in a calculated BER of 1×10^{-9}.

5.3.4.3 *Soliton shepherding results and discussion*

Figure 5.18 details the evolution of power in the 2.5, 10 and 20 GHz r.f. components of the soliton data stream with distance with and without shepherding. Without retiming the high harmonics rapidly diminish as a consequence of timing jitter increasing the effective rms pulse width. However, the presence of only a weak shepherding beam (-13 dBm mean) is sufficient to suppress the soliton decay. In this case the 20 GHz component of the microwave spectrum has dropped by less than 2 dB at 20,000 km, indicating the effectiveness of the technique in constraining the solitons to their correct time slots.

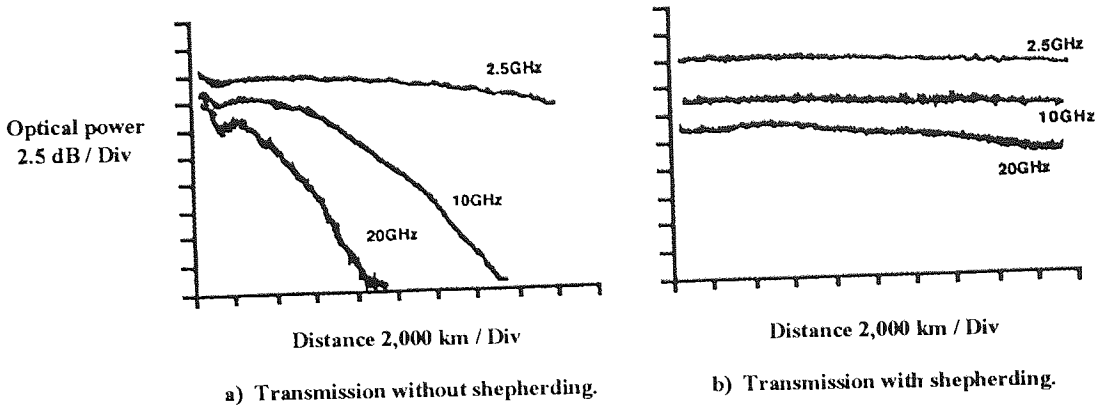

Figure 5.18. Evolution of soliton harmonics with and without shepherding.

The peak value of phase modulation obtained from the clock beam can be calculated from equation 4.12. (assuming zero walk through):

$$\phi_{\max} = \gamma P_o z_{eff} = \left(\frac{n_2 \omega_o}{c A_{eff}}\right)\left(2 P_{mean} \frac{T_o}{\tau_{shep}}\right)\left(\frac{1 - e^{-\alpha L}}{\alpha}\right) \tag{5.9}$$

where, P_{mean} is the mean clock power entering the shepherding fibre and τ_{shep} is the FWHM of the clock pulse. For the numbers appropriate to this experiment the peak phase excursion is calculated to be only ~0.01 radians.

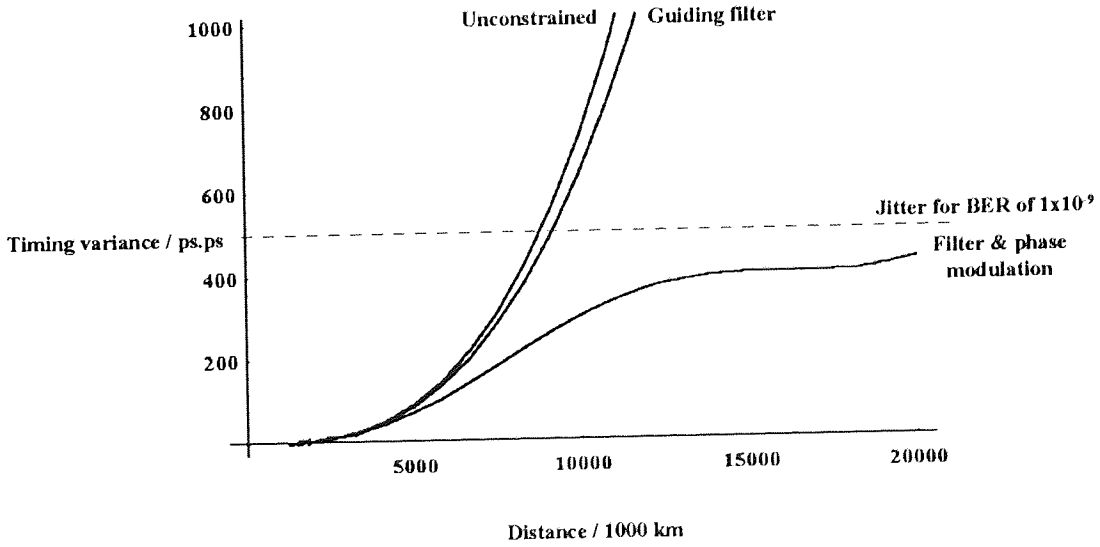

Figure 5.19. Simulation of timing jitter accumulation for soliton shepherding experiment, also shown is the unconstrained case and that of just the guiding filter.

Figure 5.19 details the theoretical evolution of timing jitter derived from equation 5.8. Also shown in Figure 5.19 is the unconstrained case and that for the action of just the guiding filter. The line on the diagram indicates the timing variance for which a BER of $1x10^{-9}$ is incurred. It can be seen that the degree of timing jitter predicted is just sufficient to obtain error free operation at 20,000 km. If the power in the shepherding beam was increased this distance would be increased further.

Experimentally, without application of the shepherding beam the error free distance was limited to 9,000 km. This is in excellent agreement with analytic theory, figure 5.19, suggesting that the acousto-optic effect was the major limitation. When the shepherding beam was applied the error free distance was extended to in excess of 20,000 km as suggested by figure 5.19. This limit on transmission distance was governed by a delay generator used in the experiment and not a restriction fundamental to the soliton shepherding technique.

5.3.4.4. Soliton shepherding summary

A stream of optical pulses has been used to retime high speed data using non-linear interaction in length of transmission fibre. This very simple all-optical 'regenerative' technique has allowed the control of soliton data over global distances.

One of the main advantages of this form of soliton control is that it is not necessary to use very high speed optical modulators and associated drive electronics. The control signal can be derived from a laser producing short pulses at a reasonable repetition rate, for example a 10 GHz laser giving 1 ps FWHM pulses[151]. The output of this device can then be passively interleaved to form the required control signal enabling soliton control at bit rates of 100's Gbit/s. Even at these data rates the power required in the retiming beam is only around 0 dBm. Alternatively, all optical clock recovery techniques[152] may be exploited in conjunction with this regenerative process allowing direct retiming of ultra-high bit rate data streams resulting in an entirely optical control scheme.

In addition to soliton shepherding, saturable absorbers can be used in the transmission path as an alternative technique for stabilising propagation at ultra-high bit rates. These may be realised from semiconductor optical amplifiers[153] or non-linear loop mirrors[154]. With these devices low power background waves, such as ASE and DWR, are discriminated against, while higher power soliton pulses switch the device into transmittance. These techniques offer significant potential for future ultra-long haul systems since they enable almost truly digital signals to be continuously processed along the transmission line.

5.4. Conclusions

The propagation of 2.5 Gbit/s soliton data has been demonstrated over the theoretical maximum distance of 17,600 km without transmission control. This results implies, for the first time, that soliton transmission with significant margin over global distances is possible with a very simple transmission path architecture. In achieving this a new stabilisation scheme has been devised for the erbium fibre ring laser.

It has been shown that polarisation rotation due to PDL in practically realisable systems precludes the use of a simple polariser as the demultiplexer. In general an OTDM demultiplexer is required and this nullifies many of the advantages of PDM. However, some benefit is obtained in terms of soliton-soliton interactions. The use of OTDM to increase the aggregate capacity is ultimately limited by the combined effects of soliton-soliton interactions and temporal jitter.

At higher bit rates timing jitter severely limits system performance and some form of soliton transmission control is required. By using synchronous modulation of amplitude 20 Gbit/s soliton data has been transmitted in excess of 100,000 km for the first time. Since, temporal jitter is significantly suppressed, the advantages offered by OTDM were also exploited. This allowed the electronics to operate at an accessible base rate and the aggregate system capacity to operate in excess of this. The technique also allowed the amplifier spacing to approach the soliton period, and this is clearly an advantageous from a system implementation view point.

At bit rates of 40 Gbit/s and above electro-optic modulators and associated drive electronics are difficult to source. To alleviate this restriction a new all optical technique for achieving soliton control by synchronous modulation of phase has been demonstrated for the first time. Modulation was achieved using Kerr non-linearity in the transmission fibre itself and consequently the technique should allow operation at ultra-high bit rates.

Chapter 6.

6. Conclusions.

This thesis has experimentally examined the viability of three options for optical fibre transmission over global distances. Clearly it is by no means complete, issues such as reliability, ageing, power consumption and cost must be addressed before any system would be considered for implementation. However, practical insight into what is possible in terms of transmission has been considered with current technologies.

The old and established technology of opto-electronic regenerators has been demonstrated to offer significant advantages over the alternatives, particularly in terms of repeater spacing and polarisation sensitivity. In this thesis, 5 Gbit/s data has been propagated over 500,000 km and 10 Gbit/s over 400,000 km. In both cases error free operation was maintained irrespective of the signal state of polarisation, and this is most desirable in terms of system robustness and reliability. Additionally, the repeater spacings in these experiments were 205 km and 160 km respectively, no other format of transmission system offers global propagation with such few repeater housings. The use of directly modulated DFB lasers allowed reduced cost and increased reliability, whilst simultaneously increasing the stimulated Brillouin scattering threshold enabling higher launch powers. It is difficult to see a more practical topology for immediate deployment since by system optimisation 10 Gbit/s operation is viable with a spacing between regenerators in excess of 200 km.

Research in to high speed electronics has realised many one off devices operating at 40 Gbit/s and given the track record of the industry it is highly probable that such components will be readily available in the not too distant future. The use of optical amplifiers as the gain medium removes many of the restrictions placed on the electronic components since far less electrical gain is required. Ultimately the possibility of fabricating 40 Gbit/s devices together with semiconductor laser amplifiers appears particularly attractive in terms of system reliability and power consumption.

It has been shown that optically amplified NRZ systems suffer from accumulated system impairments due to their inherently analogue nature. In order to maintain acceptable signal to noise ratio and also acceptable pulse distortion from optical non-linearities the amplifier spacing must be kept short. This necessities the use of many repeater housings, adversely affecting system cost and reliability. It has been demonstrated that dispersion maps must be used at bit rates of 5 Gbit/s and above to alleviate the detrimental effects of four wave mixing, self phase modulation and group velocity dispersion. Upgrading the system by multiplexing in wavelength is therefore precluded. Additionally, polarisation dependent loss and gain require the transmitted state of signal polarisation to be scrambled to minimise system fades as the signal state of polarisation evolves with time. A novel, optically passive polarisation scrambler is detailed for the first time that, unlike other techniques, is capable of operation at ultra high speeds. Upgrading amplified NRZ links by multiplexing in polarisation is thus precluded. Consequently, it appears most unlikely that such systems will be viable over oceanic distances at bit rates above 10 Gbit/s.

The use of optical solitons as the data bits to overcome transmission impairments due to non-linearity and dispersion allows distortion free transmission. However, soliton transmission without control offers very little advantage in terms of system performance over that of NRZ data format even though it is digital in nature. It has been shown that at higher bit rates temporal jitter severely restricts the maximum transmission distance achievable. Further, polarisation rotation due to PDL in practical amplifier components nullifies many of the advantages of multiplexing in polarisation. Consequently, it is not possible to double the system capacity with PDM. Additionally, the combined effects of accumulated temporal jitter and soliton-soliton interaction offset the advantages offered by OTDM. It has also been shown that to realise the ultimate in transmission performance stringent restrictions are placed on the soliton source at the transmitter. A new control scheme for the stabilisation of mode locked erbium doped fibre ring lasers has allowed 2.5 Gbit/s data to propagate to the theoretical maximum distance of 17,600 km.

With appropriate transmission control unlimited propagation is possible at very high bit rates. Retiming of the soliton data stream has been realised by synchronous amplitude modulation and allowed 20 Gbit/s data to propagate over 125,000 km. The suppression of temporal jitter enabled the benefits afforded by OTDM to be exploited. Additionally, this technique removed many of the restrictions placed on the soliton source and enabled the average soliton model to be violated allowing extended amplifier spacing.

Ultimately the speed of operation of such systems is limited by the bandwidth of the electronics available and all optical techniques offer a solution. In this thesis the use of all

optical soliton transmission control has been demonstrated for the first time. Modulation was achieved using Kerr non-linearity in the transmission fibre itself and consequently should allow operation at ultra-high bit rates. In addition to the soliton shepherding technique detailed here, saturable absorbers and non-linear loop mirrors offer alternative schemes for stabilising transmission at ultra-high bit rates. These techniques offer significant potential for future ultra-long haul systems since they enable almost truly digital signals to be continuously processed along the transmission line.

In conclusion, digital transmission using opto-electronic regenerators appears to offer the most robust implementation for bit rates up to 10 Gbit/s allowing unparalleled repeater spacings. In order to obtain similar performance for ultra-high capacities, moves towards a fully digital all optical approach needs to be taken with optical solitons as the data bits.

Appendix 1.

A.1. Transient phase errors on a recovered clock when used on a recirculating loop.

Figure A.1. schematically details data propagating around a recirculating loop with transit time τ. Part a) of the diagram shows each recirculation as a block of data. Between each block there is a gap the width, m, of which is governed by the resolution of the pulse generator used to gate the acousto-optic switch at the transmitter (in the case of the experiments detailed in this thesis the resolution of the pulse generator used was 1 μs). Part b) of the diagram shows an exploded view of the data at the end of one recirculation, the gap and the data at the start of the next recirculation. Illustrated in part c) is the phase of the data.

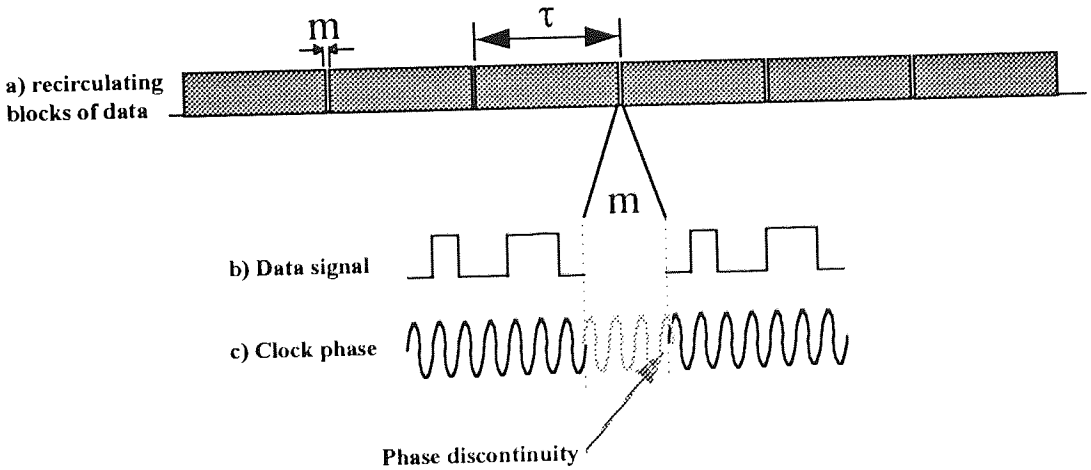

Figure A.1. Clock recovery drop out due to phase discontinuities.

Unless the transit time of the loop, τ, is an exact integer number of bit periods there will be a phase discontinuity at the start of each recirculation. By making minor adjustment to the transmitted clock frequency it is possible to establish the condition of phase coherence between successive recirculations. However, the length of the loop varies with temperature making it necessary to continuously adjust the clock frequency. One method of achieving this would be to use a phase locked loop similar to that detailed in section 4.2.1 for stabilisation of a ring laser. However, the PLL would have to integrate an error signal over many recirculations resulting in a bandwidth of ~100 Hz. With such a small bandwidth it would be

extremely difficult to lock the PLL in the first place. Consequently this solution is impractical.

If the transmitted clock frequency is fixed and the loop length allowed to vary with temperature the sign and magnitude of the phase discontinuity will vary with time. When a PLL clock recovery circuit is used on the output of the loop, as is the case for the regenerator work and that of the soliton control with synchronous retiming, the PLL has to regain phase lock at the start of each recirculation. During this time the phase output by the PLL will be errored and varying. Any phase errors incurred in previous clock recovery circuits or previous recirculations will be added to resulting in an increased phase error with time, or number of PLL circuits encountered. Thus, when this scheme is used over very long distances errors occur at the start of each recirculation towards the end of the measurement period. By manually tuning the transmitted clock it is possible to remove these errors since the PLL input can be made to be of continuous phase. In a cascaded system this problem would not occur since the data and its associated phase are continuous and, thus, it can be considered as a loop specific artefact.

References

[1] A. W. Snyder and J. D. Love.:'Optical waveguide theory', Chapman and Hall, 1983, Great Britain, pp. 122.

[2] J. E.Midwinter.:' Optical fibres for transmission.'; New York: Wiley, Chapter 8.

[3] G. P. Agrawal.:'Nonlinear fibre optics', Academic Press, 1989, United Kingdom, pp. 7.

[4] P. S. Henry.:' Lightwave primer.'; IEEE Journal of Quantum Electronics, 1985, V21-2, pp.1862-1879.

[5] A. W. Snyder and J. D. Love.:' Optical waveguide theory.'; Chapman and Hall, United Kingdom, 1983.

[6] L. J. Greenstein, L. J. Greenstein and A. A. M. Saleh.:' Optical equalisation to combat the effects of laser chirp and fibre dispersion.'; IEEE Journal of Lightwave Technology, 1990, V8-5.

[7] E. G. Bryant, S. F. Carter, A. D. Ellis, W. A. Stallard, J. V. Wright and R. Wyatt.:' Unrepeatered 2.4 Gbit/s transmission over 250 km of step index fibre using erbium power amplifier.'; Electronics Letters, 1990, V26-8, pp. 528-529.

[8] L. F. Mollenauer and R. H. Stolen,:' Solitons in optical fibres.'; Fibreoptic technology journal, 1982, pp.193-198.

[9] Y. R. Shen.:'The principles of Nonlinear optics', Wiley-Interscience, 1984, USA.

[10] P. N. Butcher and D. Cotter.:' The elements of nonlinear optics.'; Cambridge University Press, 1990, Cambridge studies in modern optics: 9. U. K. pp.12.

[11] G. P. Agrawal.:' Nonlinear fibre optics.'; Academic press inc., U.S.A., 1989. pp. chapter 2.

[12] P. N. Butcher and D. Cotter.:' The elements of nonlinear optics.'; Cambridge University Press, 1990, Cambridge studies in modern optics: 9. U. K. chapter 5.

[13] L. F. Mollenauer and R. H. Stolen.:'Solitons in optical fibres', Fibreoptic Technology, April 1982, pp. 193-198.

[14] A. W. Snyder and J. D. Love.:' Optical waveguide theory.'; Chapman and Hall, United
Kingdom, 1983.

[15] Butcher, P. N. and Cotter, D.: 'The elements of nonlinear optics.'; Cambridge University Pree, Cambridge studies in modern optics 9, 1990, pp.216.

[16] Blow, K. J., Doran, N. J., Nayar, B. K. and Nelson, B. P.: 'Two wavelength operation of the non-linear fibre loop mirror.'; Optics Letters, 1990, V15-4, pp.248-250.

[17] D. M. Patrick and A. D. Ellis.:'10 Ghz pulse train derived from a CW DFB laser using cross phase modulation in an optical fibre.', Electronics Letters, V29-15, 1993, pp. 1391-1392.

[18] D. M. Patrick and A. D. Ellis.:'Demultiplexing using crossphase modulation-induced spectral shifts and Kerr Polarisation rotation.', Electronics Letters, V29-2, 1993, pp.227-228.

[19] Widdowson, T., Malyon, D. J., Ellis, A. D., Smith, K. and Blow, K. J.:'Soliton shepherding: All active soliton transmission control over global distances', Electron. Lett, 1994, V30-12, pp. 990-991.

[20] Jinno, M. and Matsumoto, T.:' Nonlinear sagnac interferometer switch and its applications.'; IEEE Jounal of Quantum Electronics, 1992, V28-4, pp.875-882.

[21] J. F. Reintjes.:' Nonlinear optical parametric processes in liquids and gasses.';l Orlando: Academic Press. 1984.

[22] J. R. Thompson and R. Roy.:' Multiple four wave mixing processes in an optical fibre.'; Optics Letters, 1991, V16-8, pp.557-559.

[23] M W. Maeda, W. B. Sessa, W. I. Way, . A. Yi-Yan, L. Curtis, R. Spicer and R. I. Lamming.:' The effect of four wave mixing in fibres on optical frequency division multiplexed systems.'; Journal of Lightwave Technology, 1991, V8-9, pp. 1402-1408.

[24] R. H. Stolen, J. E. Bjorkholm and A. Ashkin.: Applied Physics Letters, 1974, V24, pp. 308.

[25] N. Shibata, R. P. Braun and R. G. Waarts.:' Phase-mismatch dependence on efficiency of wave generation through four wave mixing in a single mode optical fibre.'; IEEE Journal of Quantum Electronics, 1987, V23-7, pp.1205- 1210.

[26] A. Yu and M. J. Mahony.:'Effect of four wave mixing on amplified multiwavelength transmission systems.', Electronics Letters, V30-11, 1994, pp. 876-877.

[27] G. P. Agrawal.:'Nonlinear fibre optics', Academic Press, 1989, United Kingdom, pp. 43.

[28] A. Hasegawa and F. Tappert.:' Transmission of stationary non-linear optical pulses in dispersive dielectric fibres: 1 Anomalous dispersion.'; Applied Physics Letters, 1973, V23, pp. 142-144.

[29] A. Hasegawa and W. F. Brinkman.:' ';IEEE Journal of Quantum Electronics, 1980, V16, pp.694.

[30] J. R. Taylor.:' Optical solitons theory and experiment.'; Cambridge University Press, Cambridge studies in modern optics 10, 1992.

[31] M. J. Ablowitz and H. Segur.:' Solitons and the inverse scattering transform.', SIAM, 1981, USA.

[32] R. M. Shelby, M. D. Levenson and P. W. Bayer.: Physics Review Letters, 1985, V-54, pp. 939.

[33] R. G. Smith.:' Optical power handling capacity of low loss optical fibres as determined by stimulated Raman and Brillouin scattering.'; Applied Optics, 1972, V-11, pp. 2489-2494.

[34] X. P. Mao, R. W. Tkach, A. R. Chraplyvy, R. M. Jopson and R. M. Derosier.:'Stimulated Brillouin threshold dependence on fibre type and uniformity.', IEEE Photonics Technology Letters, V4-1, January 1992, pp.66-69.

[35] R. Y. Chiao, C. H. Townes and B. P. Stoicheff.: Physics Review Letters, 1964, V12, pp. 592.

[36] N. Bloembergen.:' The stimulated Raman effect.'; Am. J. Phys., 1967, V-35, pp. 989-1023.

[37] Y. Aoki.:' Properties of fibre Raman amplifiers and their applicability to digital optical communication systems.'; Journal of Lightwave Technology, 1988, V6-7, pp.1225-1239.

[38] J. P. Pocholle, J. Raffy, M. Papuchon and E. Desurvire.:'Raman and four photon mixing amplification in single mode fibres.', Optical Engineering, V24-4, July/August 1985, pp.600-608.

[39] M J. Adams, A. G. Steventon, W. J. Delvin and I. D. Henning.:' Semiconductor lasers for long wavelength optical fibre.'; Peter Peregrinus, IEE Materials & Devices 4, United Kingdom, 1987.

[40] E. E. Basch.:' Optical fibre transmission.'; H. W. Sams, U. S. A., 1987, pp. 388-389

[41] P. K. Cheo.:' Fibre optics and optoelectronics.'; Prentice Hall International Editions, U. S. A., 1990, chapter13.

[42] G. C. Valley.:' A reveiw of stimulated brillouin scattering excited with a broad band pump laser.'; IEEE Journal of Quantum Electronics, 1986, V22-5, pp. 704-712.

[43] Y. Aoki.:' Properties of fibre Raman amplifiers and thier applicability to digital optical communication systems.'; IEEE Journal of Lightwave Technology, 1988, V6-7, pp.1225-1239.

[44] M. J. O'Mahony, I. W. Marshall and H. J. Westlake.:' Semiconductor laser amplifiers for optical communications systems.'; British Telecom Technology Journal, 1987, V5-3, pp.9-18.

[45] M. J. O'Mahony.:' Semiconductor laser optical amplifiers for use in future fibre systems.'; Journal of Lightwave Technology, 1988, V6-4, pp. 531-543.

[46] P. Urquhart.:' Review of rare earth doped fibre lasers and amplifiers.'; IEE Proceedings, 1988, V135-J, No. 6, pp.385-407.

[47] A. Yariv.:' Signal to noise considerstions in fibre links with periodic or distributed optical amplification.'; Optics Letters, 1990, V15-19, pp. 1064-1066.

[48] C. R. Giles.:' Propagation of signal and noise in concatenated erbium-doped fibre optical amplifiers.'; Journal of Lightwave Technology, 1991, V9-2, pp.147-154.

[49] P. K. Cheo.:' Fibre optics and optoelectronics.'; Prentice Hall, 1990, chapter 5.

[50] R. A. Baker.:' A long haul, high bit rate transmissiom system demonstration using optical amplifiers.', L'Onde Electrique special issue coinciding with Suboptic '93.

[51] H. Taga, N. Edagawa, H. Tanaka, M. Suzuki, S. Yamamoto and H. Wakabashi.:' 10 Gbit/s 9,000 km IM-DD transmission experiments using 274 Er-doped fibre amplifier repeaters.', ECOC 1993, post dealine paper PD1-1.

[52] D. J. Malyon, T. Widdowson, E. G. Bryant, S. F. Carter, J. V. Wright and W. A. Stallard.:' Demonstration of optical pulse propagation over 10,000 km of fibre using a recirculating loop.', Electronics Letters, 1991, V27-2, pp. 120-121.

[53] P. R. Trischitta and E. L. Varma.:' Jitter in digital transmission systems.', Artech House, 1989, USA.

[54] NEL GaAs IC designers catalogue, 1994.

[55] K. Kato, A. Kozen, Y. Itaya, T. Nagatsuma and M. Yaita.: ' 110 GHz, 50% efficiency mushroom-nesa waveguide p-i-n photodiode for a 1.55 μm wavelength.'; IEEE Photonics Technology Letters, 1994, V6-6, pp. 719-721.

[56] Y. G. Wey, K. S. Giboney, J. E. Bowers, M. J. W. Rodwell, P. Silvestre, P. Thiagarajan and G. Y. Robinson.: ' 108 GHz GaInAs/InP p-i-n photodiodes with integrated bias tees and matched resistors.'; IEEE Photonics Technology Letters, 1993, V5-11, pp. 1310-1312.

[57] A. D. Ellis, T. Widdowson, X. Shan, G. E. Wickens and D. M. Spirit.:' Transmission of true single polarisation 40 Gbit/s soliton data signal over 205 km using a stabilised erbium fibre ring laser and 40 GHz electronic timing recovery.', Electronics Letters, 1993, V29-20, pp. 990-992.

[58] F. Devaux, P. Bordes, A. Ougazzaden, M. Carre and F. Huet.: 'Experimental optimisatiion of MQW electro-absorption modulators with up to 40 GHz bandwidths.'; Electronics Letters, 1994, V30-16, pp. 1347-1348.

[59] K. Noguchi, H. Miyazawa and O. Mitomi.: '75 GHz broadband Ti:$LiNbO_3$ optical modulator with ridge structure.; Electronics Letters, 1994, V30-12, pp. 949-950.

[60] E. Sano, S. Yamahata and Y. Matsuoka.: '40 GHz bandwidth amplifier IC using ALGaAs/GaAs ballistic collection transisitors with carbon doped bases.'; Electronics Letters, 1994, V30-8, pp. 635-636.

[61] Y. Kuriyama, M. Asaka, T. Sugiyama, N. Iizuka and M. Obara.: 'Over 40 Gbit/s ultrahigh speed multiplexer IC implemented with high fmax AlGaAs/GaAs HBTs.'; Electronics Letters, 1994, V30-5, pp. 401-402.

[62] Widdowson T., J. P. Hueting, A. D. Ellis, D. J. Malyon and P. J. Watkinson.:' Global fibre transmission using optically amplified regenerators for maximised repeater spacing.' To be published in Electronics Letters.

[63] F. M. Gardner.: ' Phaselock techniques'; Wiley Interscience, second edition.

[64] P. R. Trischitta and E. L. Varma.: 'Jitter in digital transmission systems.'; Artech House, U. S. A., 1989, Chapter 2.

[65] M. Amemiya and Y. Hayashi.:'Systematic jitter suppression by pattern inversion', Electronics Letters, 1985, V21-16, pp.709-710.

[66] C. Berne, B. J. Karfin and D. B. Robinson.:'Systematic jitter in a chain of digital regenerators.', Bell Systems Technical Journal, 1963, V42, pp. 2679-2714.

[67] H. Ishikawa, I. Watanabe, T. Suzaki, M. Tsuji, S. Sugou, K. Kakita and K. Taguchi.:' High sensitivity 10 Gbit/s optical receiver with superlattice APD.', Electronics Letters, 1993, V29-21, pp. 1874-1875.

[68] Y. Aoki, K. Tajima and I. Mito.:'Input power limits of single mode optical fibres due to stimulated Brillouin scattering in optical communication systems', IEEE Journal of Lightwave Technology, V6-5, May 1988, pp. 710-719

[69] D. Cotter,: ' Suppression of stimulated Brillouin scattering during transmission of high-power narrowband laser light in monomode fibre.': Electronics Letters, 1982, V18-15, pp. 638-640.

[70] S. J. Pycock and S. F. Carter.:' Measurement of wavelength chirp in advanced electro-optic devices.', 4th Bangor Communication symposium, 27-28 May 1992.

[71] T. Kataoka, Y. Miyamoto, K. Hagimoto and K. Noguchi.:'20 Gbit/s long distance transmission using a 270 photon/bit optical preamplifier receiver.', Electronics Letters, V30-9, 28 April 1994, pp. 715-716.

[72] P. S. Henry.: 'Lightwave primer.'; IEEE Journal of Quantum Electronics, 1985, V21-12, pp. 1862-1879.

[73] E. J. Greer, D. J. Lewis and W. M. Macauley.:' Polarisation dependent gain in erbium doped fibre amplifiers.', Electronics Letters, 1994, V30-1 pp. 46-47.

[74] D. J. Malyon, T. Widdowson and A. Lord.:'Assessment of the polarisation loss dependence of transoceanic systems using a recirculating loop.', Electronics Letters, 1993, V29-2, pp.207-208.

[75] P. R. Morkel, V. Syngal, D. J. Butler and R. Mewman.:' PMD-induced BER penalties in optically amplified systems.', Electronics Letters, 1994, V30-10, pp.806-807.

[76] S. Yamamoto, N. Edagawa, H. Taga, Y. Yoshida and H. Wakabayashi.:' Observation of BER degradation due to fading in long distance optical amplifier system.', Electronics Letters, 1993, V29-2, pp. 209-210.

[77] D. J. Malyon, T. Widdowson, E. G. Bryant, S. F. Carter, J. V. Wright and W. A. Stallard.:' Demonstration of optical pulse propagation over 10,000 km of fibre using a recirculating loop.', Electronics Letters, 1991, V27-2, pp. 120-121.

[78] J. P. Gordon and L. F. Mollenauer.: 'Effects of fibre nonlinearities and amplifier spacing on ultra-long distance transmission.'; Journal of Lightwave Technology, 1991, V9-2, pp. 170-173.

[79] D. J. Malyon, T. Widdowson and A. Lord.:'Assessment of the polarisation loss dependence of transoceanic systems using a recirculating loop.', Electronics Letters, 1993, V29-2, pp.207-208.

[80] C. R. Giles and E. Desurvire.: 'Propagation of signal and noise in concatenated erbium doped fibre optical amplifiers.'; Journal of Lightwave Technology, 1991, V9-2, pp. 147-154.

[81] M. G. Taylor.: 'Observation of new polarisation dependence effect in long haul optically amplified system.'; OFC 93, 1993, (San-Jose California), Post-deadline paper PD5.

[82] V. J. Mazurczyk and J. L. Zyskind.: 'Polarisation hole burning in erbium doped fibre amplifiers.'; CLEO '93, 1993, (Baltimore, Maryland), Post-deadline paper PD 26.

[83] N. S. Bergano.: 'Time dynamics of polarisation hole burning in an EDFA.'; Proc. OFC '94, Paper ff4, 1994, (San Jose, USA), pp. 305-307.

[84] V. Letellier, G. Bassier, P. Marmier, R. Morin, R. Uhel and J. Artur.: 'Polarisation scrambling in 5 Gbit/s 8100 km EDFA based system.'; Electronics Letters, 1994, V30-7, pp. 589-590.

[85] M. G. Taylor and S. J. Penticost.:' Improvement in performance of long haul EDFA link using high frequency polarisation modulation.', Electronics Letters, 1994, V30-10, pp. 805-806.

[86] A. Takada and H. Miyazawa.: '30 GHz picosecond pulse generation from actively mode locked erbium doped fibre laser.'; Electronics Letters, 1990, V26-3, pp.216-217.

[87] H. Lie, S. Oshiba, Y. Ogawa and Y. Kawai.: 'Method of generating nearly transform limited pulses from gain-switched distributed feedback laser diodes and its application to soliton transmission.';l Optics Letters, 1992, V17-1, pp.64-66.

[88] M. Suzuki, H. Tanaka, N. Edagawa, K. Utaka and Y. Matsushima.: 'Transform limited optical pulse generation up to 20 GHz repetition rate by sinusoidally driven InGaAsP electroabsorption modulator.'; Journal of Lightwave Technology, 1993, V11-3, pp.468-473.

[89] N. M. Froberg, G. Raybon, U. Koren, B. I. Miller, M. G. Young, M. Chien, G. T. Harvey, A. Gnauck and A. M. Johnson.:' Generation of 12.5 Gbit/s soliton data stream with an integrated laser modulator transmitter.', Electronics Letters, 1994, V30-22, pp. 1880-1881.

[90] I. P. Kaminow.: 'Polarisation in optical fibres.'; IEEE Jornal of Quantum Electronics, 1981, V17, pp. 15-22.

[91] C. D. Poole and C. R. Giles.: 'Polarisation dependent pulse compression and broadening due to polarisation dispersion in dispersion shifted fibre.'; Opitics Letters, 1988, V13, pp. 155-157.

[92] C. D. Poole, R. W. Trach, A. R. Chraplyvy and D. A. Fishman.: 'Fading in lightwave systems due to polarisation mode dispersion.'; Photonics Technology Letters, 1991, V3, pp. 68-70.

[93] G. J. Foschini and C. D. Poole.:' Statistical theory of polarisation dispersion in single mode fibres.', Journal of Lightwave Technology, 1991, V9-11, pp. 1439-1455.

[94] D. J. Malyon, T. Widdowson and A. Lord.:'Assessment of the polarisation loss dependence of transoceanic systems using a recirculating loop.', Electronics Letters, 1993, V29-2, pp.207-208.

[95] T. Widdowson, A. Lord and D. J. Malyon.: 'Polarisation guiding in ultra-long distance soliton transmission.'; Electronics Letters, 1994, V30-11, pp. 879-880.

[96] D. Marcuse.: 'Pulse distortion in single mode fibres.'; Applied Optics, 1980, V19-10, pp. 1653-1660.

[97] M. Lin and S. Chi.: 'Optimal transmission condition of nonlinear optical pulses in single mode fibres.'; Journal of Lightwave Technology, 1993, V11-4, pp. 542-547.

[98] M. Stern, J. P. Heritage, R. N. Thurston and S. Tu.: 'Self phase modulation and dispersion in high data rate fibre optic transmission systems.'; Journal of Lightwave Technology, 1990, V8-7, pp. 10009-1016.

[99] K. J. Blow and N. J. Doran.: 'Nonlinear effects in optical fibre and fibre devices.'; IEE Proceedings, 1987, V134-J-3, pp. 138-144.

[100] G. P. Agrawal.:'Nonlinear fibre optics', Academic Press, 1989, United Kingdom, pp. 88.

[101] M. J. Potasek and G. P. Agrawal.: 'Power dependent enhancement in repeater spacing for dispersion limited optical communication systems.'; Electronics Letters, 1986, V22-14, pp. 759-761.

[102] D. J. Malyon, T. Widdowson, E. G. Bryant, S. F. Carter, J. V. Wright and W. A. Stallard.:' Demonstration of optical pulse propagation over 10,000 km of fibre using a recirculating loop.', Electronics Letters, 1991, V27-2, pp. 120-121.

[103] N. Shibta, R. P. Braun and R. G. Waarts.: 'Phase mismatch dependence of efficiency of four wave generation through four wave mixing in a single mode optical fibre.'; IEEE Journal of Quantum Electronics, 1987, V23-7, pp. 1205-1210.

[104] M. W. Maeda, W. B. Sessa, W. I. Way, A. Yi-Yan, L. Curtis, R. Spicer and R. I. Laming.: 'The effect of four wave wixing in fibres on optical frequency division multiplexed systems.'; Journal of Lightwave Technology, 1990, V8-9, pp. 1402-1408.

[105] D. Marcuse.:' Single channel operation in very long nonlinear fibres with optical amplifiers at zero dispersion.', Journal of Lightwave Technology, 1991, V9-3, pp.356-361.

[106] N. Shibata, R. P. Braun and R. G. Waarts.:' Phase-mismatch dependence of efficiency of wave generation through four wave mixing in a single mode fibre.', IEEE Journal of Quantum Electronics. 1987, VQE23-7, pp.1205-1210.

[107] S. F. Carter, E. G. Bryant and J. V. Wright.:' Influence of self phase modulation on ultra-long span optical transmission at zero dispersion.', in Technical Digest of Topical Meeting on Nonlinear Guided Wave Phenomena (Cambridge, UK, Optical Society of America), 1991, pp. 161

[108] D. Marcuse.:' Single channel operation in very long nonlinear fibres with optical amplifiers at zero dispersion.', Journal of Lightwave Technology, 1991, V9-3, pp.356-361.

[109] J. P. Pocholle, J. Raffy, M. Papuchon and E. Desurvire.; 'Raman and four photon mixing amplification in single mode fibres.'; Optical Engineering, 1985, V24-4, pp. 600608.

[110] Y. Kodama.:' Optical solitons in a monomode fibre.', Journal of Statistical Physics, 1985, V39-5/6, pp. 597614.

[111] K. J. Blow and N. J. Doran.:' Average soliton dynamics and the operation of soliton systems with lumped amplifiers.', IEEE Photonics Technology Letters, 1991, 3, pp. 396-371.

[112] Gordon, J. P. and Haus, H. A.,: 'Random walk of coherently amplified solitons in optical fibre transmission.' Optics Lett. Vl 1-10. 1986. p 665-667.

[113] E. M. Dianov, A. V. Luchnikov, A. N. Pilipetskii and A. M. Prokhorov.:' Long-range interaction of picosecond solitons through excitation of acoustic waves in optical fibres.', Applied Physics, 1992, B 54, pp. 175-180.

[114] Gordon, J. P.: 'Interaction forces among solitons in optical fibres.' Optics Lett. V8-11, 1983, p 596-598.

[115] J. P. Gordon.:' Interaction forces among solitons in optical fibres.', Optics Letters, 1983, 8, pp. 596-598.

[116] X. Shan, D. Cleland and A. D. Ellis.:' Stabilisating Er Fibre soliton laser with pulse locking.', Electronics Letters, 1992, V28-2, pp.182-183.

[117] X. Shan and D. M. Spirit.:' Novel method to suppress noise in harmonically mode locked erbium fibre ring lasers.', Electronics Letters, 1993, V29-11, pp. 979-981.

[118] G. T. Harvey and L. F. Mollenauer.:' Harmonically mode locked fibre ring laser with an internal Fabry-Perot stabiliser for soliton transmission.', Optics Letters, 1993, V18-2, pp. 107-109.

[119] Widdowson T, Malyon D J, Watkinson P J, Shan X (1994) 'Soliton propagation without transmission control using a phase locked erbium fibre ring laser' Electron Lett 8, 661-3

[120] A. Mecozzi, J. D. Moores, H. A. Haus and Y. Lai.:' Soliton transmission contrrol.': Optics Letters, V16-23, 1991, pp. 1841-1843.

[121] L. F. Mollenauer, E. Lichtman, G. T. Harvey, M. J. Neubelt and B. M. Nyman.:' Demonstration of error free soliton transmission over more than 15,000 km at 5 Gbit/s single channel, and more than 11,000 km at 10 Gbit/s in two channel WDM.', Electronics Letters, 1992, V28-8, pp. 792-794.

[122] Evangelides, S. G., Mollenauer, L. F., Gordon, J. P. and Bergano, N. S.: ' Polarisation multiplexing with solitons.' Journal of Lightwave Technology. V10-1, 1992, p 28-35.

[123] Andrew Lord personal communication at B. T. Laboratories.

[124] A. D. Ellis, T. Widdowson, X. Shan, G. E. Wickens and D. M. Spirit.:' Transmission of true single polarisation 40 Gbit/s soliton data signal over 205 km using a stabilised erbium fibre ring laser and 40 GHz electronic timing recovery.', Electronics Letters, 1993, V29-20, pp. 990-992.

[125] Suzuki, M., Taga, H., Edagawa, N., Tanaka, H., Yamamoto, S. and Akiba, A.: 'Experimental investigation of Gordon-Haus limit on soliton transmission by using optical short pulses generated by an InGaAsP electroabsorption modulator.' Electron Lett. V29-18, 1993, p 1643-1644.

[126] Ellis A D, Spirit D M, (1993) 'Compact 40 Gbit/s optical demultiplexer using GaInAsp optical amplifier', Electon Lett 24, 2115-7

[127] I. Glesk, J. P. Sokoloff and P. R. Prucnal.:' Demonstration of all-optical demultiplexing of TDM data at 250 Gbit/s.', Electronics Letters, 1994, V30-4, pp. 339-340.

[128] Gordon, J. P. and Haus, H. A.,: 'Random walk of coherently amplified solitons in optical fibre transmission.' Optics Lett. Vl 1-10. 1986. p 665-667.

[129] E. M. Dianov, A. V. Luchnikov, A. N. Pilipetskii and A. M. Prokhorov.:' Long-range interaction of solitons in ultra-long communication systems.'; Sov. Lightwave Commun., 1991, V1, pp. 235-246

[130] L. F. Mollenauer, M .J. Neubelt, M. Haner, E. Litchman, S. G. Evangelides and B. M. Nynam.:' Demonstration of error free soliton transmission at 2.5 Gbit/s over more than 14,000 km.'; Electronics Letters, 1991, V27-22, pp.2055-2056.

[131] A. Mecozzi, J. D. Moores, H. A. Haus and Y. Lai.:' Soliton transmission control.'; Optics Letters, 1991, V16-23, pp.1841-1843.

[132] L. F. Mollenauer, E. Litchman, G. T. Harvey, M .J. Neubelt, and B. M. Nynam.:' Demonstration of error free soliton transmission over more than 15,000 km at 5 Gbit/s, single channel and over more than 11,000 km at 10 Gbit/s in two channel WDM.'; Electronics Letters, 1992, V28-8, pp. 792-793.

[133] L. F. Mollenauer, E. Litchman, G. T. Harvey, M .J. Neubelt, and B. M. Nynam.:' Demonstration of error free soliton transmission over more than 15,000 km at 5 Gbit/s, single channel and over more than 11,000 km at 10 Gbit/s in two channel WDM.'; Electronics Letters, 1992, V28-8, pp. 792-793.

[134] M. Suzuki, N. Edagawa, H. Taga, H. Tanaka, S. Yamamoto and S. Akiba.:' Feasibility demonstration of 20 Gbit/s single channel soliton transmission over 11,500 km using alternating amplitude solitons.'; Electronics Letters, 1994, V30-13, pp.1083-1084.

[135] C. Desem and P.L.Chu.:' Reducing soliton interactions in single mode optical fibres.': IEE Proceedings, 1987, V134-j-3, pp.145-151.

[136] P. L. Francois and T. Georges.:' Reduction of the averaged soliton interaction forces by amplitude modulation.'; Optics Letters, 1993, V18-8, pp. 583-585.

[137] L. F. Mollenauer, J. P. Gordon and S. G. Evangelides.:' The sliding frequency guiding filter: an improved form of soliton jitter control.'; Optics Letters, 1992, V17-22, pp. 1575-1577.

[138] L. F. Mollenauer, P. V. Mamyshev and M. J. Neubelt.:' Measurement of timing jitter in soliton transmission at 10 Gbit/s and achievement of 375 Gbit/s-Mm, error free, at 12.5 and 15 Gbit/s.'; Optics Letters, 1994, V19, pp. 704.

[139] D. Leguen, F. Favre, R. Boittin, J. Debeau, F. Devaux, M. Henry, C. Thebault and T. Georges.:' Demonstration of sliding filter controlled soliton transmission at 20 Gbit/s over 14Mm.'; Electronics Letters, 1995,

[140] L. F. Mollenauer, E. Lichtman, M. J. Neubelt and G. T. Harvey.:' Demonstration using sliding frequency guiding filters, of error free soliton transmission over more than 20 Mm at 10 Gbit/s, single channel, and over more than 13 Mm in a two channel WDM.'; Electronics Letters, 1993, V29-10, pp.910-911.

[141] M. Romagnoli and S. Wabnitz.:, Bandwidth limits of soliton transmission with sliding filters.'; Optics communications, 1994, pp. 293-297.

[142] M. Nakazawa, H. Kubota, E. Yamada and K. Suzuki.:' Infinte distance soltion transmission with soliton controls in time and frequency.', Electronics Letters, 1992, V28-12, pp.1099-1100.

[143] Nakazawa, M., Suzuki, K., Yamada, E., Kubota, H., Kimura, Y. and Takaya, M.: 'Experimental demonstration of soliton transmission over unlimited distances with soliton control in time and frequency domains.' Electron Lett. V 29-9, 1993, p 729-730.

[144] Kubota, H. and Nakazawa, M.:'Soliton transmission with long amplifier spacing under soliton control', Electron. Lett., 1993, V29-20, pp1780-1781.

[145] Ellis, A. D., Widdowson, T., Shan, X., Wickens, G. E. and Spirit, D. M.: 'Transmission of true single polarisation 40 Gbit/s soliton data over 205 km using a stabilised erbium fibre ring laser and 40 GHz electronic timing recovery.' Electron. Lett. V29-11, 1993, p990-992.

[146] Kelly, S. M. J.:'Characteristic sideband instability of periodically amplified average soliton', Electron. Lett., 1992, V28-8, pp.806-807

[147] N. J. Smith, K. J. Blow, W,J. Firth and K. Smith.:' Soliton dynamics in the presence of phase modulators.', Optics Communication, 1993, V103, pp. 324.

[148] S. Wabnitz.:' Suppression of soliton interactions by phase modulation.', Electronics Letters, 1993, V29-19, pp. 1711-1712.

[149] Widdowson, T., Malyon, D. J., Ellis, A. D., Smith, K. and Blow, K. J.:'Soliton shepherding: All active soliton transmission control over global distances', Electron. Lett, 1994, V30-12, pp. 990-991.

[150] A. D. Ellis, K. Smith and D. M. Patrick.:' All optical clock recovery at bit rates up to 40 Gbit/s.': Electronics Letters, V29-15, 1993, pp.1323-1324.

[151] A. Takada, K. Sato, M. Saruwatari and M. Yamamoto.: 'Pulse width tuneable subpicosecond pulse generation from an actively modelocked monolithic MQW laser MQW electroabsorption modulator.'; Electronics Letters, 1994, V30-11, pp. 898-900.

[152] K. Smith and J. K. Lucek.: 'All-optical clock recovery using a mode locked laser.'; Electronics Letters, 1992, 28, pp. 1814-1815.

[153] V. V. Afanasjev, W. H. Loh, A. B. Grudinin, D. Atkinson and D. N. Payne.:' Ulimited soliton propagation and noise suppression in a system with spectral filtering and saturable absorption.'; Cleo '94, CThN1.

[154] N. J. Smith and N. J. Doran.:' Picosecond soliton propagation using nonlinear optical loop mirrors as saturable absorbers.'; IEE colloquium on 'optical solitons: principle and applications.', 1994, Nov 11.